INFORMATION TO USERS

This material was produced from a microfilm copy of the original document. While the most advanced technological means to photograph and reproduce this document have been used, the quality is heavily dependent upon the quality of the original submitted.

The following explanation of techniques is provided to help you understand markings or patterns which may appear on this reproduction.

1. The sign or "target" for pages apparently lacking from the document photographed is "Missing Page(s)". If it was possible to obtain the missing page(s) or section, they are spliced into the film along with adjacent pages. This may have necessitated cutting thru an image and duplicating adjacent pages to insure you complete continuity.

2. When an image on the film is obliterated with a large round black mark, it is an indication that the photographer suspected that the copy may have moved during exposure and thus cause a blurred image. You will find a good image of the page in the adjacent frame.

3. When a map, drawing or chart, etc., was part of the material being photographed the photographer followed a definite method in "sectioning" the material. It is customary to begin photoing at the upper left hand corner of a large sheet and to continue photoing from left to right in equal sections with a small overlap. If necessary, sectioning is continued again — beginning below the first row and continuing on until complete.

4. The majority of users indicate that the textual content is of greatest value, however, a somewhat higher quality reproduction could be made from "photographs" if essential to the understanding of the dissertation. Silver prints of "photographs" may be ordered at additional charge by writing the Order Department, giving the catalog number, title, author and specific pages you wish reproduced.

5. PLEASE NOTE: Some pages may have indistinct print. Filmed as received.

University Microfilms International
300 North Zeeb Road
Ann Arbor, Michigan 48106 USA
St. John's Road, Tyler's Green
High Wycombe, Bucks, England HP10 8HR

Instrumentation for strain gage dendrography and the effects of light and temperature on the transpiration and stem strain in young trees of a populus clone

by

Edward Agyapong Baryeh

A Dissertation Submitted to the
Graduate Faculty in Partial Fulfillment of
The Requirements for the Degree of
DOCTOR OF PHILOSOPHY

Department: Engineering Science and Mechanics
Major: Engineering Mechanics

Approved:

Signature was redacted for privacy.

In Charge of Major Work

Signature was redacted for privacy.

For the Major Department

Signature was redacted for privacy.

For the Graduate College

Iowa State University
Ames, Iowa

1978

TABLE OF CONTENTS

INTRODUCTION

Preamble: Man has lived with plants ever since creation and plants have been utilized by mankind in various forms--food, decoration, medicine, manufacturing machinery, putting up buildings, making paper and making clothing. Various plant behaviors and properties have been studied by scientists to enhance peoples' knowledge and understanding of plants in order to optimize the use of plants in everyday life.

Plant physiologists and people in related fields have expressed the need for a practical and effective means whereby the internal water status of trees can be monitored in order to understand and ascertain the overall water requirements of plants. The study that form the subject of this dissertation deals with a novel method of measuring small changes in the circumference of tree trunks. It utilizes electrical resistance strain gages glued directly to the bark of the trunk. This method was originated by Schütte and Burger (1). It has been found that the progressive changes in the circumference of a tree trunk appears to correlate with variations in water stress as the environmental conditions of the tree is varied. Preliminary qualitative investigations were carried out by Iowa State University faculty members Drs. C. P. Burger and J. C. Gordon. The major advantage of this novel

method in comparison with other methods mentioned later in the literature review is that the strain gage provides a nondestructive, simple and inexpensive technique to give continuous recording as well as a point-in-time recording.

The studies in this dissertation aim to achieve a calibrated instrumentation system which is sophisticated enough to permit the running of carefully designed and controlled experiments that will look into various aspects of plant behavior as the environmental conditions change. The method uses strain gages bonded on tree trunks in the greenhouse or growth chamber, wheatstone bridge circuits, strain indicators, strain recorders, load cells and voltage amplifiers to fascilitate continuous recording of strain and weight. The transpiration, as shown later, can then be found from the weight recording. Some of the possible experiments which can be run with such equipment are:

1. The effect of temperature changes on the physiological water status of trees.
2. The effect of leaf area on water intake of trees.
3. The effect of humidity on tree growth.
4. The effect of various kinds of pollution on tree growth. This will help in selecting which trees are best suited for polluted atmospheres like avenues, parks and industrial areas.

5. The effect of atmospheric carbon dioxide concentration on tree growth.
6. The effect of light intensity on tree growth.
7. How irrigation projects can be carried out effectively and at the right time.
8. Nutrient effects on water uptake of trees.
9. Edaphic or soil effect on tree growth.

This new method of measuring the changes in circumference of tree trunks by means of electrical resistance strain gages has other advantages too. It is a quick method. The accuracy and sensitivity are high. The interpretation of results is minimal. Its application is not limited by component size. There are numerous types, sizes and forms of gages, covering practically all applications. Remote readings are possible in relatively inaccessible regions. Long-term measurements over periods of years are possible, if adequate care is taken with the installation.

The set up of instrumentation for high precision work involving electrical resistance strain gages require a lot of patience and care. The strain gages used are the thin metal foil type, fully encapsulated and with lead wires. These need to be glued very carefully to the trunk of the tree. The gage wires are soldered carefully to the lead wires.

Most strain gage applications in engineering have been in relation to metals, alloys and in some cases plastics.

The application to trees is new and therefore special care is needed in this application.

The variations in size of tree stems have been known to be affected by atmospheric conditions like temperature, humidity and light. Therefore, superimposed on any such records are the effects of such ambients. The instrumentation proposed in this study is used to investigate some of these effects on young trees.

THE PROBLEM

Studies with strain gages require a good recording and instrumentation system in order that the minute induced strains can be recorded, assessed and interpreted. Using strain gages to study the physiological behavior of trees is basically no different from other applications of the strain gage. Most strain gage applications in engineering have been in relation to metals, alloys and in some cases plastics. The application to live trees is new and, therefore, the method of bonding the gages to the trees may need special care. Like any studies with strain gages, the need for a good recording and instrumentation system cannot be overlooked. The problem basically, therefore, is the development of a good instrumentation system for the type of studies mentioned in the introduction. Such a system should reveal reliable information on short-term responses of trees caused by the diurnal cycle, and long-term changes caused by growth and fertilizer application. The instrumentation, after calibration, may then be used to investigate the effects of light and temperature on the transpiration and stem strain in young trees of a populus clone.

The instrumentation will then open up a new avenue for plant physiologists and botanists for investigating other physiological water aspects of plants.

LITERATURE REVIEW

Since the introduction of the electrical resistance strain gage in the U.S.A. in 1939 by Ruge and Simmons, as cited by Hearn (2), it has come into widespread use particularly in engineering, and to a lesser degree in biological sciences. It is now the basis of one of the most useful experimental stress analysis techniques in almost every branch of engineering. It has been used in the analysis of stress in the auto industry, in the marine industry, in the aircraft industry and in the earth moving machinery industry. Strain gages have been used for measurements of strain on all sorts of objects ranging from nuclear boilers and turbine blades to human bones. The strain gage has even measured the forces developed by a chick inside the egg (2). Dove and Adams (3) report on the use of strain gages in the medical field to measure forces of chewing, to study the mechanical behavior of the skull and to study forces acting on the leg during walking. Perry and Lissner (4) also report the use of strain gages on bones, both human and animal and also on other nonmetals such as plastics, glass and concrete. With good insulation practices, gages have been used in environments other than air such as water, concrete and engine oil.

Some of the recent works involving the use of strain gages and accompanying instruments include the work of

Goldsmith and Taylor (5). They studied the impact on ophthalmic lenses using a strain gage bridge, oscilloscope, photocell, flash unit and delay unit. Sherbourne and Haydl (6) also employed strain gage and strain gage instrumentation to investigate the postbuckling and postyielding of edge-compressed circular plates.

The use of strain gages on trees is a completely new application of strain gages in the biological field. The quantity the gage measures on the tree however, namely the diametral variations in the tree trunk diameter, has been studied by a number of investigators. They used various instruments and methods as will be outlined later. It is known that trees exhibit variations in the size of their diameters or circumferences. These variations are due both to variations in the hydration level of the tree cells and variation in water tension in the trunk. These in turn depend on environmental conditions, both past and present. This means that water status, transpiration, atmospheric conditions and stem diameter changes are inter-related. Data on diametral changes is therefore valuable in studying the way and manner in which trees respond to environmental parameters such as temperature, light and relative humidity.

One of the first instruments used in measuring stem diameters is a pair of calipers. MacDougal (7) reports that in 1879, Dr. P. Kaiser published results of hourly diametral

changes in tree trunks using a pair of calipers. This was accurate enough to detect daily variations. Although this was a simple and inexpensive method in terms of instrumentation and nondestructiveness like the strain gage, it was expensive labor-wise and results were less accurate compared to the strain gage. It also lacked the continuous recording ability of the strain gage. Zaerr (8) used calipers as recently as 1971 to measure the stem diameters of Douglas fir trees.

In 1880, Boehmerle (9) designed an auximeter that was composed of a band which was wrapped around a tree trunk. A lever mechanism and a linear scale was used to measure the changes in stem diameter. Any expansion or contraction of the tree trunk actuated the lever to move over the scale. The lever mechanism acted as an amplifier for the stem changes. A similar device involving a steel band on roller bearings was proposed in 1905 by Friedrich (10). Using a similar band dendrometer, the diurnal changes in stem circumference at a 1954 and 1963 internodes of a 22 year old Douglas fir was measured by Lassoie (11). These banding devices have one major disadvantage: they are subject to large errors associated with the thermal expansion and contraction of the material of the band.

Mallock (12) used an arrangement of prisms in connection with a tape of invar which encircled the tree trunk in 1917.

Changes in the stem diameter in turn caused observable displacements of interference bands of light. The shortcoming of this device was that it responded to external disturbances of the tree and of the prisms.

Several other investigators (13, 14, 15, 16) also obtained records of diurnal fluctuations caused by root pressure. Some (16, 17, 18) were able to predict that the trunks of trees contract during bright days and expand during cool nights. Klepper (19) has found marked diurnal variations in water potential of leaves of plants which can be correlated with the stem diurnal expansion and contraction. By observing roots in soil through transparent panels, Huck, Klepper and Taylor (20) have observed diurnal variations even in the diameter of the roots of a tree. The diurnal physiological response pattern of trees has also been demonstrated by Whipple, Ligon, Burger and Coffman using electrical resistance strain gages as the stem expansion and contraction sensor (21).

Between 1918 and 1936, MacDougal (7, 22, 23) used several dendrographs of basically the same design as the one used by Boehmerle (9), Friedrich (10) and Mallock (12). His instrument had a rigid metal frame surrounding the trunk. It had a fixed contact point and a second contact point consisting of the short bearing arm of a lever. The long arm carried a pen which traced out a record of the

diameter changes. MacDougal is one of the few investigators who has paid careful attention to temperature effects. He did so by constructing the frames of his dendrograph with bario, invar or permant. All these materials have a very small thermal coefficient of expansion. For frames constructed out of permant, he found that the maximum error introduced by temperature changes under field conditions was 111 x 10^{-6} or 111 με. Most of his experiments were carried out with invar frames which has a coefficient of thermal expansion of 0.7/°C, 1/5 that of permant. The reliability and the accuracy of the data obtained by MacDougal in the 1920's has not been surpassed by the data obtained using other instruments developed during the subsequent period of almost 50 years. The strain gage dendrograph proposed in this dissertation, however, is capable of surpassing the accuracy of MacDougal's dendrograph.

Some recent investigators like Reineke (24), Fowells (25), Daubenmire (26), Byram and Doolittle (27) and Fritts and Fritts (28) have written about devices which must be screwed or bolted to the tree trunk. The wood is assumed rigid so the screws or bolts do not move -- an assumption which has been found to be untrue. Measurements of stem diameter variations are made between the bark and the device. This type of dendrograph has some disadvantages. The behavior of the tree around the device is affected to an unknown

degree due to the insertion of the screws or bolts in the tree. The fact that the wood is not rigid has been supported by MacDougal (7). He found in the case of Monterey Pine that the expansion of the wood could account for 20% of the total diametral expansion.

A modification to the Fritts dendrograph (28) was made by Kozlowski (29) in 1967. He eliminated the screw or bolts inserted into the stem of the tree by supporting the dendrograph on a 30 inch (76 cm) high steel frame. This had an inherent error due to the thermal expansion of the material for the instrument. The data indicated that similar trees subjected to identical conditions gave nonidentical results, making the technique unreliable.

Another instrument that has been used for recording stem diameter changes is the LVDT (linear variable differential transformer). This was first proposed by Impens and Schalck (30) in 1965. This instrument was also screwed or bolted to the tree stem making it suffer the same disadvantage outlined previously in connection with the other instruments that are also screwed or bolted to the stem. In addition to this, it had the disadvantage of not being useful for work on small trees because of its bulkiness. Despite the shortcomings, several other investigators (31, 32, 33, 34) have used the LVDT in ascertaining a record of the diametral changes of trees. A description of this method of stem diameter measure-

ment is given in reference 34. In 1969, Splinter (35) proposed a LVDT which did not require mounting screws. This device and all modifications of it require a framework for holding the LVDT in contact with the stem. This makes the system susceptible to temperature errors.

Water movement in trees and transpiration of trees have been studied by plant physiologists and botanists using other methods too. Peel (36) quotes that in 1954, Wiebe and Kramer used labelled ions to study water intake by trees. The corona hygrometer was used by Anderson, Hertz and Rufelt in 1954 to study transpiration of palnts, as quoted by Sutcliffe (37). Gregory, Milthorpe, Pearse and Spencer (1950) measured water absorption potometrically (37). Ogata, Richards and Gardner (1960) tried to measure water consumption by means of tensiometers (37). In 1971, Jordan and Ritchie (31) measured evaporation rates by means of an energy balance technique. Jordan and Ritchie (31) quotes Black, Tanner, Gardner, Ritchie and Burnett as using precision weighable lysimeters in recent field studies to measure absolute transpiration rates. The lysimeter method of measuring evaporation or water loss as opposed to the method proposed in this study is expensive to set up and it requires some field excavation. This tends to disturb the environment to some extent.

Other fairly recent related studies which can also be performed with the strain gage and correlated with stem

strain include the works of Marais and Wiersma (38), Sionit and Kramer (39), Bielorai and Hopmans (40), Ackerson, Krieg, Miller and Zartman (41), Thomas, Brown and Jordan (42) and Lang, Klepper and Cumming (43).

With a strain gage dendrometer capable of recording strain changes at a sensitivity of 20×10^{-6} or 20 $\mu\varepsilon$ per inch of chart width and a pen recorder which can move at 4 inches per minute (10 cm per minute), it is possible to record response times to watering simply, inexpensively and nondestructively.

A tabulation of various techniques for measuring water stress which have been used by various investigators is given in Appendix A. The major portion of the table was originally compiled by Ligon and Whipple.

It has been confirmed by various investigators (1, 11, 21, 31, 32) that the diametral changes of the stem is greatly affected by ambients such as humidity, temperature and light. The need to study some of the effects of these ambients on the water status of trees cannot therefore be overemphasized. The study presented in this dissertation looks at some of these effects.

OBJECTIVES

The objectives of this study are:

1. To assemble and build an instrumentation system for data collection and recording which is suitable for the types of strain gage applications stated under the introduction.
2. To calibrate the instrumentation.
3. To use the instrumentation to investigate the effect of light and temperature on the transpiration and stem strain in young trees of a populus clone.

INSTRUMENTATION

Gage Selection

All experiments described here were conducted on nursery trees growing in pots. The basic quantities to be measured on the tree are diametral or circumferential strain of the stem and transpiration of the tree. Circumferential strain can be measured, as described later, by bonding a gage along the circumference of the stem and hooking the gage into a wheatstone bridge. Transpiration can be assessed by designing a special load cell which can measure continuously the total weight of the potted tree at any instant of time. Hence, if evaporation from the soil in the pot is eliminated, the change in weight of the system will be due to the transpiration by the tree.

As mentioned in the introduction, electrical resistance strain gages are used extensively in engineering and medicine. They are, in fact, the sensing elements in most sensitive transducers for measuring pressure, forces, flow rates and displacements. Due to the usefulness and high demand for strain gages, strain gage manufacturers have perfected the design of gages and have made available a wide and complete variety of gages for various applications. These gages vary in material of construction, geometry, size and backing material. Most commercial gages have a resistance of

120 ohms or 350 ohms. The 120 ohms gage was selected for this work due to its greater availability and lower cost. There is a complete list of gage properties and gage selection techniques for various applications in references 2, 3, 4 and 44. The important factors among these for the work presented here are:

1. Duration of strain
2. Size of gage
3. Operating temperature
4. Strain limits expected
5. Gage resistance and sensitivity
6. Method of installation and protection
7. Material on which gage is to be bonded

Bearing in mind that wood is essentially a bad heat sink, the fact that a live tree contains moisture and the size of the tree to be experimented on, the gage type selected was Micro-Measurements gage EA-06-125BT-120. It has a gage factor of 2.075 $\pm$ 0.5% at 75°F (24°C), and a resistance of 120.0 $\pm$ 0.3% ohms. These gages are fully encapsulated to seal gage foil against moisture from both the tree and the atmosphere. They have lead wires for easy soldering without burning or overheating the tree trunk with soldering heat. This series of gages are a general purpose family of constantan gages used in experimental stress analysis. They have a 1 mil (0.03 mm) tough, flexible polymide film backing.

They can stand a temperature range of -75°C to 175°C (-104°F to 346°F) for continuous use in static measurements, and -195°C to 205°C (-318°F to 402°F) for special or short term exposure. The strain limit is 5% for gage lengths of 3.2 mm (0.126 in) and 3% for gage lengths less than 3.2 mm (0.126 in) and they are linear within this strain range. The length of the gage used is 0.125 in.

The Wheatstone Bridge

Metals and alloys used for manufacturing strain gages work on the principle that when they increase in length, their resistances increase and when they decrease in length, their resistances decrease. This means that when a gage of resistance R_g is bonded to any material, any strain imparted to the material is transmitted to the material of the gage foil giving a change in resistance ΔR_g of the gage. The resistance change per unit resistance is proportional to the strain on the material at the point where the gage is glued.

$$\text{ie} \quad \frac{\Delta R_g}{R_g} = G\varepsilon \tag{1}$$

where

G = the gage factor, and

ε = strain in material

The strain that appear in this work can be classified as quasi-static. The use of a wheatstone bridge, (Figure 1a), is therefore preferred to its counterpart, the potentiometer

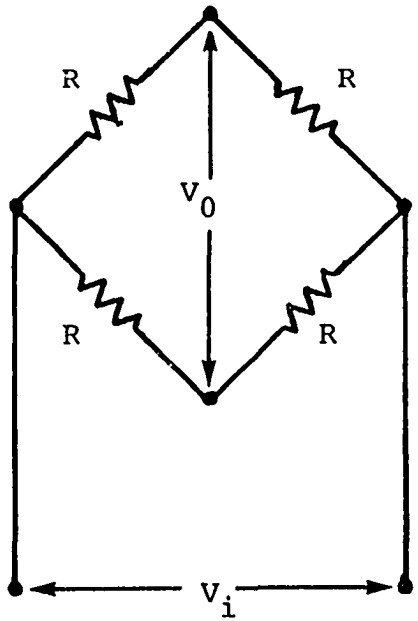

Figure 1a. Wheatstone Bridge

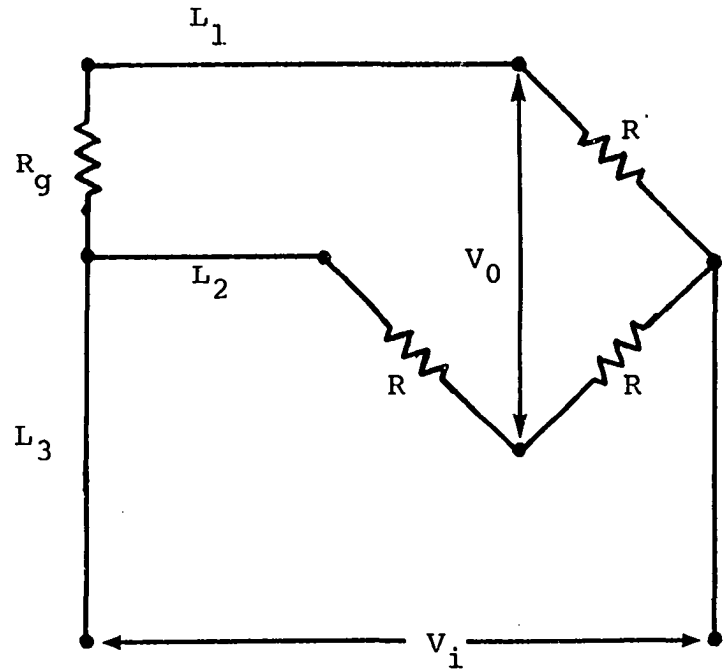

Figure 1b. Quarter bridge or single arm bridge with 3 lead wires (L_1=L_2=L_3)

for measuring the small resistance changes of the gages.

The wheatstone bridge is essentially four resistors, usually of the same magnitude, connected as in Figure 1a with a voltage input V_i. Any of the resistors can be a strain gage. When the resistance of the strain gage changes due to a strain transmitted to the gage, the change in resistance of the gage yields an output voltage V_0 which can be displayed on a galvanometer or on a pen recorder.

The principle of operation of the wheatstone bridge as a direct readout device, where ΔE is measured to determine the strain is outlined in reference 44, in which ΔE is given by:

$$\Delta E = \frac{VR_1R_2}{(R_1+R_2)^2}\left(\frac{\Delta R_1}{R_1} - \frac{\Delta R_2}{R_2} + \frac{\Delta R_3}{R_3} - \frac{\Delta R_4}{R_4}\right) \qquad (2)$$

Equation 2 is inherently nonlinear but the nonlinear term is quite small and can be neglected if the strains being measured are less than 0.05 (50,000 $\mu\varepsilon$).

The wheatstone bridge in conjunction with sensitive amplifiers can measure the small changes in the resistance of the gages. The results can then be displayed on a continuous chart recorder. The chart can then be calibrated to read directly as strain. These instruments have good stability over long periods of time and over a wide range of ambient conditions. A resolution of 5 $\mu\varepsilon$ or 5×10^{-6} can be

achieved for long term strains while for short term the resolution improves to 1 $\mu\varepsilon$ or 1 x 10^{-6}.

Bonding Gages on Trees

One successful method of mounting gages on trees is outlined in reference 21. This method uses an epoxy cement with epoxy backed gages. For long term application this bonding method was good although the epoxy bond is quite stiff and there is a fairly high reinforcement provided when used on young trees which usually have soft barks.

The quality and success of a strain gage installation are influenced greatly by the care and precision of the installation procedure and the correct choice of adhesive.

The trees used in this investigation were young greenhouse grown poplar clone 5377 (also known as the Wisconsin 5). The trees were about four months old and therefore had soft bark. Hence, a slightly different method of bonding was used.

Before bonding the gage, a small area on the bark (a little larger than the gage and its carrier) is carefully and gently smoothened with 500 grade emery paper. It is then wiped gently a few times with cotton wool which is moistened with acetone. This removes dirt and grease from the smoothened area. The gage is then transferred on to a glass plate which has been cleaned with acetone. Gages are handled with tweezers so that they do not get greasy. The

gage is lifted by means of a Scotch tape and placed on the tree in a horizontal manner as in Figure 2. One end of the tape is then lifted off the tree so that the whole gage is off the tree but with the tape still on the tree. A thin layer of the catalyst for Eastman 910 bond is smeared on the side of the gage which will eventually be in contact with the tree and on the smoothened part of the bark. After the catalyst has dried, a small drop of Eastman 910 is dropped at one end of the gage. Bonding is achieved by pressing the gage down on the bark with the thumb for about ten to fifteen minutes keeping the glue line thickness as small as possible. The gage is then soldered using three lead wires and hooked into a wheatstone bridge like Figure 1b or Figure 2. Solder flux is used to facilitate easy soldering. Excess solder flux at the soldering points is cleaned with rosin solvent after soldering. The leads are prevented from touching each other and/or the bark of the tree by insulating them with Scotch tape. When the greenhouse is cool it is usually necessary to warm the bark a bit with a hair dryer before bonding the gage and again after bonding the gage. This is necessary because the bonding sets faster at slightly elevated temperatures. It is worth noting that the Eastman 910 adhesive is good only for short term applications such as in the investigation presented in this dissertation. For long term applications, epoxy cement with epoxy backed gages is

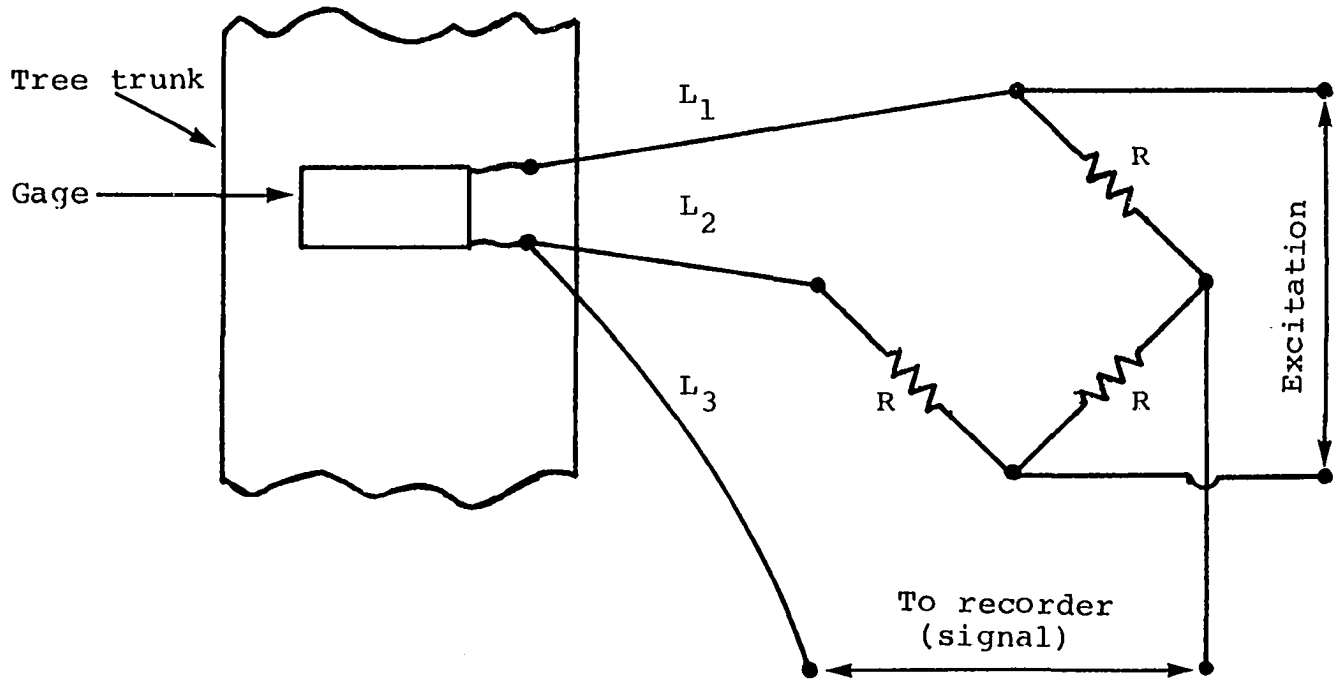

Figure 2. Gage on tree trunk and hooked into a quarter bridge with three lead wires (L_1=L_2=L_3)

a better choice.

From reference 45, the error in strain indication due to angular misalignment of the gage is given by:

$$\varepsilon = \frac{\varepsilon_1 - \varepsilon_2}{2} [\cos 2(\phi \pm \beta) - \cos 2\phi] \quad (3)$$

where

$\varepsilon_1, \varepsilon_2$ = maximum and minimum principal strains, respectively

ϕ = angle between the maximum principal strain axis and the intended axis of strain measurement

β = the angular mounting error between the gage axis after bonding and the intended axis of strain measurement.

For the work on the trees, $\phi = 0$. Therefore, for an angular mounting error of 5°, which is larger than expected, ε works out to be 7.5 $\mu\varepsilon$ or 7.5×10^{-6} for a principal strain difference of 1000 $\mu\varepsilon$ or 1000×10^{-6}. Since great care was taken in aligning the gages horizontally, gage misalignment errors were kept negligible.

According to references 46 and 47, the curvature induced incremental apparent strain is a second order effect which can usually be ignored. This apparent strain is due to the fact that the strain sensitive grid of the gage is above the surface of the bark of the tree by the thickness of the gage backing and adhesive layer.

After bonding the gage to the tree trunk, the quality of the bond is tested by going through the following sequence of simple tests:

1. The gage resistance is checked to ensure that it is as quoted by the manufacturer and that the installation process has not changed the gage.
2. The resistance to earth is checked using an ohmmeter which does not apply too high a voltage capable of causing breakdown of the gage or adhesive. This resistance should normally not be less than 1000 megohms. This check ensures completeness of adhesive cure since the dielectric properties of adhesives are related to their state of polymerization.
3. The presence of air bubble or void in the glue line is checked by connecting the gage to a strain indicator. The face of the gage is then pressed lightly with an eraser. The indicator should record a strain value which disappears when the pressure is removed if there is no air bubble or void in the glue line.
4. To test for creep the gage is hooked into a strain indicator. The tree is then given a gentle bending. If there is no creep of glue line, the indicator will indicate a small bending strain and on release of the bending, the strain indicated

will gradually disappear. This is repeated at the end of each test run to make sure that the glue line did not deteriorate during the test.

Load Cell

Existing methods of measuring transpiration were not satisfactory for the studies presented in this dissertation. The measurement of transpiration by placing dry cobalt chloride paper in contact with the leaf upsets heat transfer by convection, shades leaf on one side, increases humidity between the paper and the leaf and protects the leaf from wind. This method also has no quantitative value. The potometric method is destructive. With a small potted plant, the pot may be sealed with water-proof plastic or aluminum foil and weighed during transpiration. The environment is disturbed in this method.

In order to overcome the limitations mentioned above and assess transpiration of the potted trees accurately, a load cell was designed. Requirements of the load cell are:

1. It should be able to measure weights up to 10 kg (22 lb).
2. The material of the load cell must have a low value for Young's Modulus E, to maximize the strain.

3. The material of the cell must not exceed its elastic limit under the maximum load of 10 kg (22 lb).
4. The cross sectional area of the cell must be small to achieve a high stress and in turn a high strain sensitivity.
5. The cell must be easy and cheap to manufacture yet rugged enough to stand light shocks.
6. It should be simple to use.
7. The material used must have good atmospheric corrosion properties.
8. The cell must have a good long term stability.
9. The cell should be insensitive to temperature and vibrations.

The metal ring type of load cell, Figure 3 was selected. This combines the strength of a loop with the high sensitivity of a small cross sectional area to give a reasonably high sensitivity. Aluminum was selected as the ring material because of its reasonably low value of E and its excellent resistance to corrosion. The cell was constructed out of a 5.08 cm (2 inch) diameter aluminum ring, 0.159 cm. (0.0625 inch) thick and 0.95 cm. (0.375 inch) wide. This type of cell is simple to use, cheap and easy to manufacture.

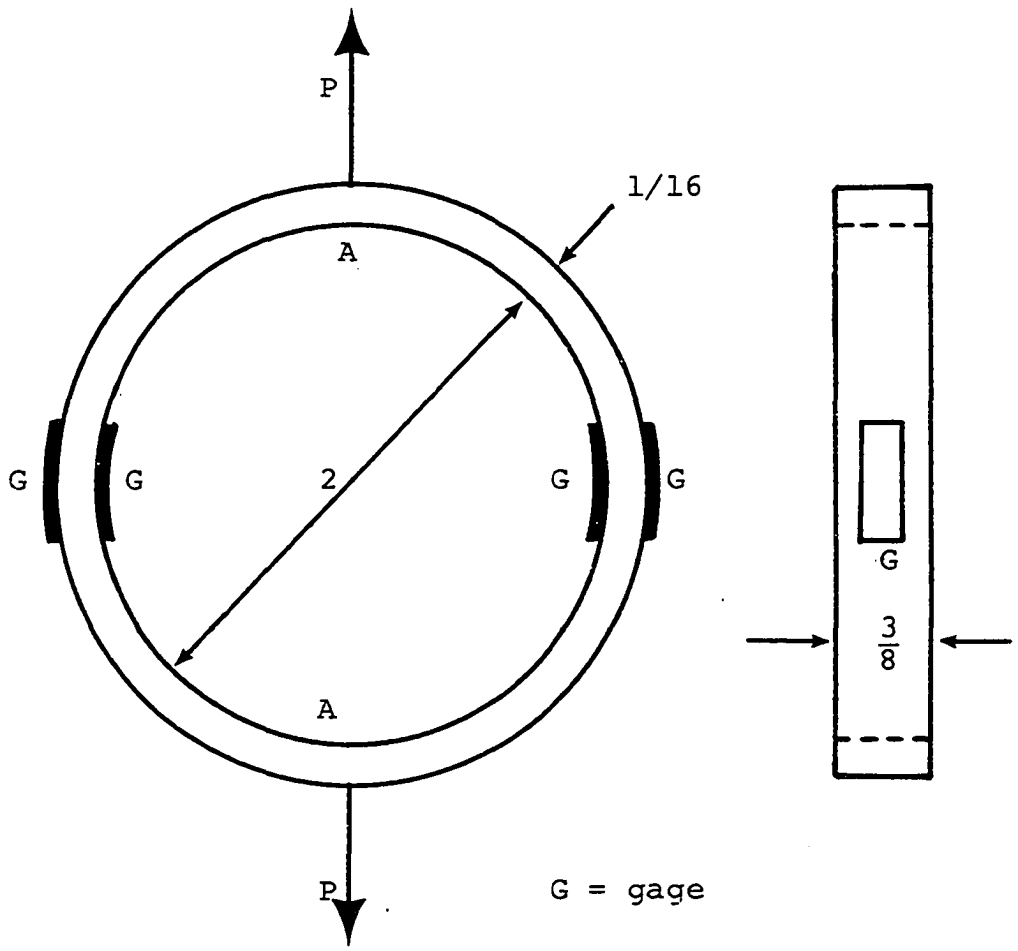

Figure 3. Load cell (dimensions are in inches)

For a ring, it can be found from references 48 and 49 that the moment, M at the gage is given by:

$$M = \frac{PR}{2}\left(1 - \frac{2}{\pi}\right) \qquad (4)$$

where

P = applied load

R = radius of curvature of the ring

∴ For the ring used:

$$M = \frac{10(2.54)(10^{-2})(9.80665)}{2}\left[1 - \frac{2}{\pi}\right]$$

$$= 45.257 \times 10^{-2} \text{ N-m}$$

$$I = \frac{1}{12}(0.95)(0.159)^3 = 32 \times 10^{-13} \text{ m}^4$$

$$\sigma = \frac{P}{A} + \frac{M_y}{I}$$

$$= \frac{10(9.80665)}{(0.95 \times 0.159) \times 10^{-4}} + \frac{45.257(10^{-2})(0.159)10^{-2}}{(32 \times 10^{-13})(2)}$$

$$= 11{,}893 \times 10^4 \text{ N/m}^2$$

The yield stress of the aluminum alloy used is 210×10^6 N/m^2. Thus, the ring will be safe.

The gage used for the load cell was micro-measurements type EA-13-125AD-120 which has a resistance of 120 ± 0.15% ohms. It has a gage factor of 2.09 ± 0.5% at 75°F (24°C). This type of gage is temperature compensated for aluminum. The

four gages on the ring were connected as a full bridge in such a way that temperature compensation could be achieved. The gage chosen is a general purpose family of constantan strain gages widely used in experimental stress analysis. The gage has a 1 mil (0.03 mm) tough, flexible polymide film backing. It can stand a temperature range of -75°C to 175°C (-104°F to 346°F) for continuous use in static measurements and -195°C to 205°C (-318°F to 402°F) for special or short term exposure. The strain limit is 5% for gage lengths of 3.2 mm (0.126 in) and larger.

The gages were mounted as outlined on page 21 with Eastman 910 adhesive. The bond of the mounted gages were tested as before except that the resistance to earth should be greater than 10,000 megohms. The gages were coated to protect them from atmospheric attack. Two lead wires were soldered to each of the gages.

The load cell was then drilled 0.119 cm (3/64 in) at points A, Figure 3, to make it possible to carry suspension wires.

When the gage bonds on the load cell had cured for a day, the cell was loaded in an oven. The temperature was then varied from 10°C to 60°C (50°F to 140°F) to check how good the temperature compensation on the cell was. The graph of apparent strain vs. temperature difference for the cells used is shown in Figure 4. For complete temperature compensation,

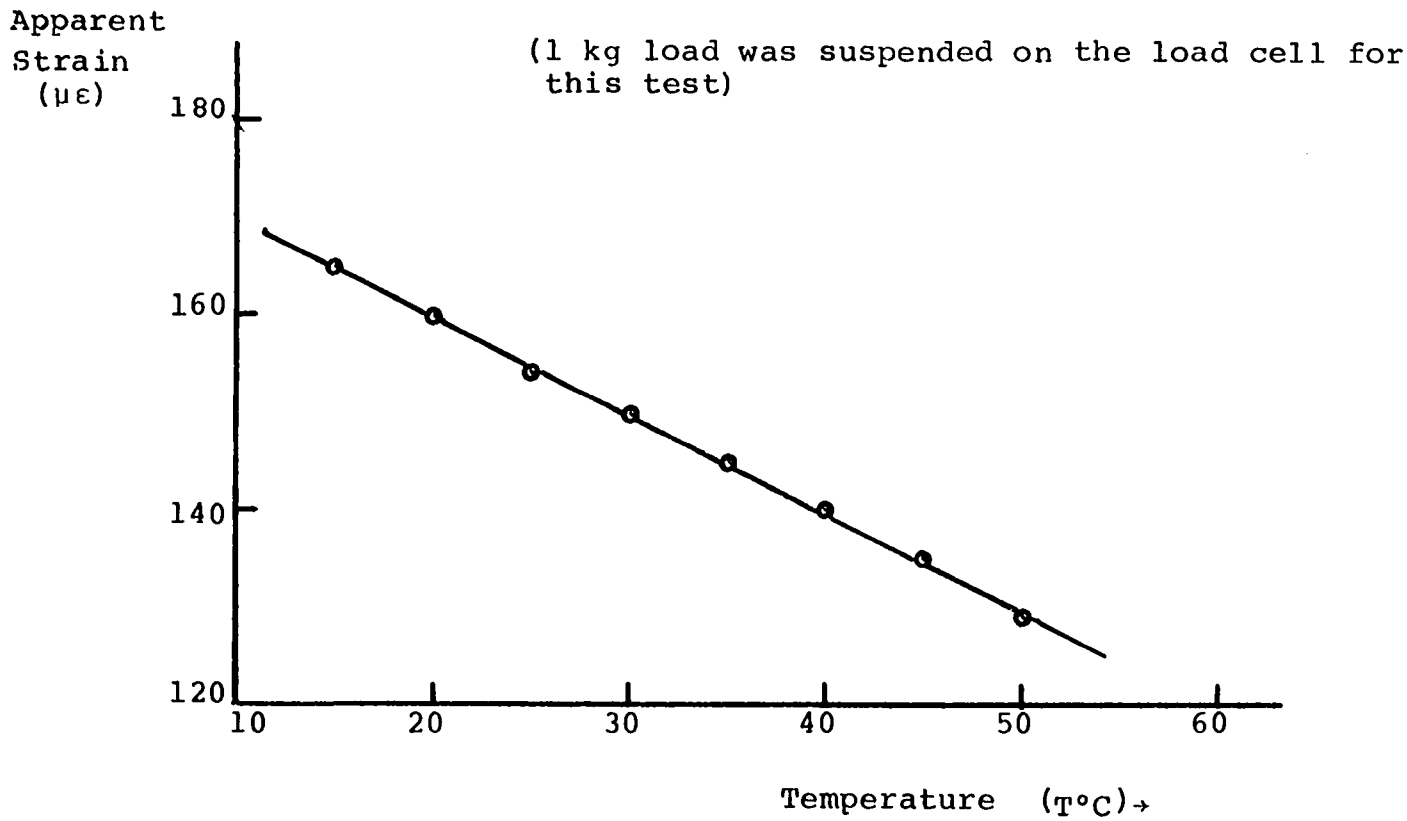

Figure 4. Apparent strain vs. temperature, for load cell

the slope of the graph must be zero. The slope, however, works out to be 1 με/°C. This is negligible for the strain magnitudes expected and the temperature rise used. This small error could be due to unequal lead wire length in or out of the oven.

After this the cell is checked for linearity. This was done by hooking the cell into a strain indicator as a full bridge and loading it with different weights and noting the corresponding strains on the indicator. The linearity curve for the cells used is shown in Figure 5. This curve can also be regarded as a calibration curve.

In order to isolate the cell from outside vibrations, the cell is suspended on a soft spring and the spring is in turn hooked to a rigid support such as a roof rafter.

Recording Instrument

The data was recorded on electrical strip chart recorders. This gives a continuous record of quantities like strain, weight, light and temperature as a function of time on a chart.

Two types of continuous recording were used. One is the Esterline Angus Speed Servo II Model L1102S strip chart recorder. This does not have a wheatstone bridge of its own. It can, however, work with the Vishay Digital Strain Indicator Model P-350A or the Model 520 Digital Strain Indicator

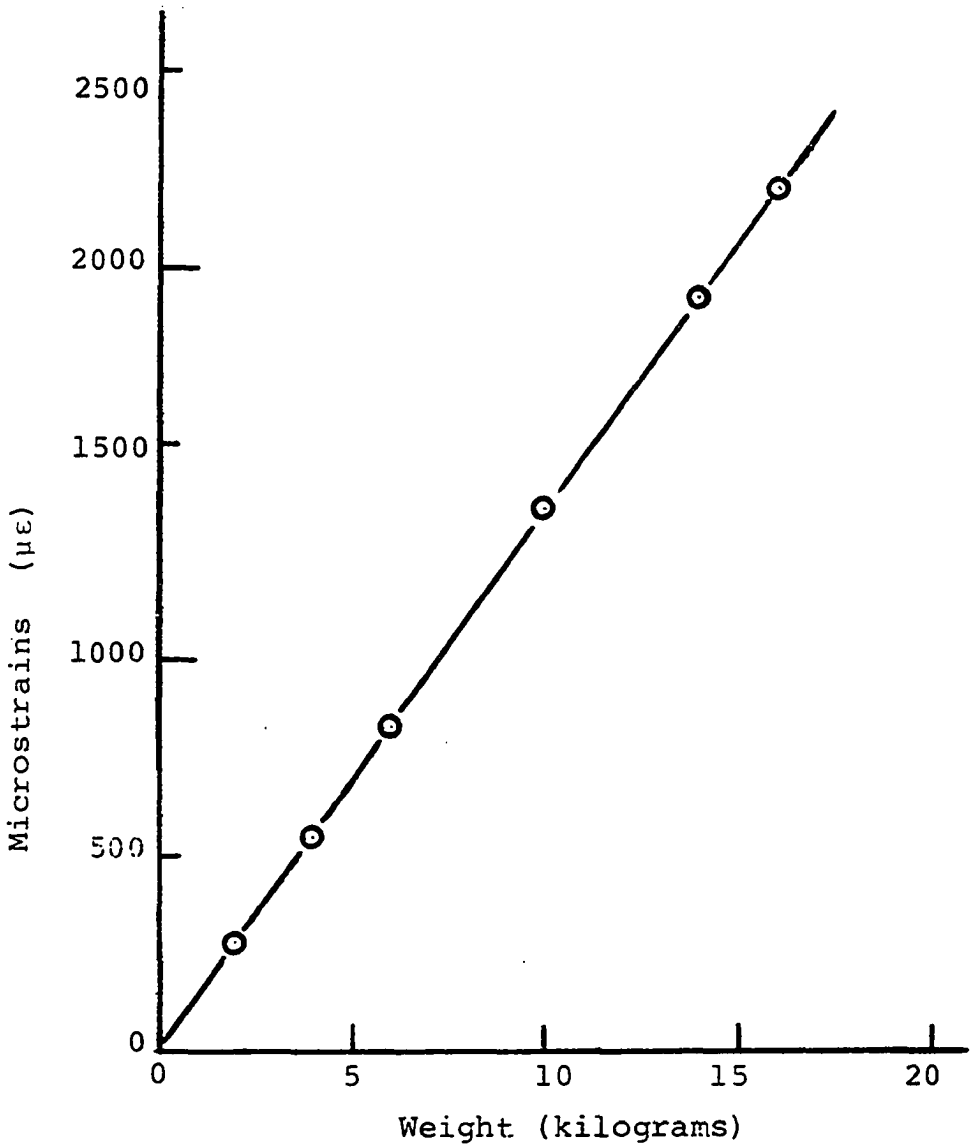

Figure 5. Linearity test for load cell

manufactured by the Northern Technical Services. Both indicators have a wheatstone bridge. They are capable of taking quarter, half or full bridge connections. The strain indicator represents the bridge completion board and amplifier unit which will be referred to later in the other recorder proposed.

Strain indicators

The Vishay strain indicator works on the null balance principle with carrier. It has a 1.5 Volts RMS bridge excitation. By means of the sensitivity control knob, the sensitivity of the meter can be varied by a factor of approximately 100:1. It has a self-contained shunt calibration across internal dummy gages. It is equipped with a 10-turn lock balance knob for zeroing strain prior to load application. It also incorporates an AC transistorized amplifier. The gage factor can be set anywhere from 0.10 to 10.00. This setting is calibrated only from 1.50 to 4.50. The strain range is 0 to 49,999 με. It has a resolution of 2 με. The indicator has an output jack which supplies a DC voltage to the strip chart recorder for recording purposes. When the Vishay indicator is used with the strip chart recorder, it is linear only over 8 inches of chart width.

The model 520 digital strain indicator gives a direct readout of micro-strain. It can display gage factors with a

resolution of 0.001. It accepts quarter, half or full bridge. It is simple to use. The gage factor control is essentially a 10-turn potentiometer giving a gage factor range of 0.5 to 20. The balance knob is a high resolution 10-turn potentiometer internally connected so that it does not load the bridge output. The strain range is 0 to 19,000 με. The bridge excitation voltage is 2.5 volts DC at a gage factor of 2.0. It has a resolution of 1 με. This can be increased with the recorder sensitivity when used in conjunction with the recorder.

Strip chart recorder

The Esterline Angus strip chart recorder operates on a precision null balance servo principle. It has high sensitivity, fast wide-chart response and its operation is interference-free. It is, therefore versatile and reliable. In operation, the instrument graphically displays input analog data on a calibrated 10 inch span of continuous strip chart. It requires a minimum of operator adjustment. It has two recording channels. Each channel features a linear-motion pen motor which is servo-actuated. All operator controls are accessible from the front of the recorder. The instrument needs to be warmed at least 30 minutes before using to record anything. The pen is a simple direct-writing type with a fast response. The chart is driven by a combina-

tion of gear and belt arrangements.

The recorder has a span selector which enables six different spans and six sensitivities to be selected. It has a zero offset. This is capable of suppressing zero from 1 to 10 times span in its -1 through -10 positions. It also elevates zero one full span in its +1 position. There is a 10 turn potentiometer provision for zero positioning between the offset switch steps.

The Vishay strain indicator or the Model 520 digital strain indicator in combination with the strip chart recorder can give sensitivities of the order of 25 με per inch of strip chart paper.

Ten chart speeds are possible with this recorder. The lowest is 1 inch/hour and the highest is 16 inch/minute.

The Gould brush recorder

The other type of recorder used is the Gould 260 recorder. It has six channels. This enables six quantities to be recorded simultaneously. This recorder uses the Brush DC Bridge amplifier Model 13-4312-00. A bridge completion board is provided at the back of the amplifier. The bridge completion board enables the amplifier to take quarter, half or full bridges.

All operator controls of both the amplifier and the recorder are in front of the instruments. A sensi-

tivity knob is provided on the amplifier which enables 5%, 10%, 20%, 50% or 100% of transducer load to be supplied to recorder. A balance knob is provided for bridge balancing. The amplifier features a zero signal positioning knob. It also has a ten turn counting dial which enables the gage factor of a strain gage to be set.

Each channel on the recorder has a sensitivity dial which allows sensitivity settings of 1, 2, 5, 10, 20, 50, 100, 200, 500 millivolts/division and 1, 2, 5 and 10 volts/div. Four push buttons and a millimeter per minute/millimeter per second switch enables eight chart speeds to be selected. The chart speed varies from 1 millimeter per minute to 125 millimeters per second.

The inking system is pressurized. It produces smudge-proof traces which are of uniform width at any pen velocity. Each channel width is 40 mm and there are 50 divisions per channel. This recorder can record more items compared with the strip chart recorder. It, however, requires a little more attention due to the narrowness of the channels.

Temperature Measurement

The temperature range in which the trees under observation grow is about 50°F to 90°F (10°C to 32.2°C). Copper vs. constantan thermocouple was used in measuring temperatures of

trees and ambient. The temperature range of this thermocouple is from sub-zero to an upper limit of about 700°F (371°C). This is more than adequate for the temperature range in which the trees grow.

Among the factors to be considered in making a thermocouple are the maximum service temperature and the required response time of the probe. A small diameter thermocouple has a faster response than a heavier diameter thermocouple, but its service temperature and life are correspondingly lower. Thus, for short term applications, it is advisable to use small diameter wires while for long term applications, it is better to use heavier diameter wires. With these in mind and the fact that the medium of submersion for the thermocouple is air, a 0.01 inch diameter wire was used for the thermocouple. This has a time constant of 1.0 sec in still air. The copper and constantan junctions are fused together by means of an oxyacetylene flame.

The thermocouple output is 0.04 mV/°C. Therefore, the output can be fed to a recorder after amplification to obtain a continuous temperature recording.

Light Measurement

Light measurements were made with the Lambda LI-185 radiometer. This is a precision instrument designed to function over a wide dynamic range. It gives a direct readout

with excellent linearity from Lambda photometric sensor, LI-210S. The instrument features a chopper stabilized amplifier for automatic zeroing. The high gain of the amplifier gives an extremely low impedance load to the silicon sensors resulting in excellent linearity from the sensors. The meter can be used to measure as low as 3 millivolts full scale with 1% accuracy from low impedance sources such as thermocouples. The LI-210S photometric sensor features a cosine corrected response and a filtered silicon photodiode which provides a high degree of stability.

The instrument has a sensitivity of 10 millivolts per 10^4 micro-einsteins $m^{-2}s^{-1}$ (1 micro-einsteins $m^{-2}s^{-1}$ = 0.1 watts m^{-2} = 10 lux) when used with a 200 ohm resistor. It has a maximum linearity deviation of 1% up to 10^4 micro-einsteins/m^2s. The change in stability is less than 2% over one year period. It has a response time of 10 micro-seconds and readings can vary by $\pm$ 0.15%/°C maximum.

A 1 K-ohm resistor in series with the meter provides a 0 to 100 millivolt recorder output. Hence the output of the meter in millivolts can be fed into a recorder for recording purposes.

Instrumentation Hook-up

Strain gages on trees were connected by the three lead wire method to minimize lead wire errors. They were hooked as a single arm wheatstone bridge. For the Vishay strain indicator, the bridge is completed by 120 ohm resistors. In the Brush six channel recorder arrangement, the bridge is also completed on a bridge completion board with 120 ohm resistors. In such situations where resistors are needed to complete the bridge, hermetically sealed resistors are recommended instead of plastic encapsulated resistors since the latter drifts with time (50), due to moisture absorption. The three wire hook up for the Vishay strain indicator the model 520 strain indicator and the Brush recorder system are shown in Figure 6a, Figure 7a and Figure 8a, respectively.

The load cells were hooked up as a full bridge. The hook up diagrams for the Vishay strain indicator, the model 520 strain indicator and Brush recorder are as shown in Figure 6b, Figure 7b and Figure 8b, respectively.

For light and temperature recordings, the Vishay strain indicator and the bridge completion board for the Brush DC bridge amplifier are eliminated from the instrumentation. The voltage output from the light meter or thermocouple can be connected directly to the strip chart recorder which can

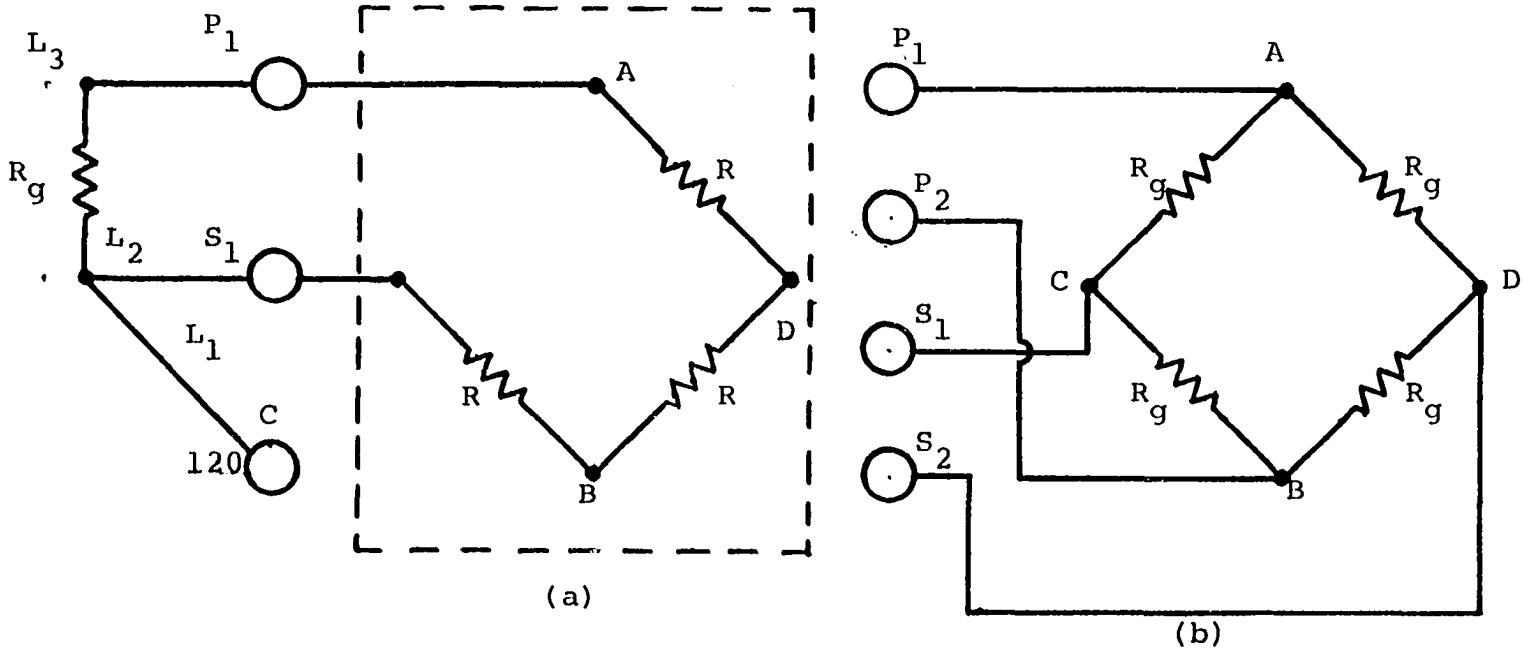

Figure 6. Connection for the Vishay indicator
(a) Quarter bridge connection for the Vishay indicator. Excitation is across AB. Signal is across CD ($L_1=L_2=L_3$). (b) Full bridge connection for the Vishay indicator. Excitation is across AB. Signal is across CD

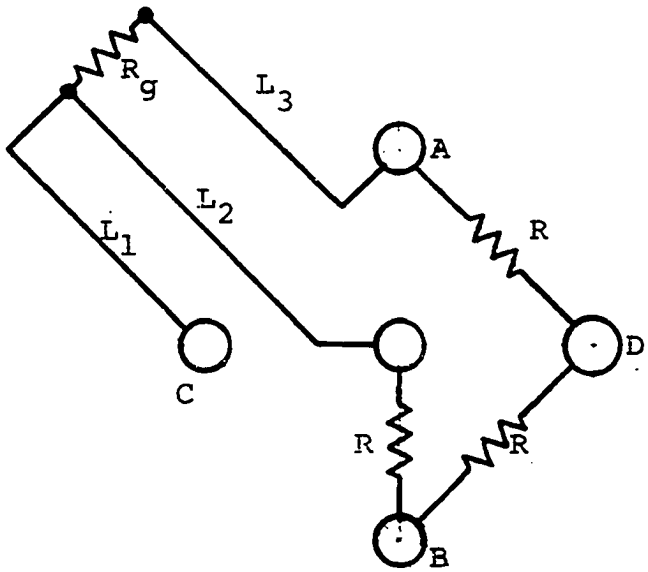

Figure 7a. Quarter bridge connection for the model 520 digital strain indicator. Excitation is across AB. Signal is across CD (L_1=L_2=L_3)

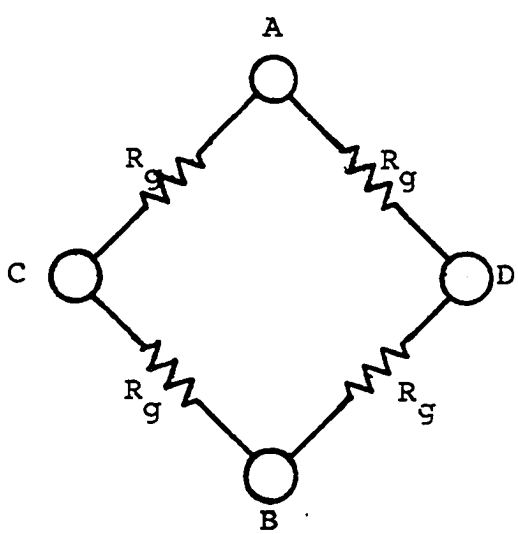

Figure 7b. Full bridge connection for the model 520 digital strain indicator. Excitation is across AB. Signal is across CD

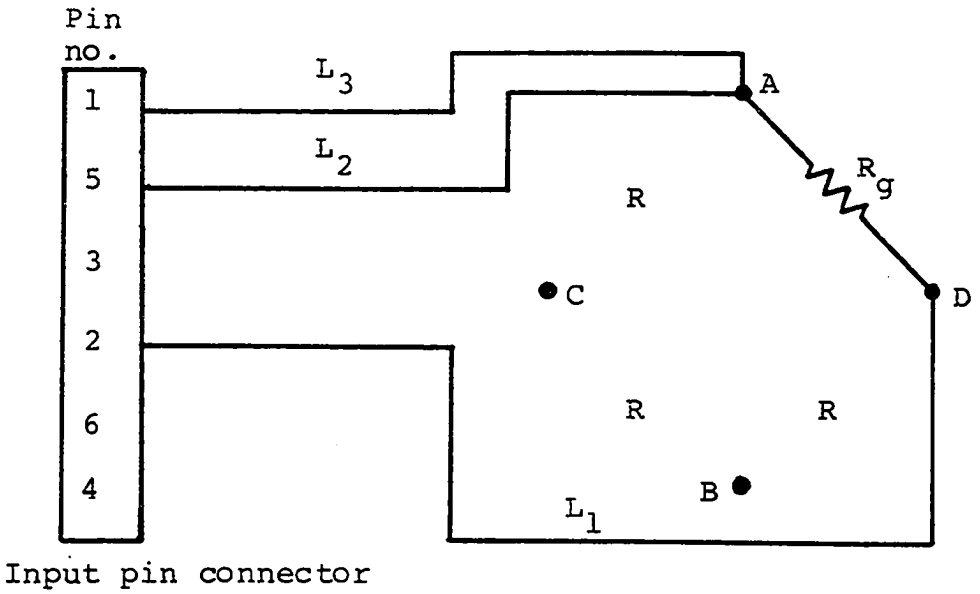

Figure 8a. Quarter bridge connection for Brush amplifier and recorder system. Excitation is across AB. Signal is across CD (L_1=L_2=L_3)

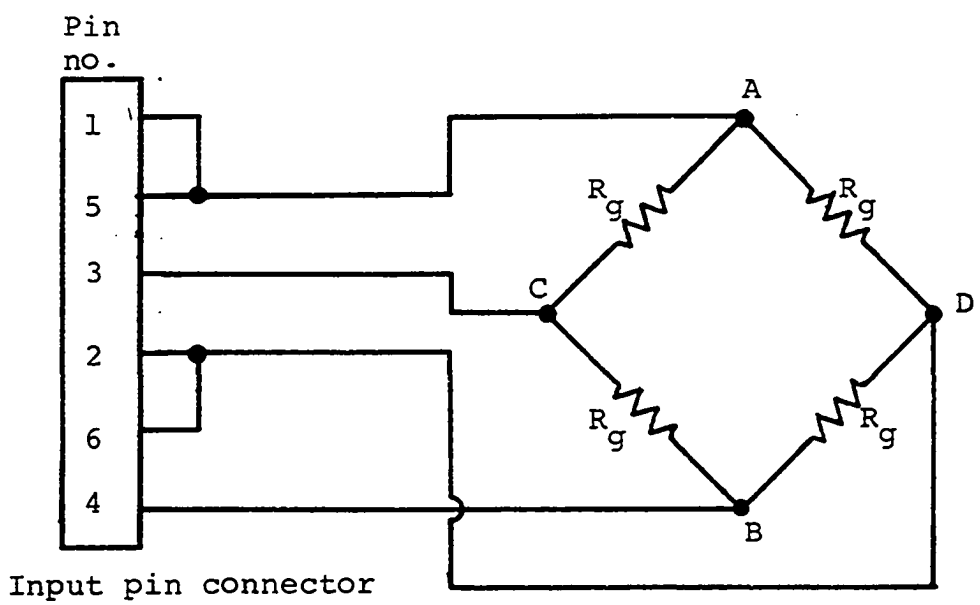

Figure 8b. Full bridge connection for Brush amplifier and recorder system. Excitation is across AB. Signal is across CD

amplify and record the signal. The light meter or thermocouple outputs can also be connected to the input of the Brush DC bridge amplifier (with the bridge completion board removed) for amplification and recording by the Brush recorder.

For light recordings, the photometric sensor is mounted in the tree half way between the top and the bottom of the canopy.

For temperature measurements, thermocouples are taped as close to the gages on the trees as possible and on the same side of the tree as the gage. The other junction of the thermocouple is kept in a mixture of ice and water. In ambient temperature measurements, the hot junction of the thermocouple is kept close to the canopy.

At the beginning of every experiment, it is advisable to balance strain gage and load cell bridges.

Calibration

In any calibration technique, one must select a body or system for which the theoretical distribution of the quantity to be measured is accurately known. A thermometer can be calibrated against a thermocouple and vice versa. A photoelastic stress distribution can be calibrated against a circular plate model or a tensile model. A brittle coat can be calibrated against a tensile model. In the case of a

transducer, a complete calibration usually involves the determination of environmental effects on sensitivity and behavior. In the case of the load cell (which is a transducer) the gages were coated to protect them against atmospheric humidity. They were hooked into a full bridge to compensate for temperature. The only environmental effect is temperature changes when direct light rays hit a single gage. This difficulty is overcome by shielding the load cells from direct light rays with aluminum foil.

Gages on the trees were calibrated by the usual shunt calibration technique. In this method, a high quality known resistor is connected in parallel with the gage and a known change in strain is effected. For example, a 60 K-ohm resistor shunted across a 120 ohm gage gives a strain reading of 998 με (998×10^{-6}). A 120 K-ohm shunt resistor gives 499.5 με (499.5×10^{-6}). According to Troke (51) it makes a difference as to whether tensile or compressive strain is being calibrated. The expression for the apparent strain is:

$$\varepsilon_a = \frac{R_g}{G(R_s+R_g)} \tag{5}$$

for calibration of compressive strain and

$$\varepsilon_a = \frac{R_g}{G(R_s)} \tag{6}$$

for calibration of tensile strain where:

R_g = resistance of gage

R_s = shunt resistor

G = gage factor of gage

The shunt calibration is also discussed in references 3, 4 and 44. All the gages used had a gage factor of approximately 2 because the gage factor of such gages is unchanged by strains even in the plastic region (3, 52).

The load cells were calibrated by putting various known weights in the pot of the potted tree. The corresponding deflection on the recording chart is noted. This deflection could be changed to any convenient value using the recorder sensitivity. The weights used were 100 gm, 500 gm, 1000 gm and 1500 gm. In this way, the linearity of the calibration could also be checked.

The thermocouples were calibrated against a thermometer. The hot junction of the thermocouple and the thermometer were dipped into water at various temperatures and the chart readings were noted. The readings on the chart could be changed to a convenient value by means of the sensitivity on the recorder. The water temperatures commonly used were 0°C, 20°C, 30°C, 40°C and 50°C (32°F, 68°F, 86°F, 105°F and 122°F).

The light meter was calibrated against the scale provided on the meter.

EXPERIMENT AND DATA ACQUISITION

Preamble

Most of the results on water stress studies cited in the literature review, have superimposed on them the effects of ambient conditions such as light, temperature, humidity, carbon dioxide content of the air and in the case of field studies, wind. The way ambient conditions effect water stress studies is therefore important since trees undergo various ambient conditions at different stages of their lives. The experiments performed in this study, look at what happens to young trees of a populus clone as the temperature and light vary simultaneously. Constant temperature and constant light levels were investigated. This is not exactly what happens in practice. But the complexity of the variations of these ambient conditions makes it difficult to consider the practical case now. The experimental results, therefore, provide a model which can, as a first stage approximation, be applied to such young trees.

Preliminary studies revealed that gages mounted vertically on the trunk could not compensate for temperature. This is due to the fact that the vertical gage responded physiologically too. The horizontal gage responded to a larger degree compared to the vertical gage. This anomaly may be due to the fact that wood is anisotropic both mechanically and

thermally. For a live tree, the degree of hydration can complicate the anisotropic problem considerably. Thus, temperature compensation could not be achieved in the conventional way of using a dummy gage. To overcome this difficulty, mounted gages were covered with cotton wool. The cotton wool was in turn covered with aluminum foil to reflect light away from the gage vicinity. This stabilized the temperature around the gage and reduced the temperature effect to a negligible amount.

Tree Preparation

The study was conducted on young trees of the populus clone 5377 (also known as Wisconsin 5). The trees were grown under greenhouse conditions in two gallon capacity black, plastic nursery containers. The containers had drain holes at the base. The drain holes were covered with bronze wire gauze to prevent the roots of the trees from growing out of the container.

The plastic containers were filled about 2/3 full with soilless mix. This mix was composed of 2/3 Jiffy mix and 1/3 Perlite by volume mixed with Mag-Amp (Magnesium Ammonium Phosphate) slow release fertilizer: NPK in the ratio 7:40:6 by weight. The phosphorus was largest in weight because it is a good starter for growth and root formation. The Jiffy

mix comprises 1/2 Vermiculite and 1/2 milled sphagnum peat by volume. This is a normal mix for greenhouse growth.

The propagation technique used utilized the intermittent mist system for rooting softwood tip cuttings. The trees took two weeks to root and they went through one to two weeks hardening (weaning from mist).

In addition to the initial Mag-Amp fertilizer, the trees had a twice weekly irrigation with Peters water soluble NPK in the ratio 20:20:20 by weight. The concentration of the components of the fertilizer was N: 100 ppm, P: 44 ppm and K: 84 ppm. Periodically (every two weeks), chelated iron (FeEDTA) of 5 ppm concentration was given to the trees. Watering was done on as needed basis depending on the weather, tree size and humidity conditions. At any watering time, all the trees were watered.

The trees went through such preparation and treatment for about four months before tests were run on them.

Growth Chamber

The growth chamber used in the investigation was the Percival Phytotron 80 which measures 66 inches (168 cm) in length by 30 inches (76.2 cm) in width by 50 inches (127 cm) in height inside. It is constructed of welded steel insulated with 2 inches (5 cm) of fiberglass with a 1 inch diameter floor drain. It has 14 sq ft (1.3 m^2) of working area. It

is provided with a 30 in by 48 in (76.2 cm x 122 cm) door the edges of which is provided with magnetic gasket for positive air seal. The door has a 12 in by 12 in (30 cm x 30 cm) light-tight, covered observation window. The chamber is shown in Figure 9a.

The chamber is equipped with 16 fluorescent lamps (340 micro-einsteins $m^{-2}s^{-1}$) and ten 100W incandescent lamps (60 micro-einsteins $m^{-2}s^{-1}$). These lights are automatically programmed by three 24 hour time clocks. The first controls all the fluorescent lights. The second controls half the fluorescent lights. The third controls the incandescent lights. This enables five light settings to be achieved in the chamber. Further light setting can be achieved by removing some bulbs. The lamps are separated from the environmental chamber by a removable translucent diffusing barrier. The lights are cooled by filtered ambient air.

Heating within the chamber is done through two 300 watt heater strips. Achievable temperature range is 40°F to 110°F (4°C to 44°C) $\pm$ 2°F with dual set points and 24 hour time clock for diurnal cycle.

The chamber is maintained at a temperature uniformity of $\pm$ 1°F in any horizontal plane. This is achieved by diffusing conditioned air gently into the bottom of the controlled area and drawing off at the top, on both sides, by a balanced system of dual air handlers. The air is

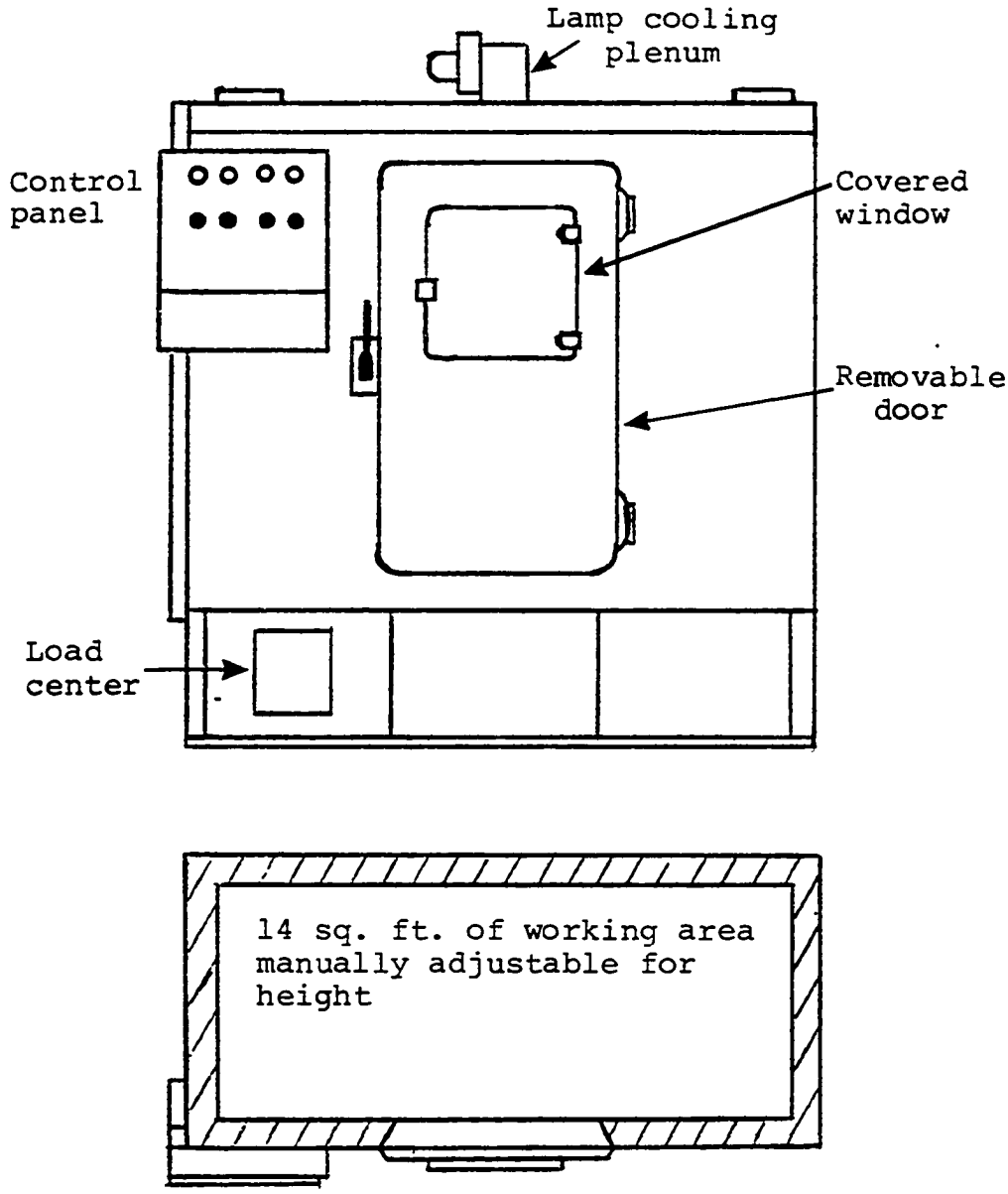

Figure 9a. Growth chamber

recirculated through dual air handlers which contain the evaporator coils, heaters, fans, drip pans and other mechanical components. This forced recirculation dissipates heat produced by the radiant energy of the lamps without causing drafts. This is adjustable from 0 to 20 air changes per hour. Thus, the air circulating through the chamber is the medium by which the temperature of the objects in the chamber is controlled.

Fans located at the top of the air duct, Figure 9b, in each end of the chamber draw the air from the top and move it down through the ducts containing heaters and cooling coils. This adds to or removes heat from the air as required to maintain the desired temperature in the chamber. The air enters the chamber at the floor through a distributor. The distributor breaks up the air stream and directs the air evenly distributed from the floor upward through the bench to the ceiling.

The exhaust ports are located to draw off air at the highest level. This will also be the air with the highest absolute humidity. Consequently, the highest relative humidity is obtained with the ports closed so that humid air inside is not replaced with dryer outside air.

The air intake slide is used in conjunction with the exhaust slide to permit outside air to replace the air exhausted. About ten changes per hour can be obtained. This

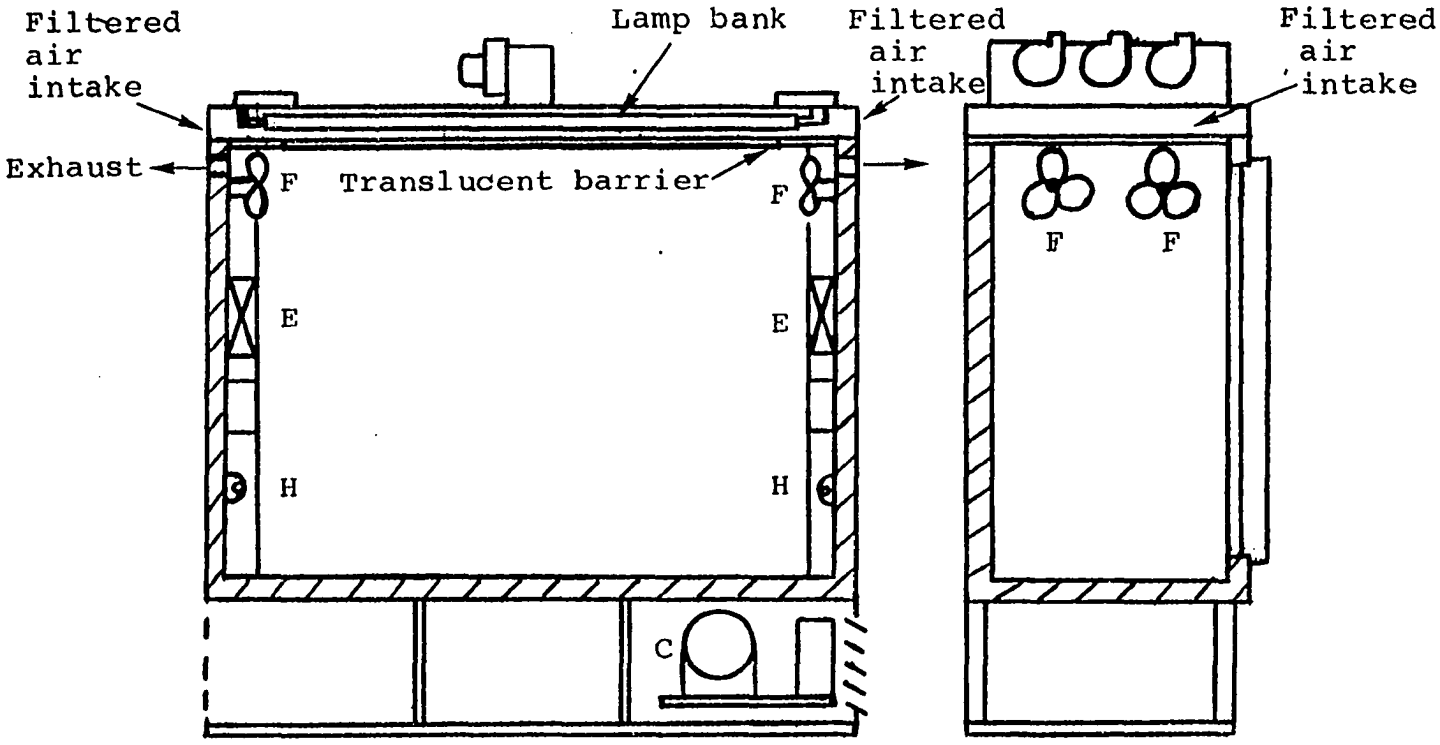

Figure 9b. Sectional view of growth chamber (F = fan, E = evaporator coil, H = heater strip, C = condensing unit)

quantity, however, is rarely necessary since the air change rate is usually dependent on temperature and humidity of the ambient versus the laboratory conditions required and the load.

Refrigeration is provided by a conventional refrigeration system. It comprises a hermetically sealed motor and compressor, a condenser, receiver, dryer, pressure limiting expansion valve and evaporator.

Relative humidity is normally 50% to 70% subject to temperature in the environmental chamber and the nature of the experiment.

Test Procedure

After four months of greenhouse growth, two of the trees were selected and their stems were bonded with gages using M-Bond 200 adhesive. The gage was bonded 6 inches (15 cm) above the soilless mix on the stem. The bonding procedure on page 21 was used. The trees were selected in a statistically random manner to eliminate biasness in results. Forty trees were provided for the investigation. These were numbered 1 to 40. Forty papers also numbered 1 to 40 were put in a bag and given a shake. Two of the papers in the bag were picked at random. The trees with the same numbers as those on the papers picked were selected for one set of test run. All pairs of trees were selected in the

same manner for the various test runs. The stem diameters at the location of the gage for all the trees were measured with calipers before each test run.

A suspension structure for the potted trees was made out of three 1/2 inch (1.27 cm) diameter aluminum rods of lengths 2 ft, 2 ft and 5 ft (61 cm, 61 cm and 152 cm) as shown in Figure 10. The rods were fastened together at A and B by means of Lee Lattice connectors. The structure was set on four supports at C, D, E and F in the growth chamber. The supports were 4 ft (122 cm) from the chamber floor.

The plastic pots carrying the trees were drilled on the sides with 3/16 in (0.476 cm) drill in order to carry two 3/16 in (0.476 cm) diameter steel rods for suspension purposes. Each of the steel rods was 2 ft (61 cm) in length. Four such holes were drilled. Two of the holes were opposite each other and the other two were opposite each other. The center line of any two opposite holes was roughly at right angles to the center line of the other two opposite holes. Two holes opposite each other were made about 1 cm (0.39 in) above or below the other two. This ensures that the axes of the steel rods did not coincide.

Two small steel cylinders measuring 3/16 in (0.476 cm) in diameter by 0.5 in (1.27 cm) in length were cut out of a 3/16 in (0.476 cm) diameter rod. The cylinders were drilled 0.047 in (0.119 cm) at the mid-point along the center line

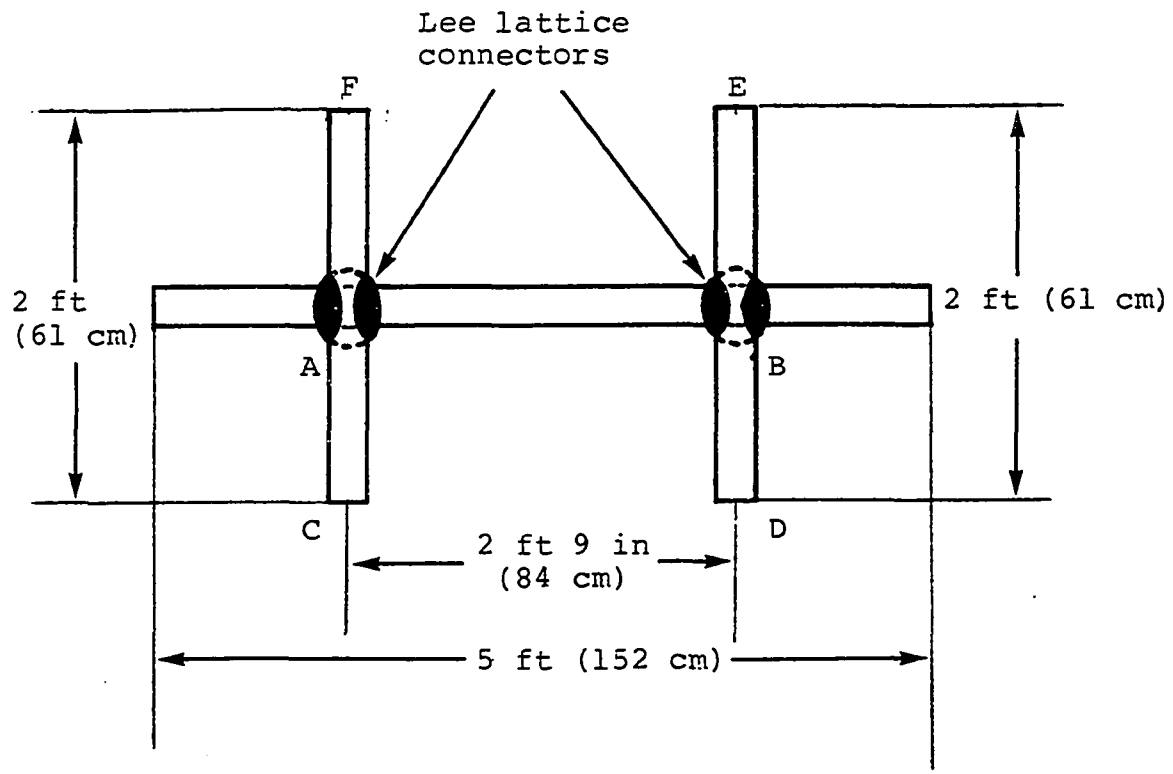

Figure 10. Suspension structure for potted tree (rods are of 1/2 inch (1.27 cm) diameter)

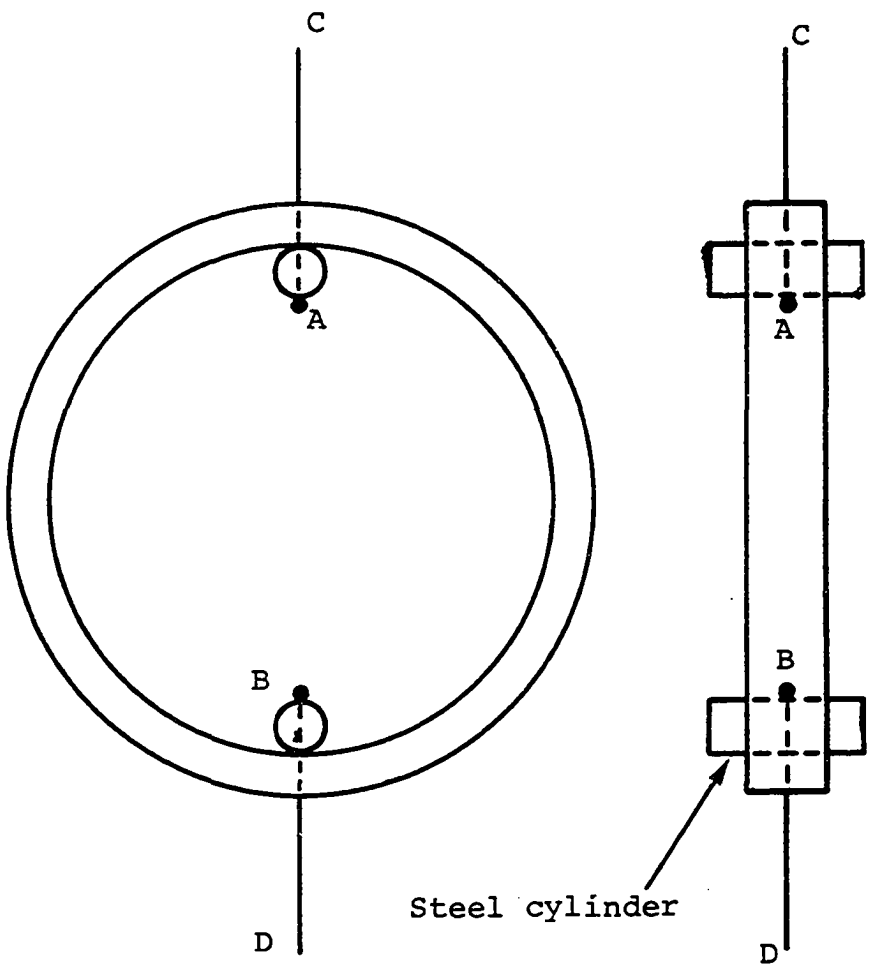

Figure 11. Load cell with suspension wires: AC and BD are steel

of the cross section. The small cylinders were set in the load cell as in Figure 11, such that the 0.047 in (0.119 cm) holes in the ring and the cylinders coincided. Two 3/64 in (0.119 cm) diameter steel wires were pushed through the holes in the cylinder and load cell. The arrangement was soldered at A and B (Figure 10). The arrangement made it possible for the load cell to be suspended from the aluminum frame structure by coiling the wire AC (Figure 11) around the bar AB (Figure 10). The potted trees were suspended from a loop at the lower end of wire BD (Figure 11). This was done by connecting four polyester chords from each end of the 3/16 inch (0.476 cm) diameter steel rods in the pot to the loop. The assembled system is shown in Figures 12a and 12b. The system was assembled out of the growth chamber in Figure 12b in order to accommodate all the instruments.

The gages and load cells were hooked up as outlined on page 40 to the brush recorder and amplifier system. Another set of two trees under different light and temperature combination was put in a second chamber. This second set was hooked to the Esterline Angus strip chart recorder through the strain indicators. There were two trees per chamber. Each such two trees were subjected to the same ambient conditions. A light meter and a thermo-hydrograph were placed in each chamber during the tests to give a recording of the light

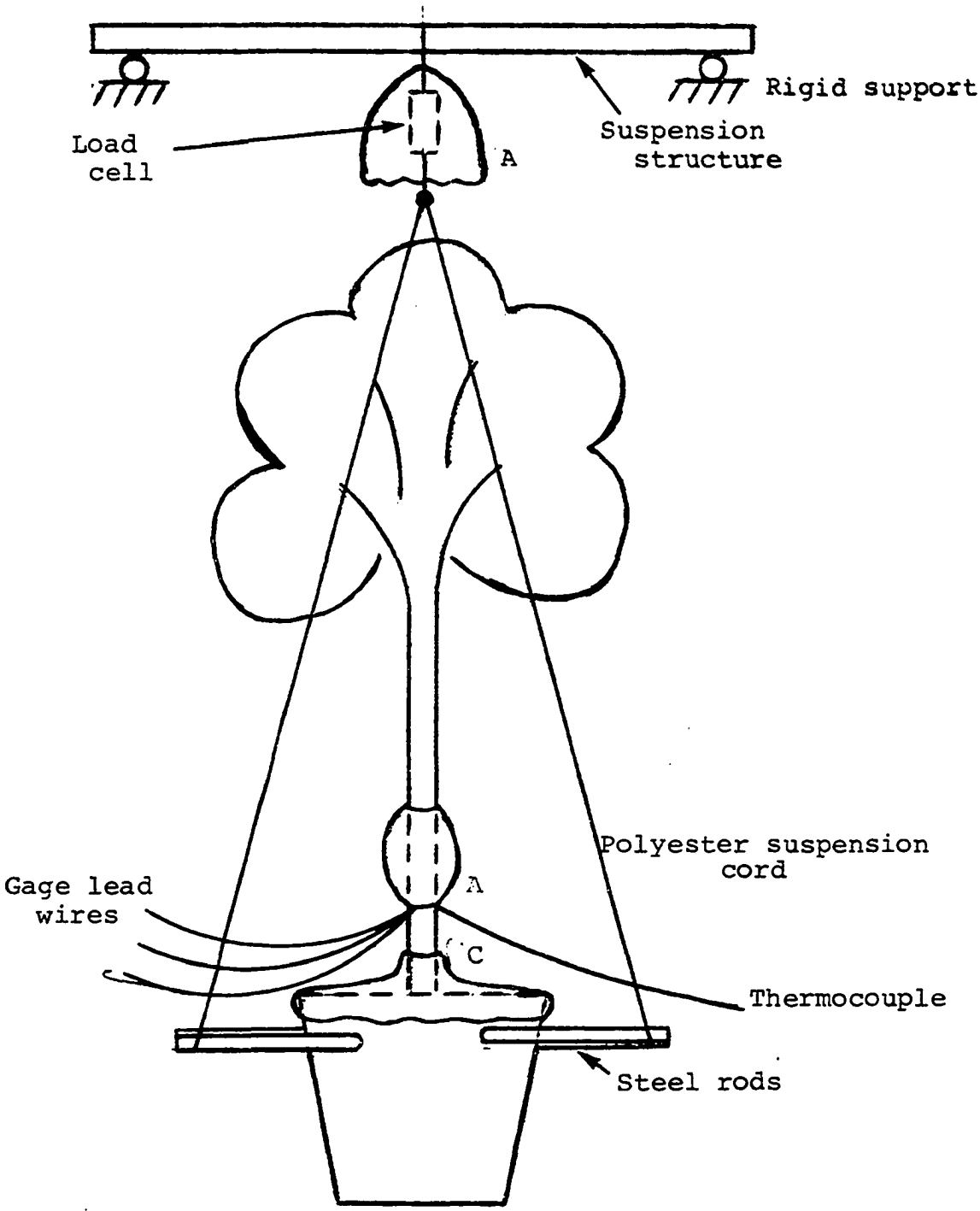

Figure 12a. Assembled test tree (A = aluminum foil cover to shield gages from direct radiant heat, C = aluminum foil cover over pot to reduce evaporation)

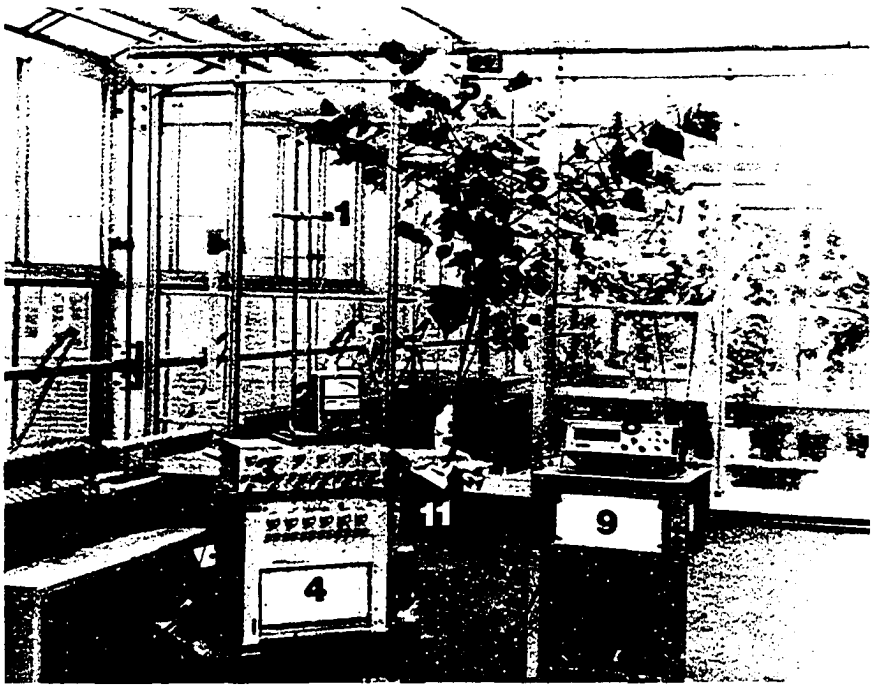

1 LIGHT SENSOR

2 LIGHT METER

3 BRUSH AMPLIFIERS

4 BRUSH RECORDER

5 LOAD CELL SHIELDED WITH ALUMINUM FOIL

6 TEST TREE

7 STRAIN GAGE AND THERMOCOUPLE SHIELDED WITH ALUMINUM FOIL

8 STRAIN INDICATOR

9 ESTERLINE ANGUS STRIP CHART RECORDER

10 ICE POINT

11 PLASTIC POT COVERED WITH ALUMINUM FOIL

Fig. 12b. Assembled test tree with instrumentation

level, the temperature and the relative humidity in the chamber. A copper-constantan thermocouple was put on the bark of one of the trees. This gave a continuous recording of the tree temperature on hooking into the recorder.

The pots were covered with aluminum foil. This reduced the amount of water loss due to evaporation from the surface of the soilless mix to negligibility. The amount of evaporation from the surface of the soilless mix in an uncovered pot will normally depend on the ambient conditions. On a normal sunny day, the amount lost from a surface of 350 cm^2 (55 in^2) (which is equal to the surface area of the soilless mix used in the test runs) is 120 gm per day. A covered pot placed in the growth chamber did not loose weight for a day. An uncovered pot in the chamber under the conditions for R_{33} lost 80 gm of water per day. The load cell was also covered with aluminum foil. The aluminum foil shaded the cell from the direct rays of the light bulbs. This was necessary because when the light rays hit one of the gages directly, the temperature compensation of the cells was not complete.

Each set of two trees experienced 18 hours of day and 8 hours of darkness. Daytime was initiated by simultaneously and automatically switching on the lights and the heaters in the growth chamber. Night was established by simultaneously and automatically switching off the lights and the heaters.

All day temperatures were 15°F (8.3°C) above their respective night temperatures. This difference is close to optimum for good plant growth. Darkness started 11 hours after watering and lasted for 8 hours. Watering was done 5 hours after the light and temperature come on. Each set of two trees was run for two days in the growth chamber to acclimatize it. It was then test run for four days. The trees were watered to field capacity at 24 hour intervals. The circumferential strain, weight lost by potted tree or transpiration of potted tree, tree bark temperature and light were recorded continuously on strip chart recorders. At each watering, the load cell recording on the chart was zeroed. The loss in weight or the transpiration of the potted tree was recorded on the chart.

The four levels of day temperatures used were 85°F (29.4°C), 75°F (23.9°C), 65°F (18.3°C) and 55°F (12.8°C). The corresponding night temperatures were 70°F (20.1°C), 60°F (15.6°C), 50°F (10°C) and 40°F (4.4°C). The four light levels used were 26, 100, 180 and 330 micro-einsteins $m^{-2}s^{-1}$.

Each of the four temperature levels was combined with each of the four light levels for the runs. Hence, there was a total of sixteen runs, and there were two trees per run.

The calibration of the gages and load cells follow those

outlined in the section on calibration, page 44.

At the end of each run, the length of each leaf was measured. The maximum width at right angles to the length of each leaf was also measured. These measurements were used to evaluate the leaf areas of the trees as outlined later.

The temperature combinations, light levels and runs made are as symbolized and explained below:

T_1 First temperature combination level - 55°F day (12.8°C); 40°F night (4.4°C)

T_2 Second temperature combination level - 65°F day (18.3°C); 50°F night (10°C)

T_3 Third temperature combination level - 75°F day (23.9°C); 60°F night (15.6°C)

T_4 Fourth temperature combination level - 85°F day (29.4°C); 70°F night (21.1°C)

L_1 First light level - 26 micro-einsteins $m^{-2}s^{-1}$

L_2 Second light level - 100 micro-einsteins $m^{-2}s^{-1}$

L_3 Third light level - 180 micro-einsteins $m^{-2}s^{-1}$

L_4 Fourth light level - 330 micro-einsteins $m^{-2}s^{-1}$

R_{ab} Run at a^{th} temperature combination level and b^{th} light level, where a = 1,2,3,4 and b = 1,2,3,4

To make the water loss or transpiration of the trees more meaningful for comparison purposes, the transpiration of each tree was reduced to transpiration per unit leaf area basis. The leaf area of each tree was calculated from Zuuring's (53) model:

$$\text{LEAF AREA} = a + b(LW) + c(W^2) \qquad (7)$$

for the populus clone used in the investigation. In Equation 7,

L = length of leaf (cm), (Figure 13)

W = maximum width (cm) at right angles to the length (Figure 13)

a = 1.26054

b = 0.21245

c = 0.36252

The total leaf area of each tree was then found by adding the areas of each leaf on the tree. The number of leaves on a tree varied from a low of 20 to a high of 105. The total leaf areas ranged from 1735 cm^2 to 5026 cm^2.

When the temperature changes, the tree reacts both physiologically and thermally. The gage senses both reactions of the tree. In order to have a feel of how much of the changes in the tree and the gage is physiological and how much is thermal, two temperature tests were run.

One test was run in the growth chamber along with run R_{33}. A gage was bonded to the stem of one of the test trees. The gage was wired with three lead wires. The trunk of the tree was cut 5 cm (1.97 in) above and below the gage. The cut ends of the piece of the stem was quickly coated with paraffin wax to seal it from absorbing or giving out moisture. The piece was placed in the growth chamber together with the regular test tree for R_{33}. The gage was hooked to the brush

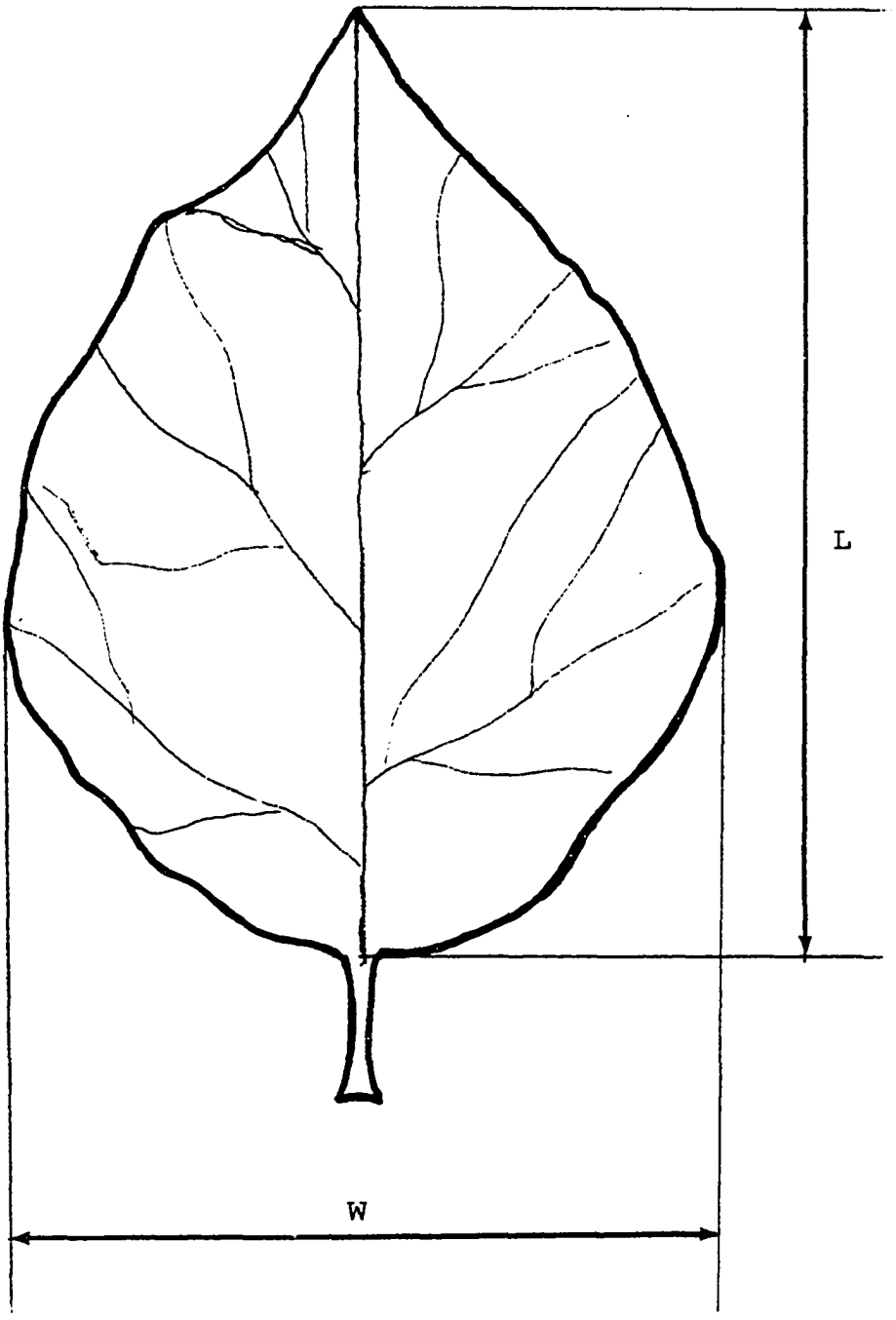

Figure 13. Typical leaf of populus clone

recorder through the amplifier.

This experiment revealed that when the light and temperature change from day conditions to night conditions, the live tree (R_{33}) expands while the severed piece of trunk contracts (Figure 14). Similarly, when the light and the temperature change from night conditions to day conditions, the live tree contracts while the chopped tree expands (Figure 15). This leads to the conclusion that the expansion of the live tree as recorded on the chart is less than the actual expansion by the amount that the severed piece expanded. Similarly, the actual contraction of the live tree is higher than what is recorded on the chart by the amount the severed piece contracted.

From Figure 14, when the lights shut off and the temperature reduces by 15°F (8.3°C), the live tree expands 250 με and the dummy piece contracts 102 με. The actual expansion on the live tree can therefore be approximated to 352 με. From Figure 15, when the lights come on and the temperature increases by 15°F (8.3°C), the live tree contracts 250 με and the chopped tree expands 100 με. The actual contraction on the live tree is thus 350 με. Thus the thermal expansion or contraction was approximately 12.3 με/°C.

In another experiment, two horizontal gages and two vertical gages were bonded to the trunk of a tree. The two

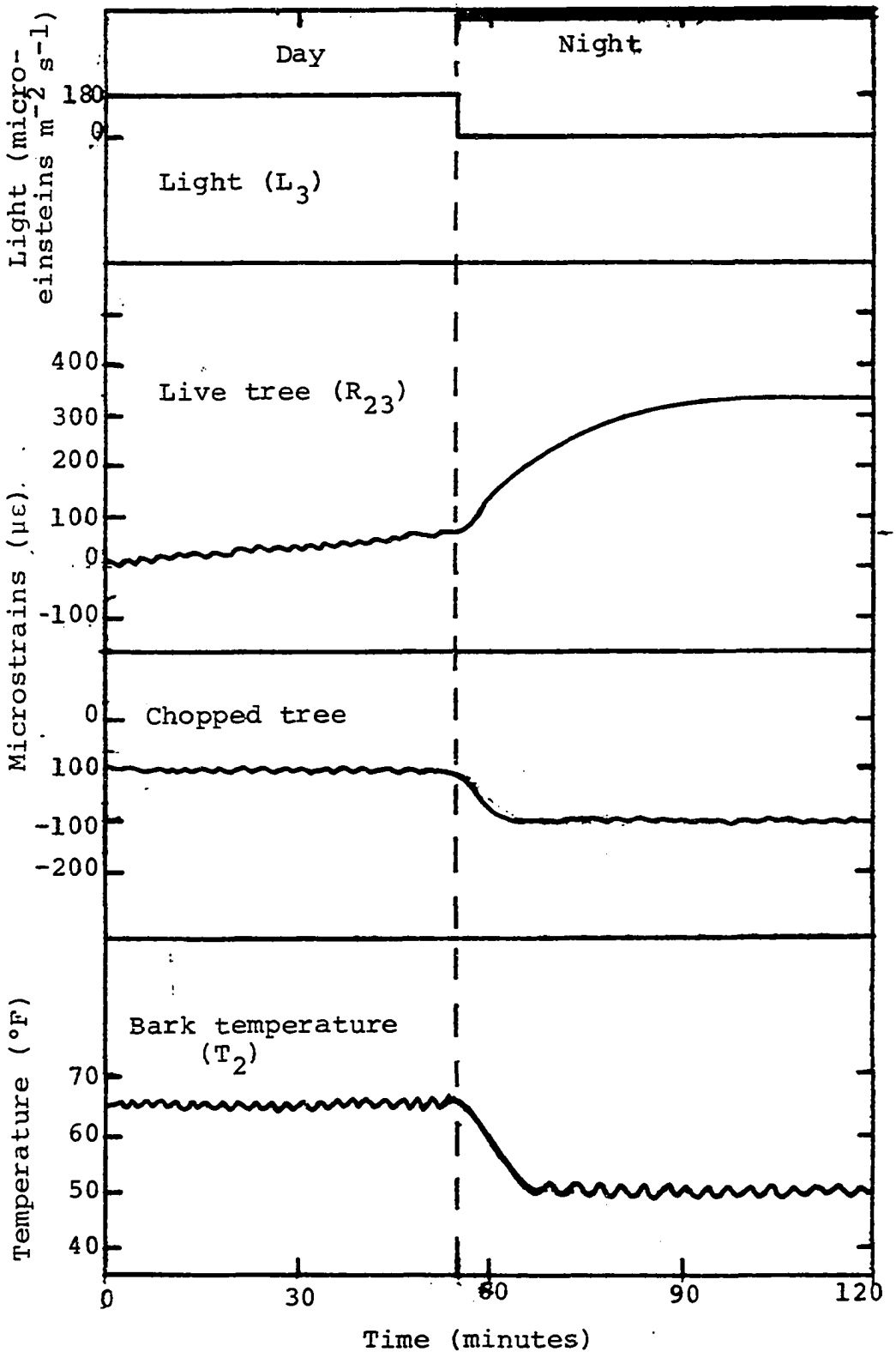

Figure 14. Temperature test in growth chamber. T_2 was measured with a thermometer in contact with the tree

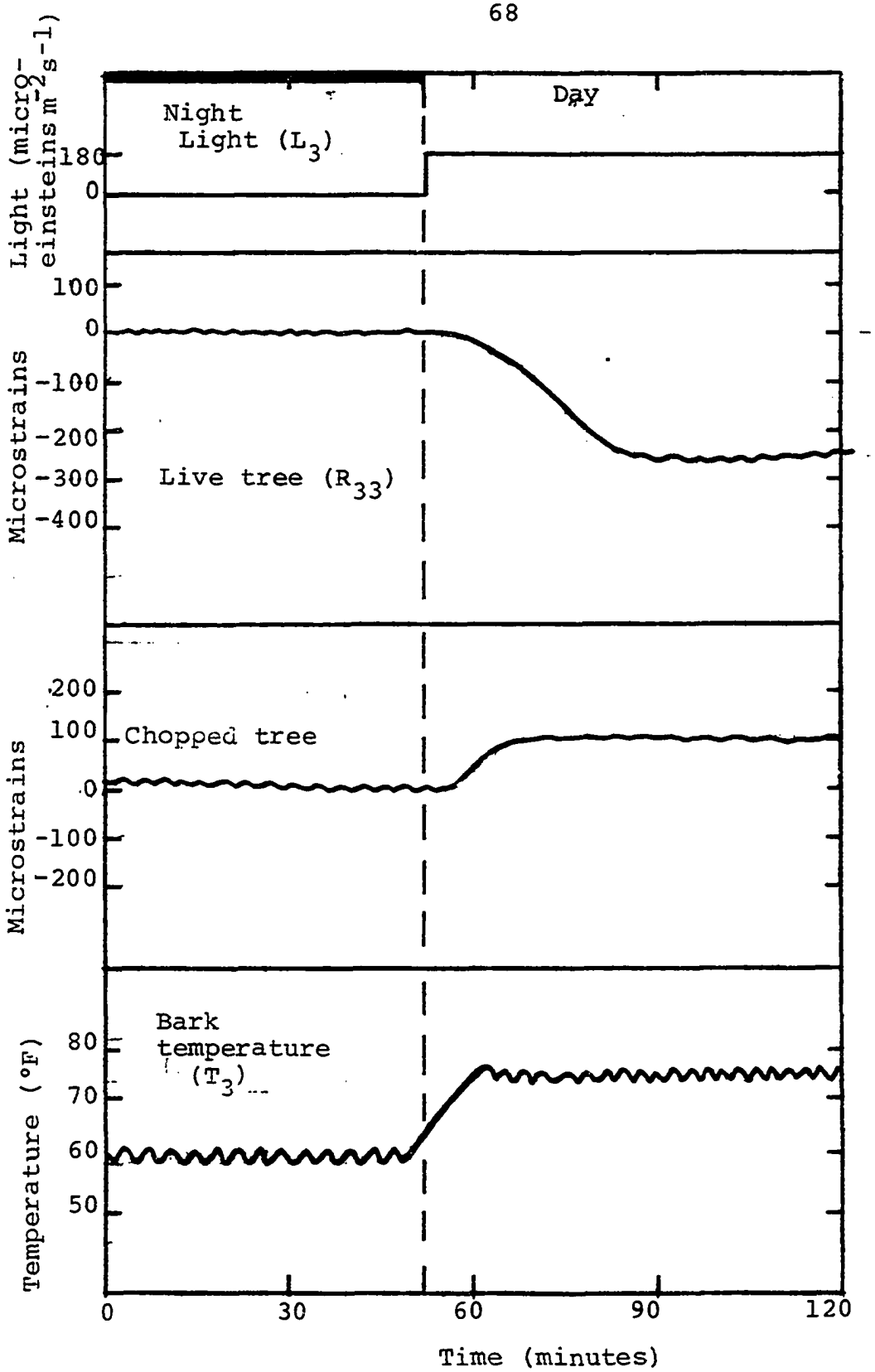

Figure 15. Temperature test in growth chamber T_3 was measured with a thermocouple in contact with the tree

horizontal gages were opposite each other and the two vertical gages were also opposite each other. Each of the four gages were connected with three lead wires. The horizontal gages were mounted just below the vertical gages. The trunk was cut about 5 cm above and 5 cm below the gages. The cut piece was quickly immersed in a bath that was filled with Dow Corning 200 fluid. The Dow Corning 200 fluid is a clear silicone fluid which has excellent water repellency. The fluid thus sealed the cut tree from absorbing or giving out moisture. The bath of fluid was then placed in an oven. The gages on the wood were hooked into the Brush recorder and amplifier assembly. The oven temperature was increased by 22°C (39.6°F) and held at that temperature until all conditions stabilized. The output obtained from the recorder (Figure 16), shows that both horizontal gages expanded the same amount as the temperature increased. One of the vertical gages expanded while the other contracted. This means that there was a little bit of bending too on the stick. This is not contrary to expectation due to the fact that wood is nonaxisymmetric.

An oven temperature reduction of 16°C (28.8°F) gave the opposite effect (Figure 17). The horizontal gages contracted about the same amount. The vertical gage which expanded before, contracted and the one which contracted before expanded.

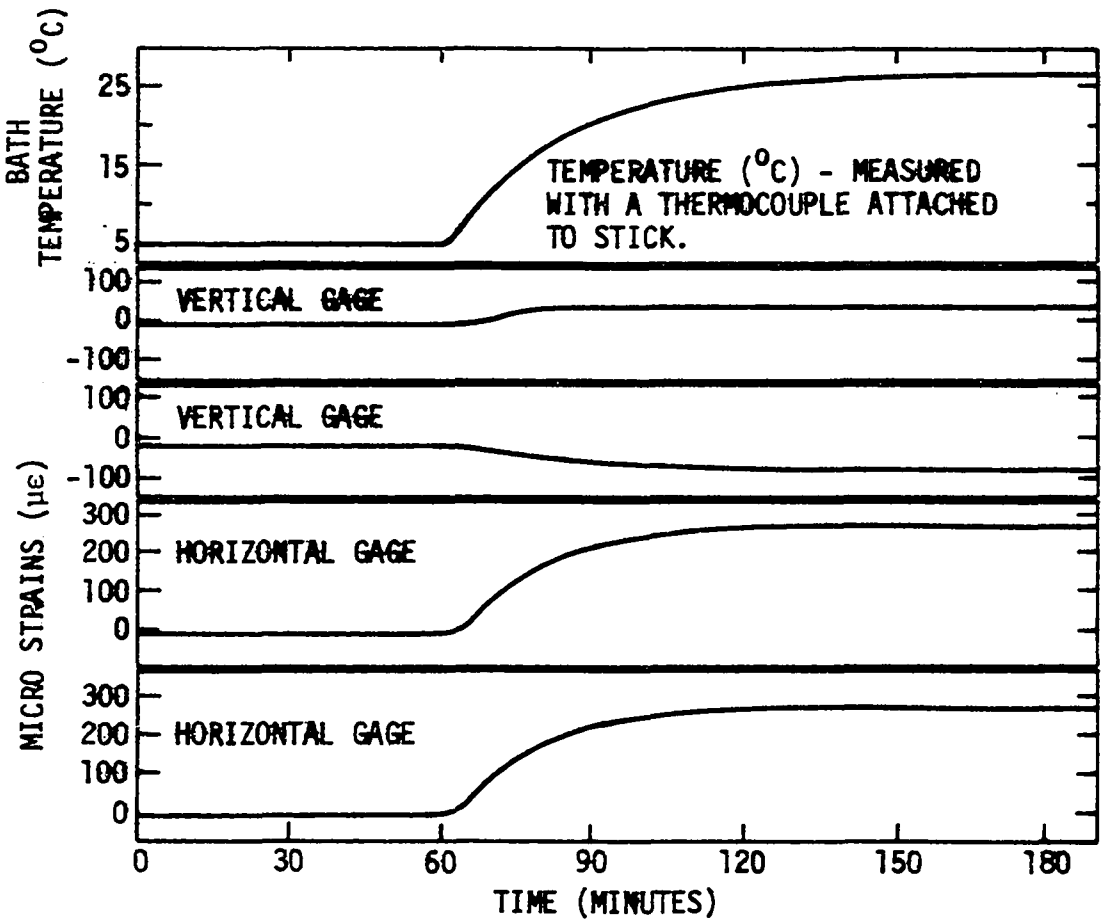

Fig. 16. Temperature correction test

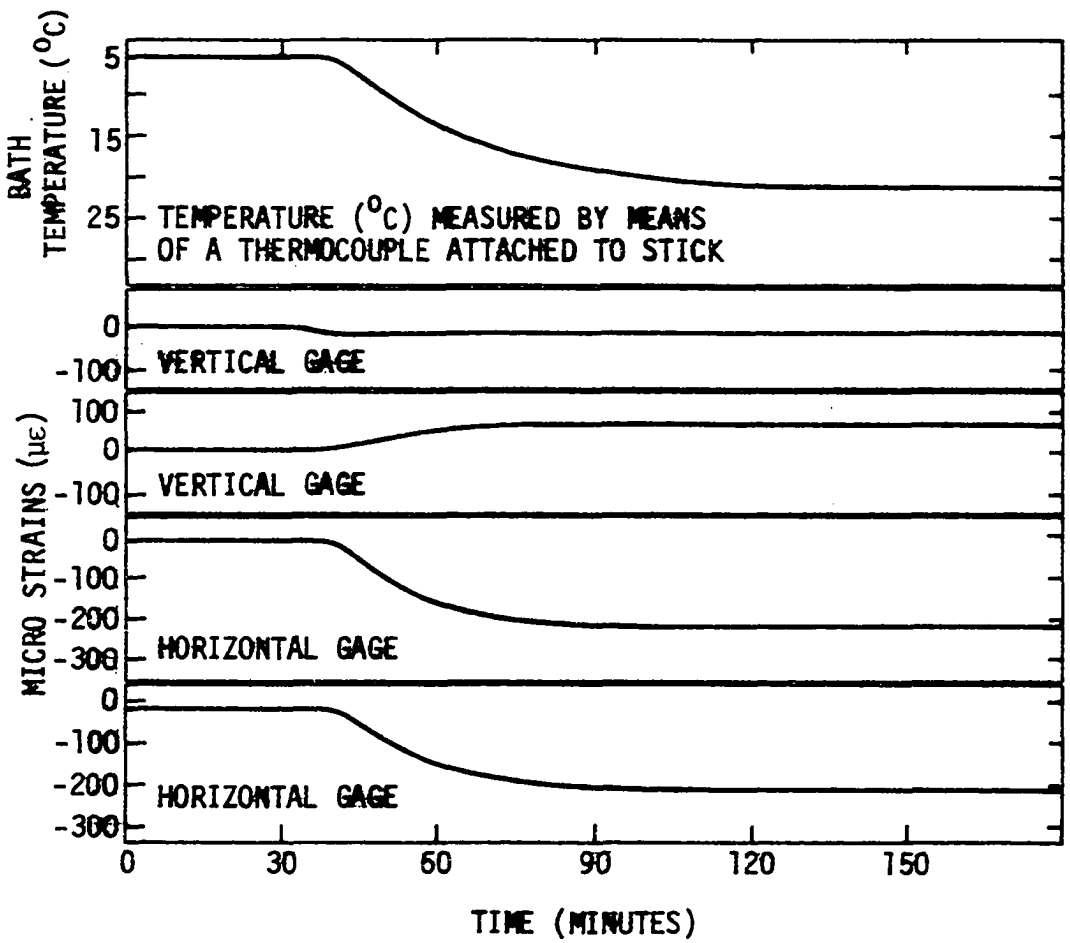

Fig. 17. Temperature correction test

A plot of the strain vs. temperature change obtained from Figure 16 is shown in Figure 18 for the horizontal gage. The graph is linear within the temperature range that trees normally thrive. The slope of the graph is 13 με/°C. This compares well with the value of 12.3 με/°C obtained for the one ran in the growth chamber. Figure 18 can be used to correct for the strain on the stem when the temperature changes. The correction is good for both positive and negative temperature changes.

Along with the experiment run in the silicone fluid, an experiment was run in which an isolated gage was connected with three lead wires. The gage was immersed in the silicone fluid and hooked to the model 520 digital strain indicator. The output from the gage when the temperature of the oven was increased is shown in Figure 19. This curve is steeper than the one in Figure 18. This is due to the high expansion coefficient of the polymide backing of the gage. This test is not directly relevant to the study presented but it helps to explain a few things. If the gage is loose on the tree, the result will be like Figure 19. The reaction to temperature of the live tree must be physiological for the greater part otherwise the strain on the live tree will not have an opposite sign to that in Figure 19.

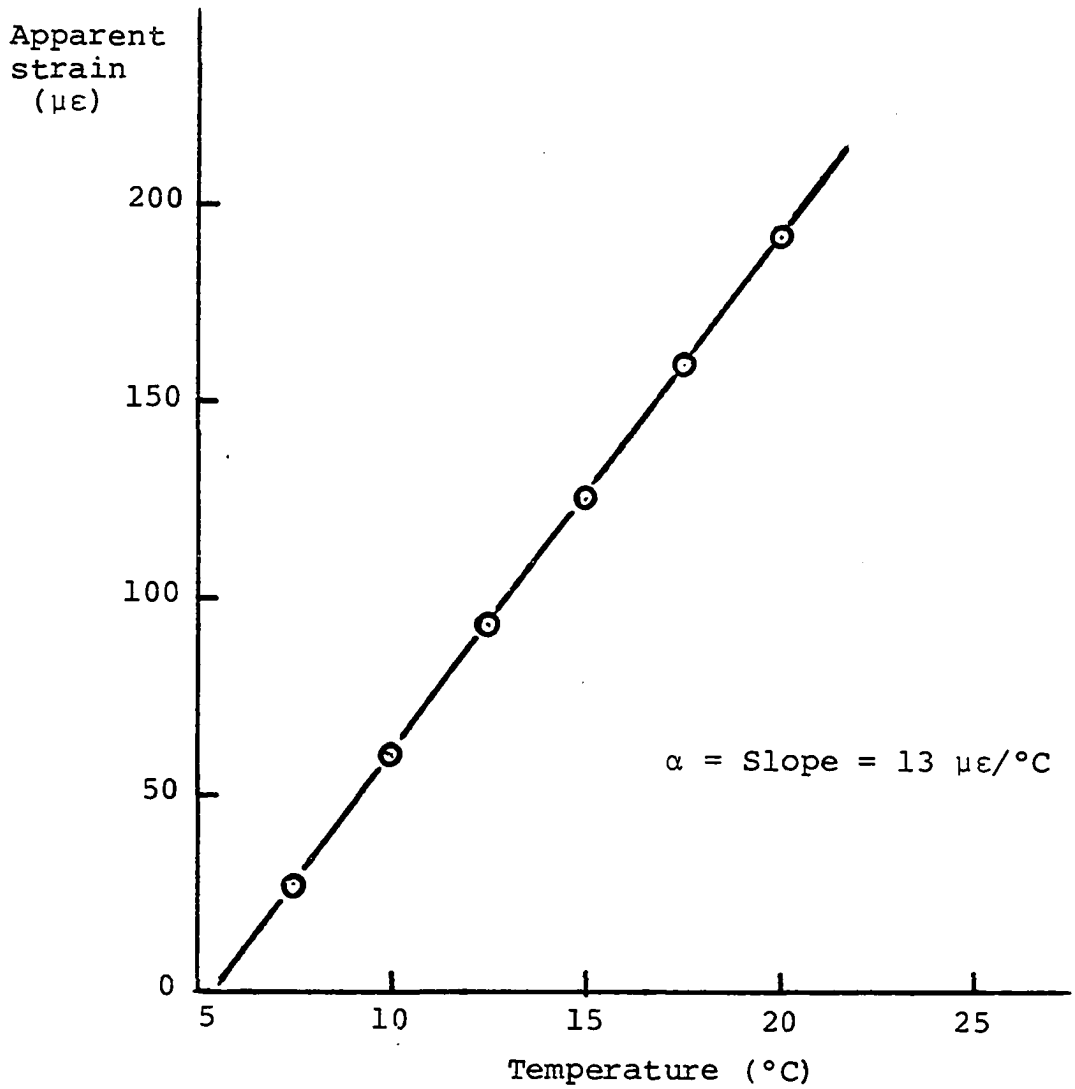

Figure 18. Correction curve for strain as temperature changes

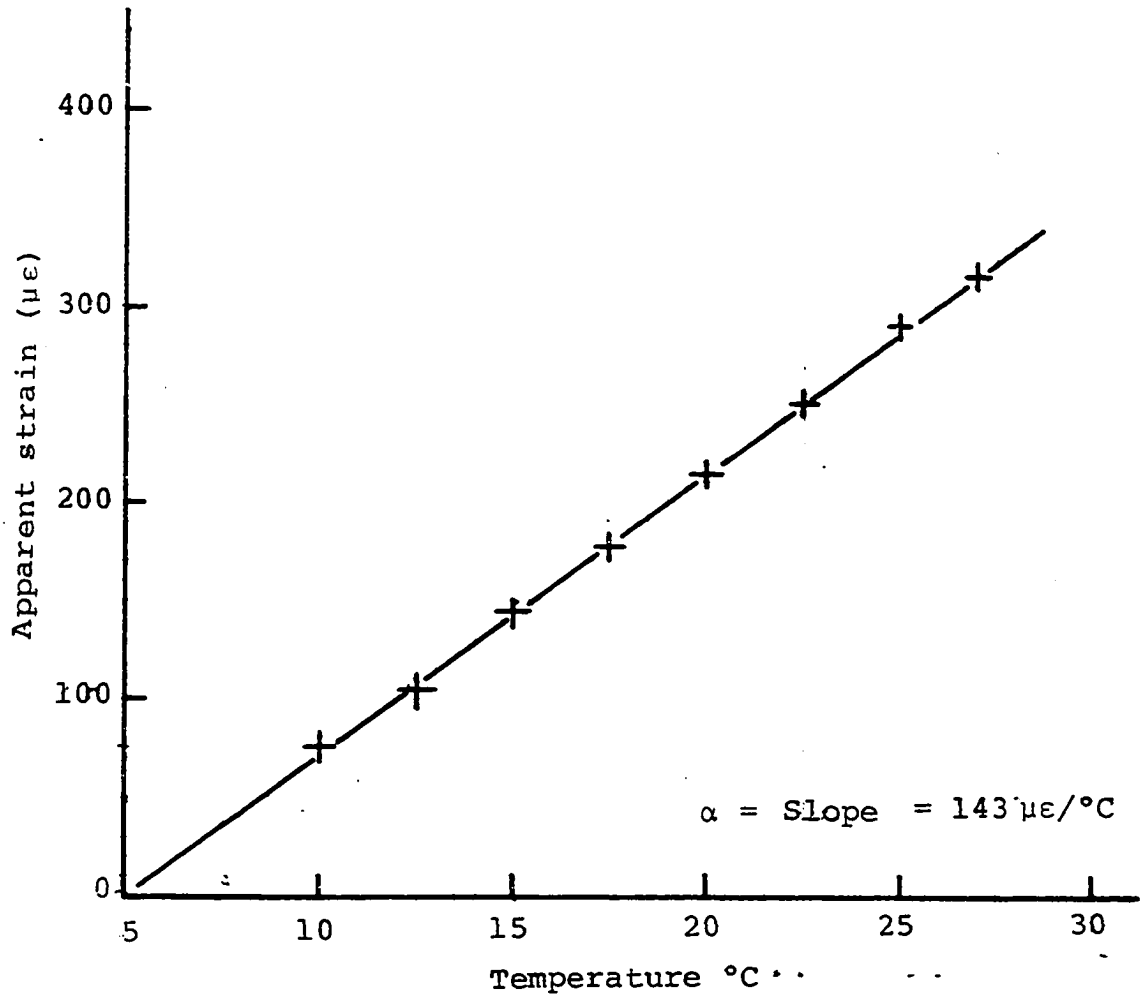

Figure 19. Apparent strain on loose gage in silicone fluid

The relative effect of temperature and light was also investigated in a separate run in the growth chamber. The stem of one of the test trees was instrumented with a tangential gage. The gage was wired in the manner outlined previously. The stem was cut 5 cm (1.97 in) above and below the gage. The cut piece was quickly sealed at the ends with paraffin wax to seal in moisture in the wood. A live tree was selected. A gage was bonded onto the stem in the horizontal sense. This gage was wired in the usual way. The live tree was put into the growth chamber. The cut piece was also placed in the chamber. The chamber was set to run under the temperature and light combinations of R_{23} except that the temperature was made to lag the light by one hour.

The strains on both the live tree and the severed piece as the night changed to day are shown in Figure 20a. The results show that:

1. Light had very little effect on the cut piece compared to the live tree. When the light came on, the temperature of the tree as measured with a thermocouple in contact with the bark increased by 1.5°F. The chopped tree expanded by 15 με. The live tree contracted by 170 με.
2. The effect of light on the cut piece was much less than the effect of temperature. When the temperature of the chamber rose by 12°F, the severed piece

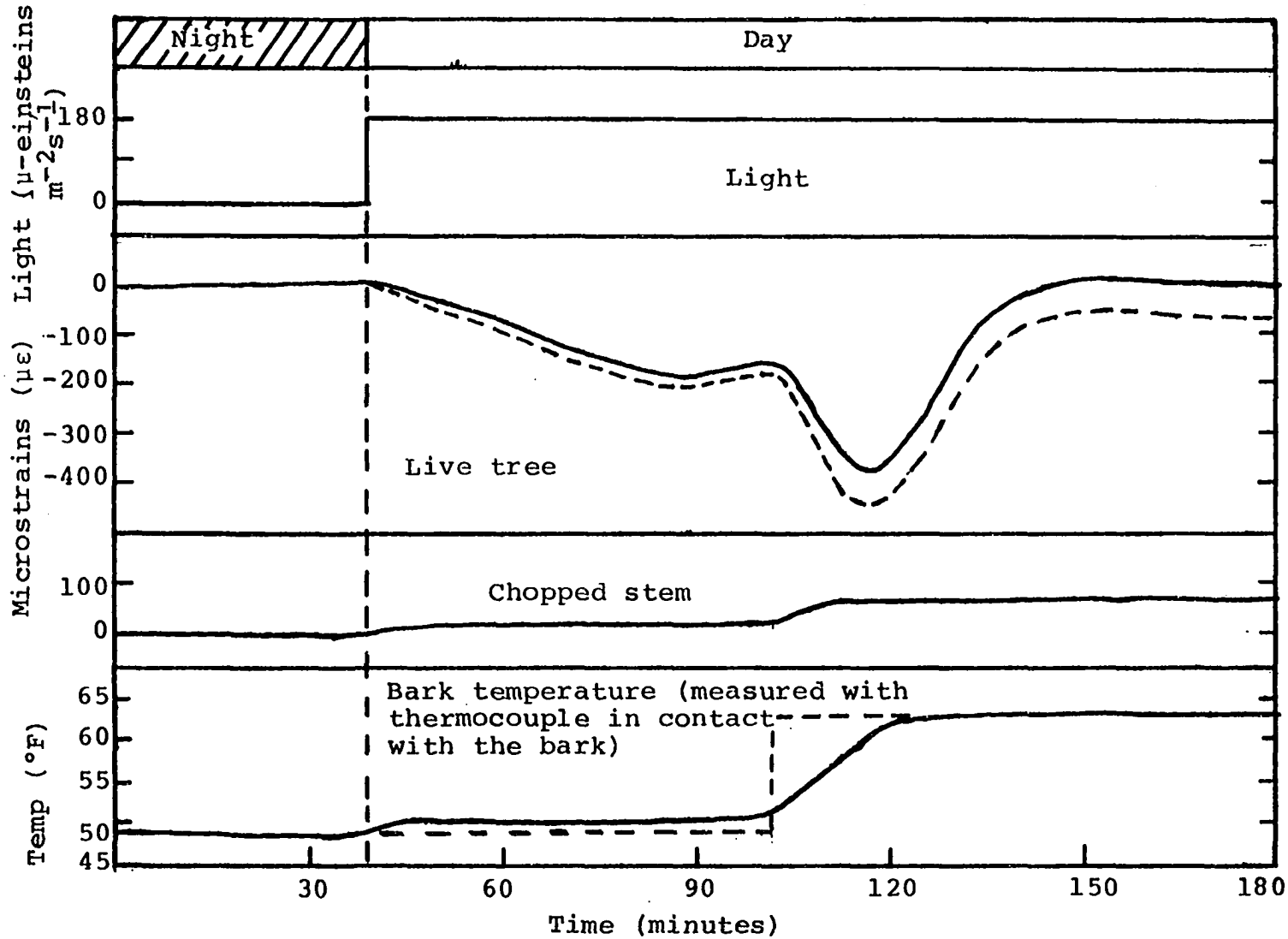

Figure 20a. Relative effect of light and temperature (dotted line shows strain corrected for temperature effect)

expanded an additional 50 με.

3. The effect of temperature on the live tree was higher than the effect on the severed piece. A 12°F temperature rise in the chamber gave a 200 με contraction in the stem of the live tree.
4. The effect of a 12°F temperature rise in the chamber was greater on both the live tree and the chopped piece compared to that of a 180 μ-einsteins $m^{-2}s^{-1}$ increase in light intensity.
5. The live tree took 40 minutes to get to its maximum contraction when the lights came on.
6. The live tree took only 15 minutes to get to its maximum contraction when the temperature of the chamber rose by 12°F.

The strains on the live tree and the severed piece as the day changed to night are shown in Figure 20b. The figure shows that:

1. When the lights went off, the temperature of the bark reduced by 2°F. The severed piece contracted by 15 με and the live tree expanded by 130 με.
2. When the temperature of the chamber dropped by 12°F, the severed piece contracted another 50 με and the live tree expanded an additional 200 με. Thus the effect of a 12°F temperature drop in the

chamber on both the live tree and the severed piece was greater compared to that of a reduction in light intensity from 180 μ-einsteins $m^{-2}s^{-1}$ to darkness. The reason why light has an effect on the chopped piece is that an increase or decrease in light intensity increases or decreases the chamber temperature respectively.

3. The live tree took 39 minutes to get to its maximum expansion when the light went off. It however took 18 minutes to get to its maximum expansion when the temperature reduced by 12°F.

The following general comments can be made on the live tree on comparing Figures 20a and 20b:

1. The numerical value of the maximum stem strain change when the light changed from darkness to 180 μ-einsteins $m^{-2}s^{-1}$ was 40 με larger than the numerical value of the maximum stem strain change when the light changed from 180 μ-einsteins $m^{-2}S^{-1}$ to darkness.
2. The expansion in the stem when the temperature increased by 12°F was numerically equal to the contraction in the stem when the temperature decreased by 12°F.
3. The response time when the light changed from darkness to 180 μ-einsteins $m^{-2}S^{-1}$ was essentially

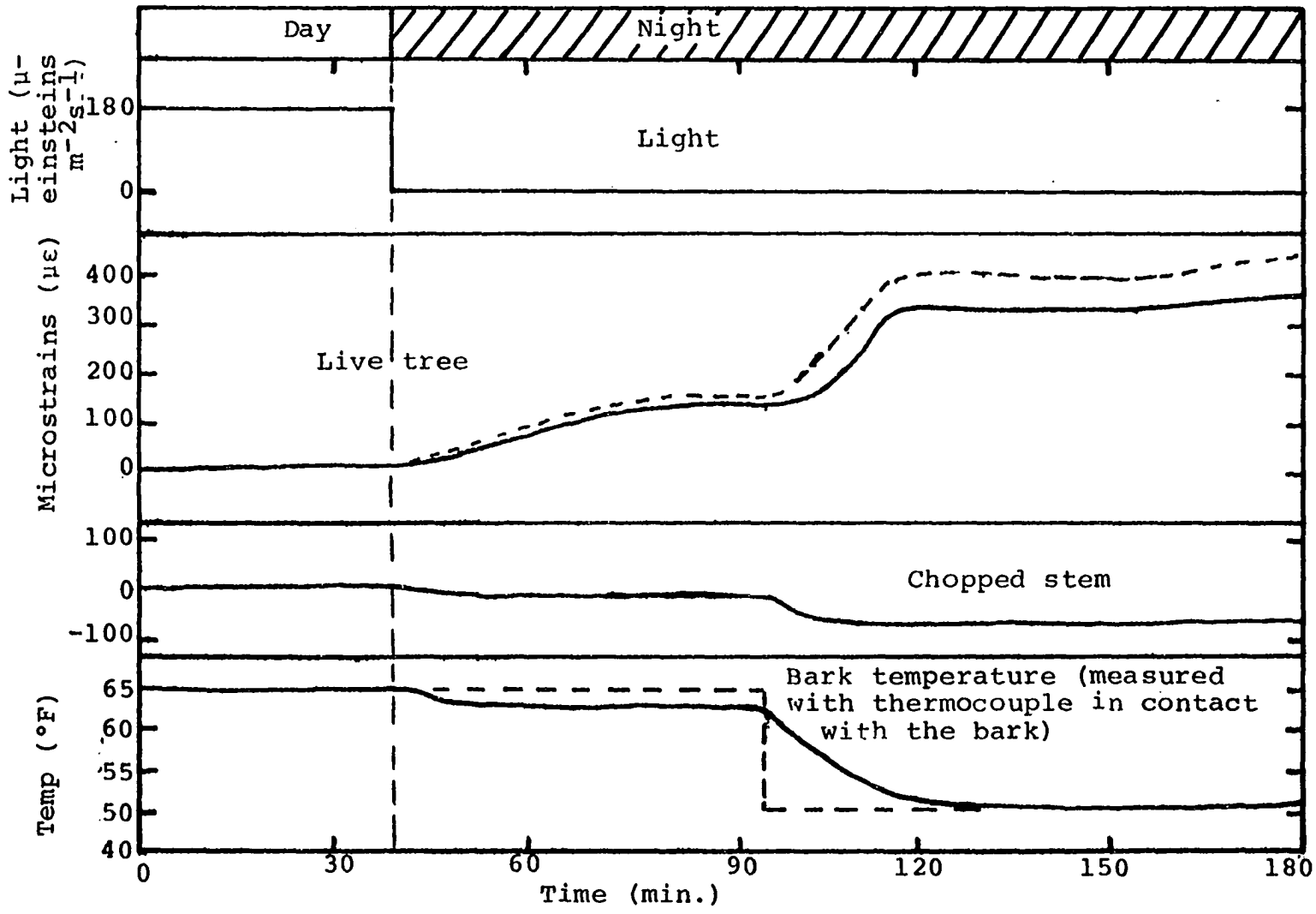

Figure 20b. Relative effect of light and temperature (dotted line shows strain corrected for temperature effect)

the same as the response time when the light changed from 180 μ-einsteins to darkness.

4. The response time to a 12°F temperature rise was 3 minutes less than that of a 12°F temperature drop.

The dotted lines in the second graphs of Figures 20a and 20b show the stem strain after correcting for temperature effects as measured on the chopped stem. The dotted lines in the bottom graphs show the chamber temperature as measured with a thermohydrograph. It can be noted from the bottom graphs that the chamber temperature changed almost instantly while the bark temperature took 24 minutes to establish an equilibrium temperature. This test also demonstrated that the nonphysiological part of the response of the live tree to temperature was small. It also confirmed the fact that the recorded stem strain when the temperature changed was actually less than the true stem strain.

The full stem strain recorded for the live tree for the same day as Figures 20a and 20b is given in Figure 20c. The figure shows that after the day, the stem strain settled at a night time value which was larger than the settling value for the previous night. A permanent strain of 565 με was imparted to the stem. The stem diameter at the point where the gage was mounted for the test was 1.77 cm. This means that there was a growth of 1000×10^{-6} cm for that day. The

average growth for three days for similar trees under similar light and temperature levels was 3350 x 10^{-6} cm (see Table 2b, p.137). Thus the one hour temperature lag did not make much difference in the growth. The strain recovery on watering was 280 με. This is 47 με larger than the average of 243 με given in Table 1, p. 106. Thus the one hour temperature lag increased the amount of stem strain recovered on watering.

The strain pattern in Figure 20c is a little different from the one in Figure 23 for R_{23}. After the daybreak stem contraction, there was a large stem expansion such that the tree recovered all the daybreak contraction. The strain was then fairly steady until when the tree was watered. This change in strain pattern could be due to the fact that the tree used for this test was a month and a half older than those used for the tests reported in Table 1. Another possible reason for the slight difference in the strains is that watering for this test was done 2 hours later than those of the tests reported in Table 1. It can be noted that the total contraction at daybreak in this test was 370 με compared to 615 με reported in Table 1 for R_{23}. The night time increase of 330 με in the stem strain however is not too different from the 300 με reported in Table 1 for R_{23}.

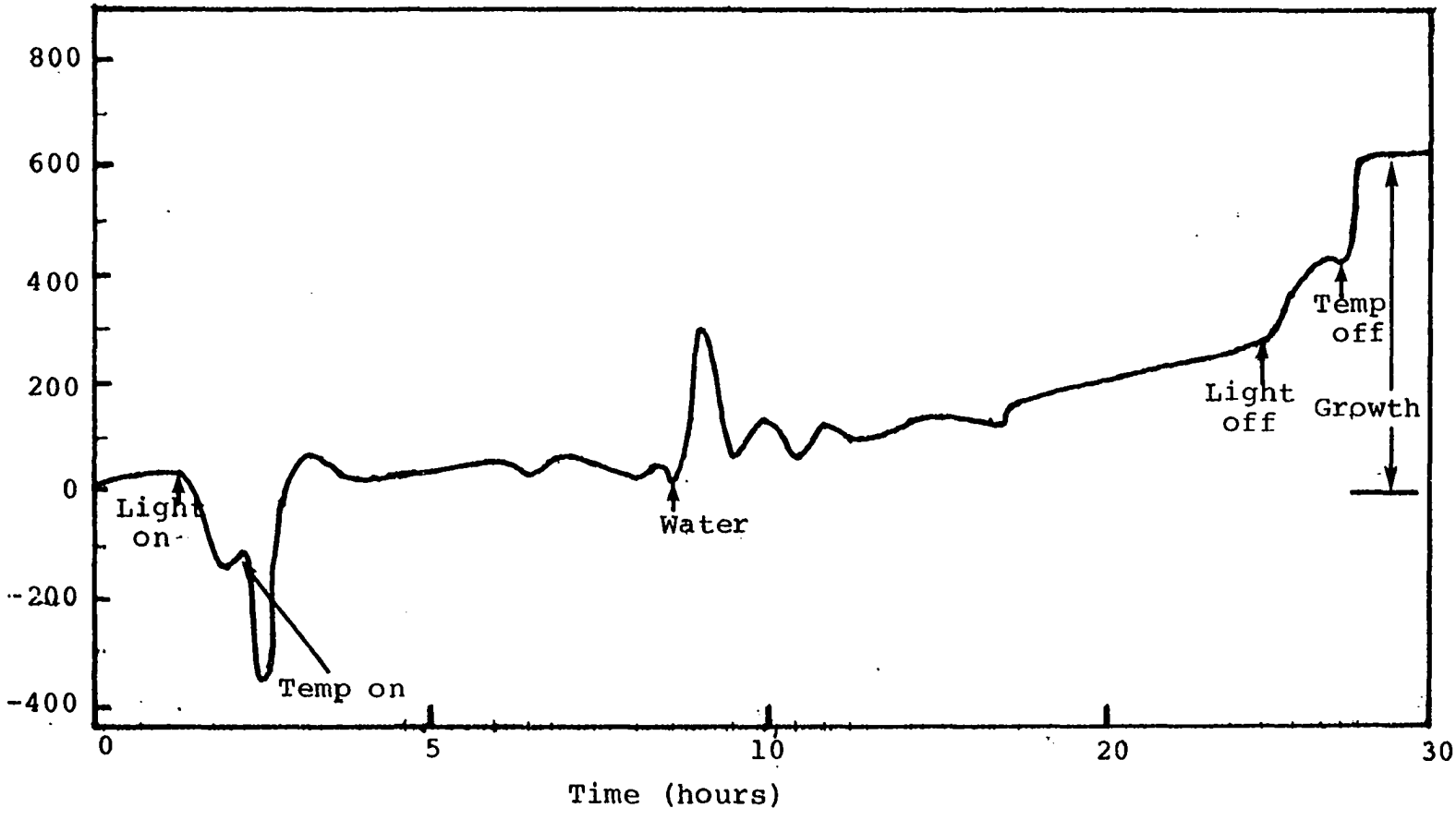

Figure 20c. Relative effect of light and temperature

RESULTS AND CONCLUSIONS

The average height of the trees used in the investigation was 90 cm and the diameters varied from 1.133 cm to 1.77 cm. The trees had healthy green leaves and the leaf areas varied from 1735 cm^2 to 5026 cm^2. The number of leaves per tree ranged from 20 to 105. The pertinent properties of the trees used in the investigation are given in Appendix B. Throughout this investigation the strain units ($\mu\varepsilon$) are meant to indicate parts per million. For example 1000 $\mu\varepsilon = 1000 \times 10^{-6}$ cm/cm. Strain by definition is the change in dimension per unit dimension. An increase in strain in the studies presented here does not mean that this particular tree is under stress. When a tree loses water and the cells begin to dry out, the stem contracts and the tree is under stress. When water is made available to the tree, the cells fill up, enlarge and the tree recovers from the stress it had when it had insufficient water, thereby imparting positive strain to the gage. The light intensity units used is the micro-einstein $m^{-2}s^{-1}$. The light intensity on a bright sunny day is about 1200 μ-einsteins $m^{-2}s^{-1}$. The μ-einstein is an energy unit (1 μ-einstein = 0.1 joule). That is 1 μ-einstein $m^{-2}s^{-1}$ is equivalent to 0.1 watt m^{-2}. This energy form of measuring light is currently preferred to former units like lux, ft-candle, candella and lumen because all these units give the density of luminous flux (the time rate of flow of light)

with respect to the eye. Thus the energy unit gives a better indication of the intensity of light. Light meters which are graduated in μ-einsteins $m^{-2}s^{-1}$ are commercially available too. The notations used for the light levels, the temperature levels and the different test runs are as explained on page 63.

When the temperature of the growth chamber is set at some value the inner part of the chamber achieves this set value and fluctuates $\pm 2°F$ about this set value as the temperature controls cut in and out. The stem strain results as obtained from the recorder show that the trees responded physiologically to these small temperature fluctuations (see Figures 21a and 21b). The lowest graphs show the temperature fluctuations for both day and night as recorded by a thermocouple mounted on the bark of a tree during the interval when the conditions changed from day to night (see top graph of Figure 21a) and from night to day (see top graph of Figure 21b). In Figure 21a, the stem temperature fluctuation is $\pm \frac{1}{2}°F$ or a total swing of 1°F. Eliminating the noise superimposed on the temperature recording in Figure 21b, the temperature can be seen to fluctuate $\pm 2°F$ or a total swing of 4°F. Figure 21a is for a day temperature of 55°F and Figure 21b for a day temperature of 75°F. The results for a day temperature of 65°F was similar to Figure 21a and that for a day temperature of 85°F was similar to Figure 21b. It seems,

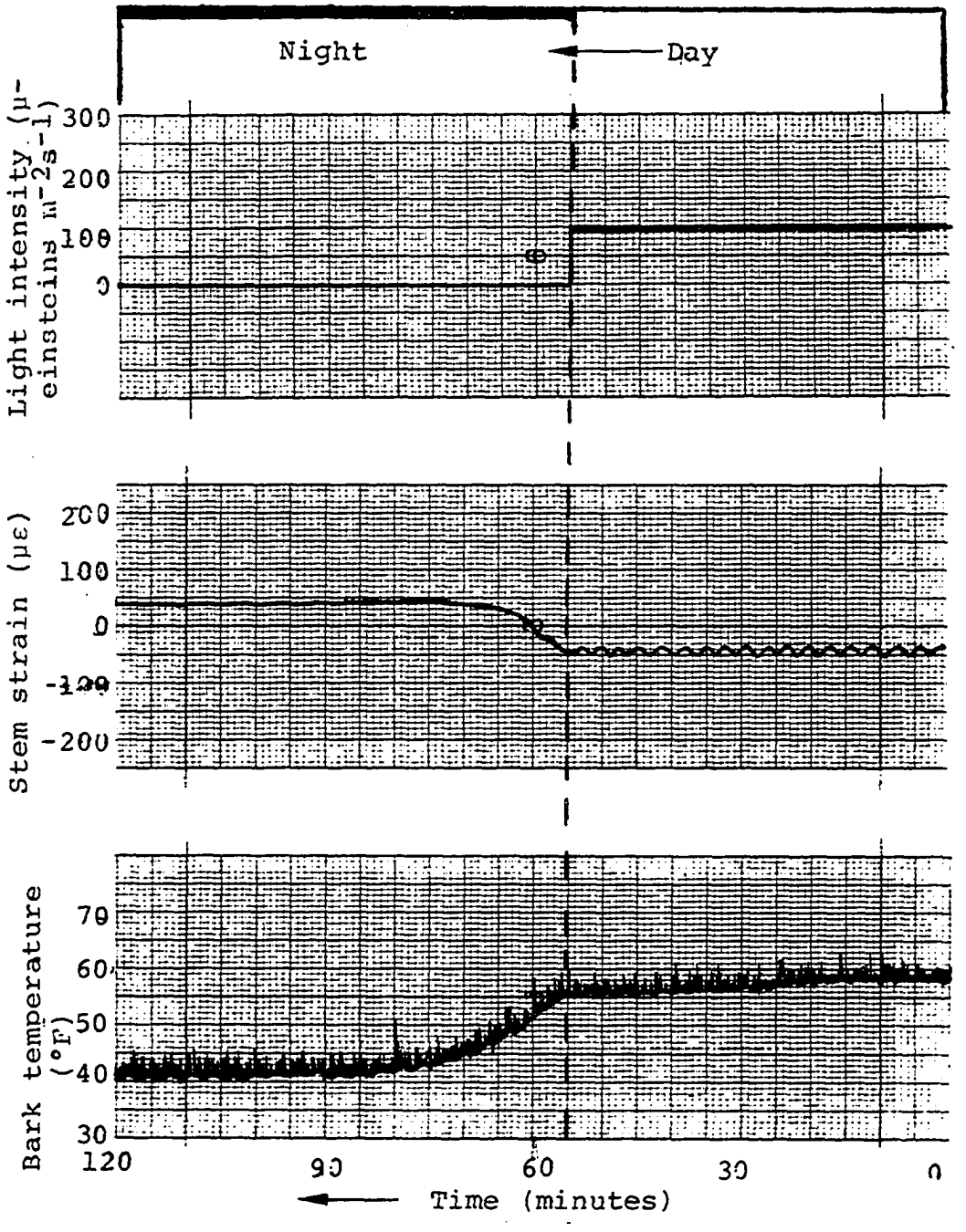

Figure 21a. Physiological response of tree to temperature cycling in growth chamber during night (40°F) and day (56°F). Bark temperature measured with thermocouple attached to bark

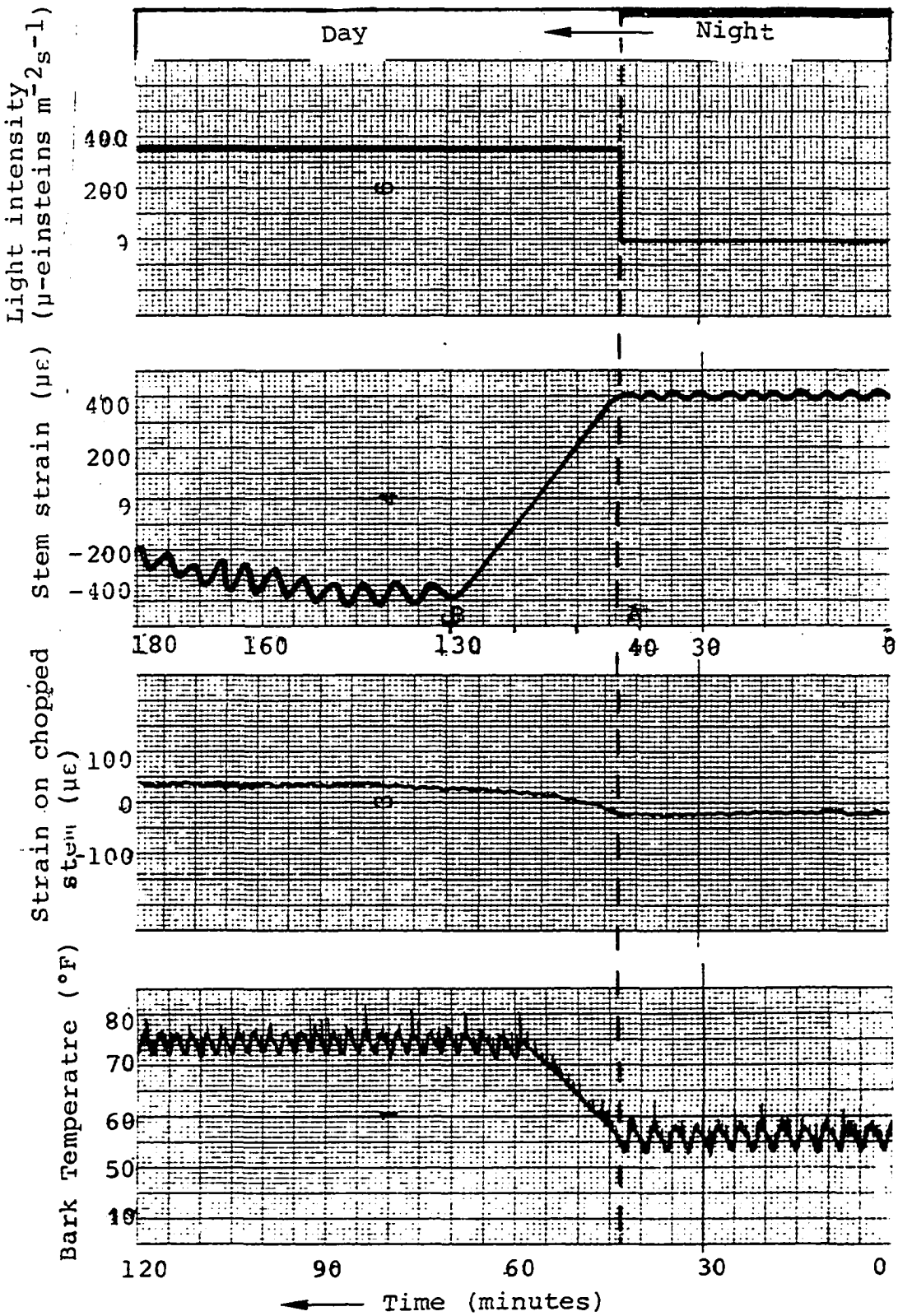

Figure 21b. Physiological response of live tree and chopped stem to temperature cycling in growth chamber

therefore, that the chamber temperature control was better between 40°F and 65°F compared to between 65°F and 85°F. Due to unavailability of excess recording channels, the chamber temperature itself was recorded on a thermohydrograph which was not sensitive enough to see the ±2°F quoted by the manufacturer of the chamber. The time scale for the second graph has been squeezed between points A and B in order to accommodate the fluctuations after the temperature change. The second graphs show the stem strain variations for the same periods of time. The stem strain clearly fluctuates as the temperature in the chamber fluctuates. At temperatures T_1 and T_2 (40°F night; 55°F day and 50°F night; 65°F day respectively) the stem strain fluctuations were seen during the day but not at night (see middle graph in Figure 21a) for all light intensities considered. At temperature levels T_3 and T_4 (60°F night; 75°F day and 70°F night and 85°F day respectively) the stem strain fluctuations were seen both during the day and at night (see second graph in Figure 21b) for all light intensities considered. The amplitude of the stem strain fluctuations were larger during the day compared to the night, Figure 21b. This may be due to the added effect of the light during the day. It could also be due to the fact that the tree is more active during the day compared to the night. A dummy piece of the stem which was sealed against moisture loss with paraffin was also responded to the

temperature fluctuations in the chamber but to a lesser degree (see third graph in Figure 21b. This shows that the stem strain fluctuations on the live tree is physiological. The fact that the stem strain fluctuations were seen at some temperatures but not at other temperatures also supports the conclusion that the stem strain fluctuations on the live tree is physiological. The third result which supports this conclusion is the fact that the stem strain fluctuations during the day are larger than those that occurred during the night. It can be seen from Figures 21a and 21b that the stem srain fluctuations were larger when the day temperature was 75°F compared to a day temperature of 55°F. This could be due to the fact that the activities of the cells in the stem tend to increase with increasing temperature within the temperature limits in which the tree thrives.

The results as obtained from the recorders have been redrawn in Figures 22 to 29. The short term temperature related stem strain fluctuations mentioned above are not shown in these figures. The mean values about which the strains fluctuated have been used in redrawing the strain curves. Each curve in Figures 22 to 29 is the average for two different trees which were subjected to the same light and temperature levels. The largest strain variation between any two trees which were subjected to the same light and temperature levels was 55 $\mu\varepsilon$. This occurred 9 hours after

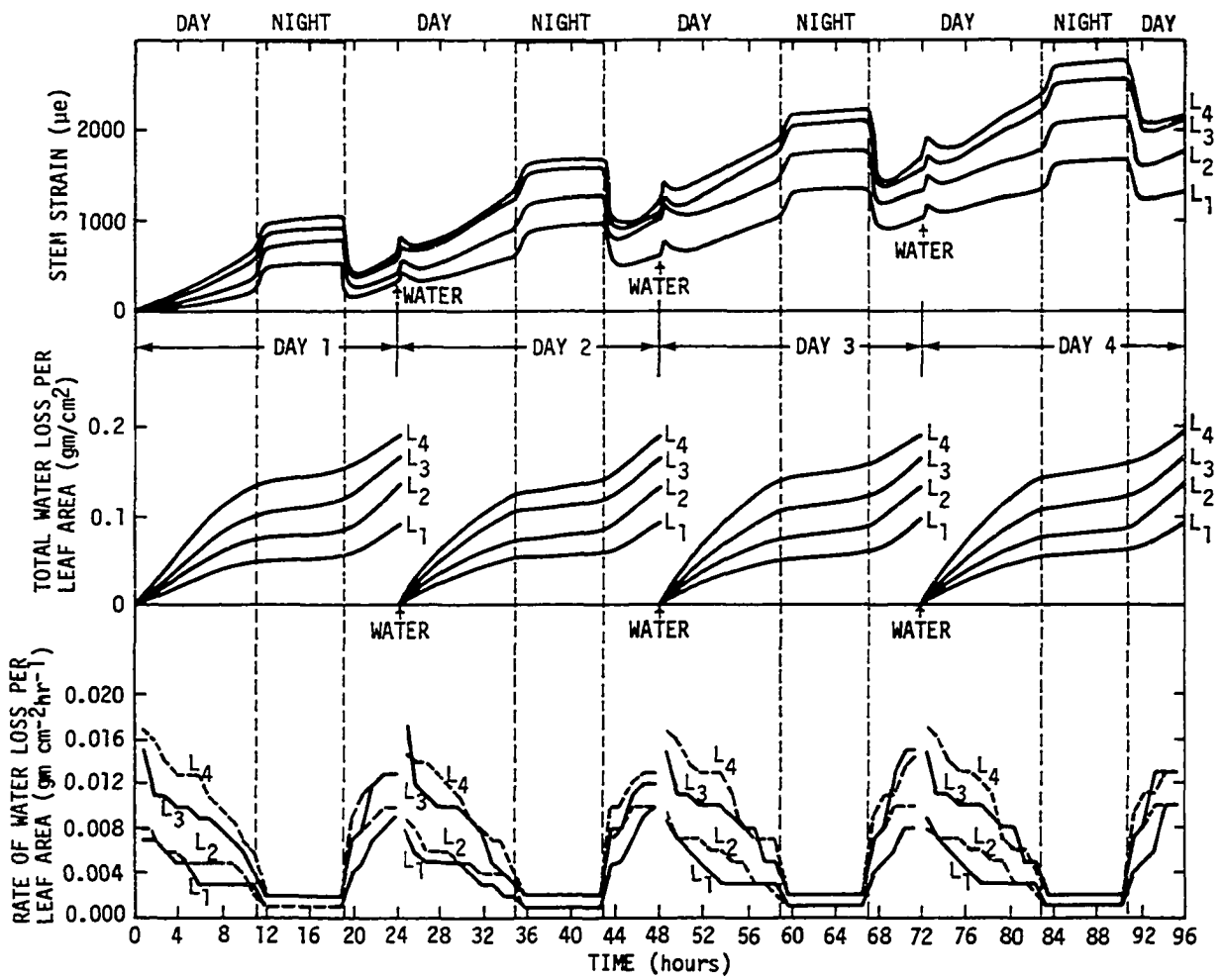

Fig. 22. Variation of stem strain, total water loss per leaf area and rate of water loss per leaf area with time for daytime temperature 55°F for various light levels

L_1 = μ26 μ-einsteins $m^{-2}s^{-1}$ L_3 = 180 μ-einsteins $m^{-2}s^{-1}$

L_2 = 100 μ-einsteins $m^{-2}s^{-1}$ L_4 = 330 μ-einsteins $m^{-2}s^{-1}$

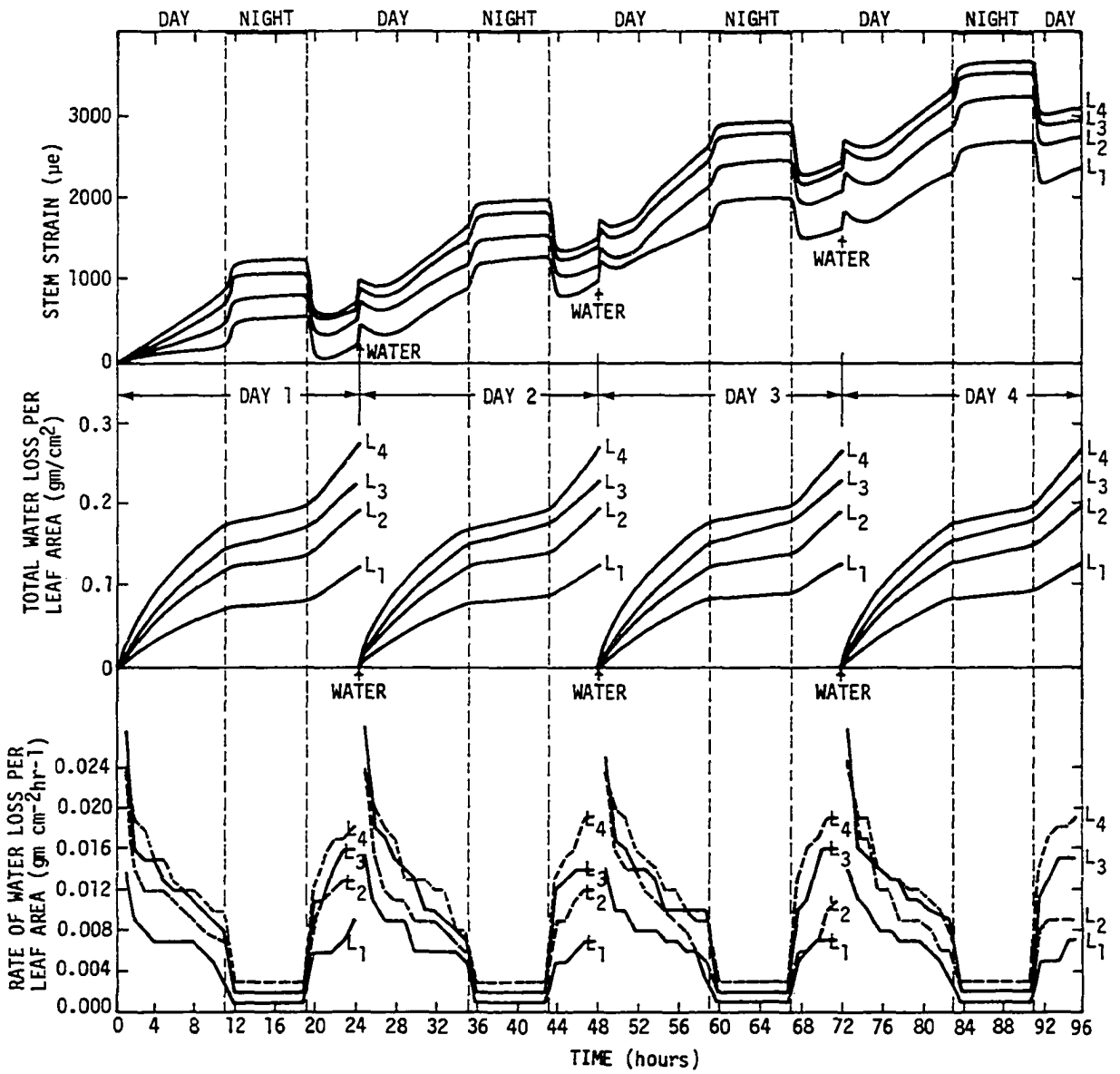

Fig. 23. Variation of stem strain, total water loss per leaf area and rate of water loss per leaf area with time for daytime temperature 65°F for various light levels

L_1 = 26 μ-einsteins $m^{-2}s^{-1}$ L_3 = 180 μ-einsteins $m^{-2}s^{-1}$

L_2 = 100 μ-einsteins $m^{-2}s^{-1}$ L_4 = 330 μ-einsteins $m^{-2}s^{-1}$

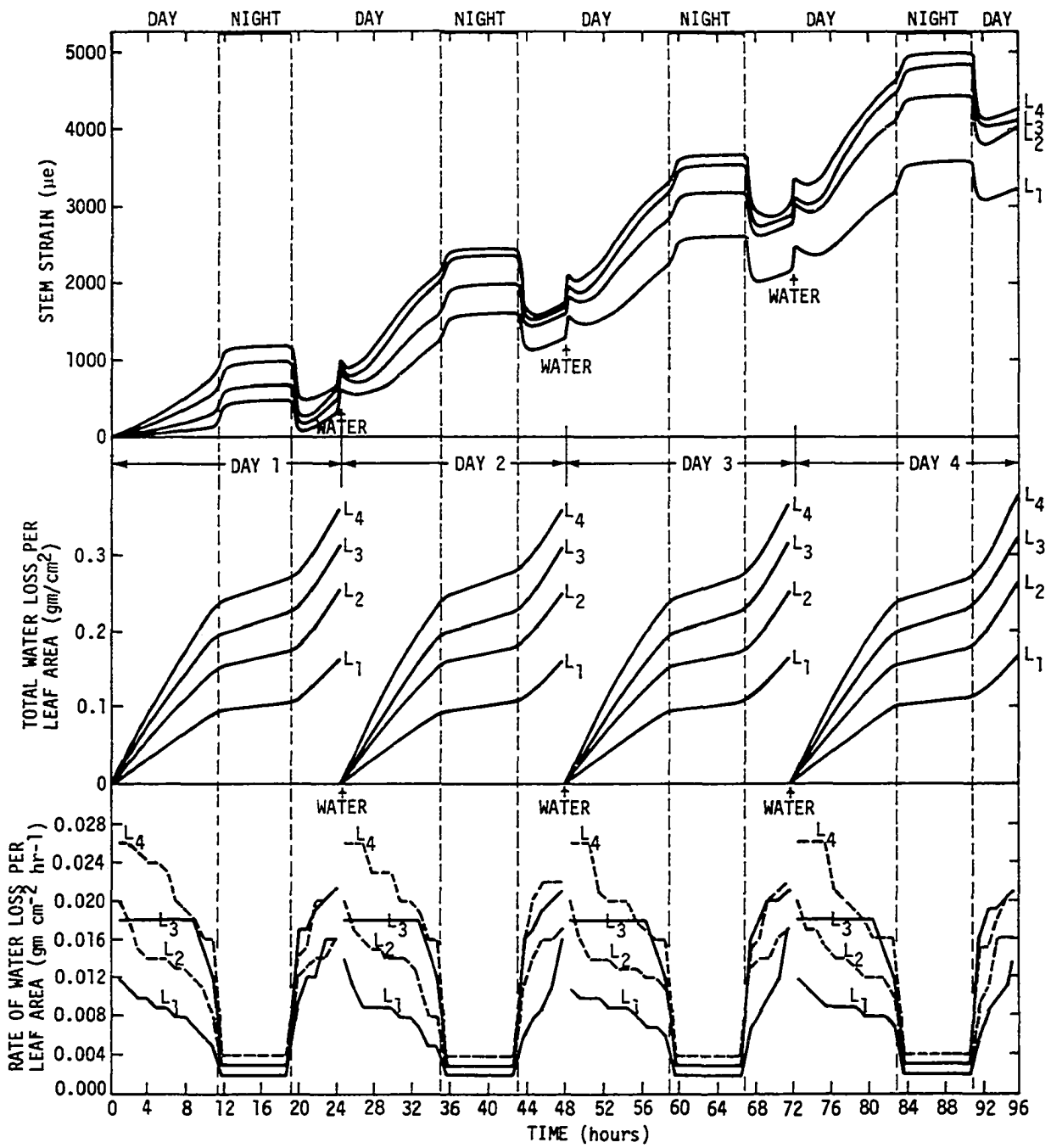

Fig. 24. Variation of stem strain, total water loss per leaf area and rate of water loss per leaf area with time for daytime temperature 75°F for various light levels

L_1 = 26 μ-einsteins $m^{-2}s^{-1}$ L_3 = 180 μ-einsteins $m^{-2}s^{-1}$

L_2 = 100 μ-einsteins $m^{-2}s^{-1}$ L_4 = 330 μ-einsteins $m^{-2}s^{-1}$

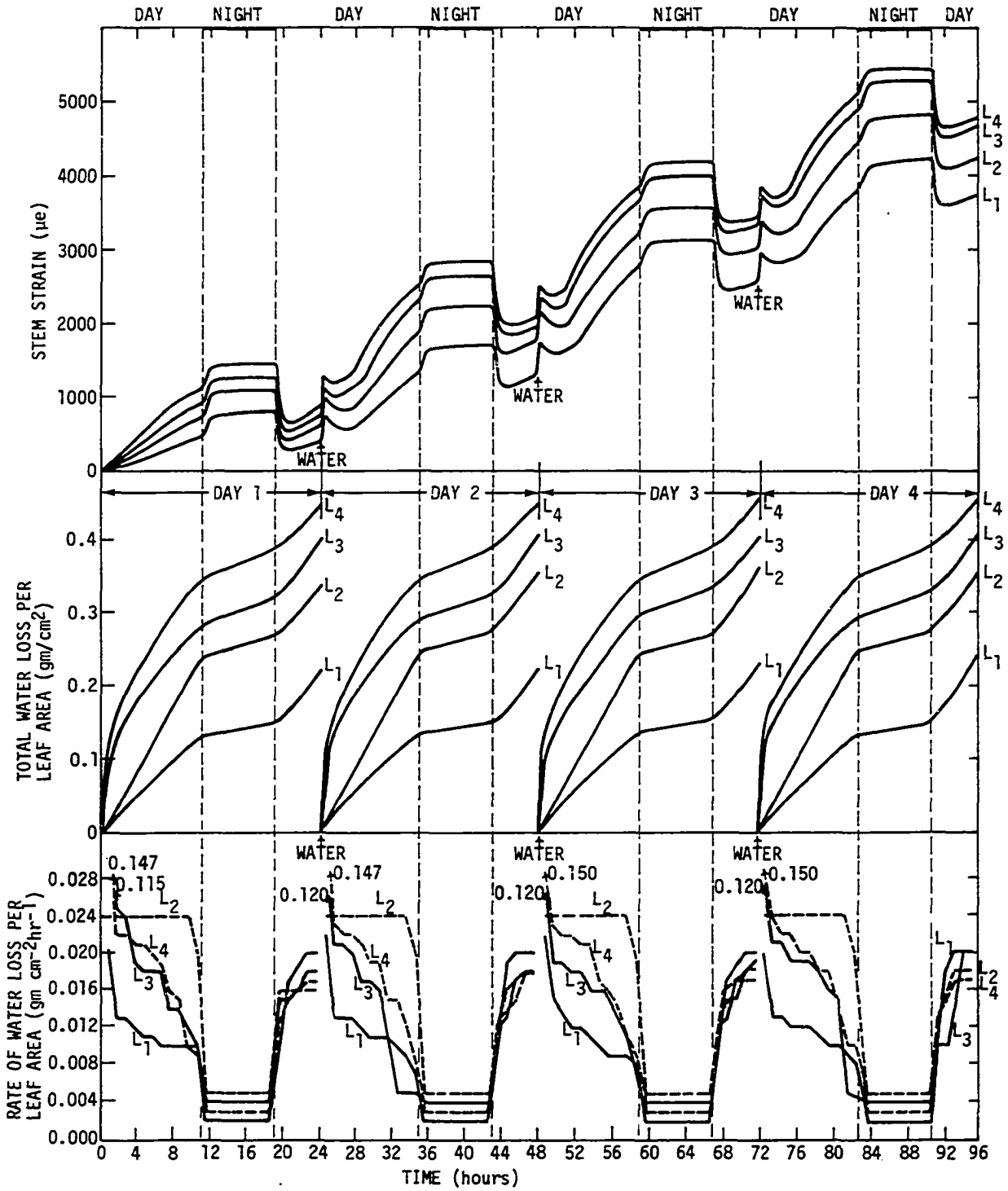

Fig. 25. Variation of stem strain, total water loss per leaf area and rate of water loss per leaf area with time for daytime temperature 85°F for various light levels

L_1 = 26 μ-einsteins $m^{-2}s^{-1}$ L_3 = 180 μ-einsteins $m^{-2}s^{-1}$

L_2 = 100 μ-einsteins $m^{-2}s^{-1}$ L_4 = 330 μ-einsteins $m^{-2}s^{-1}$

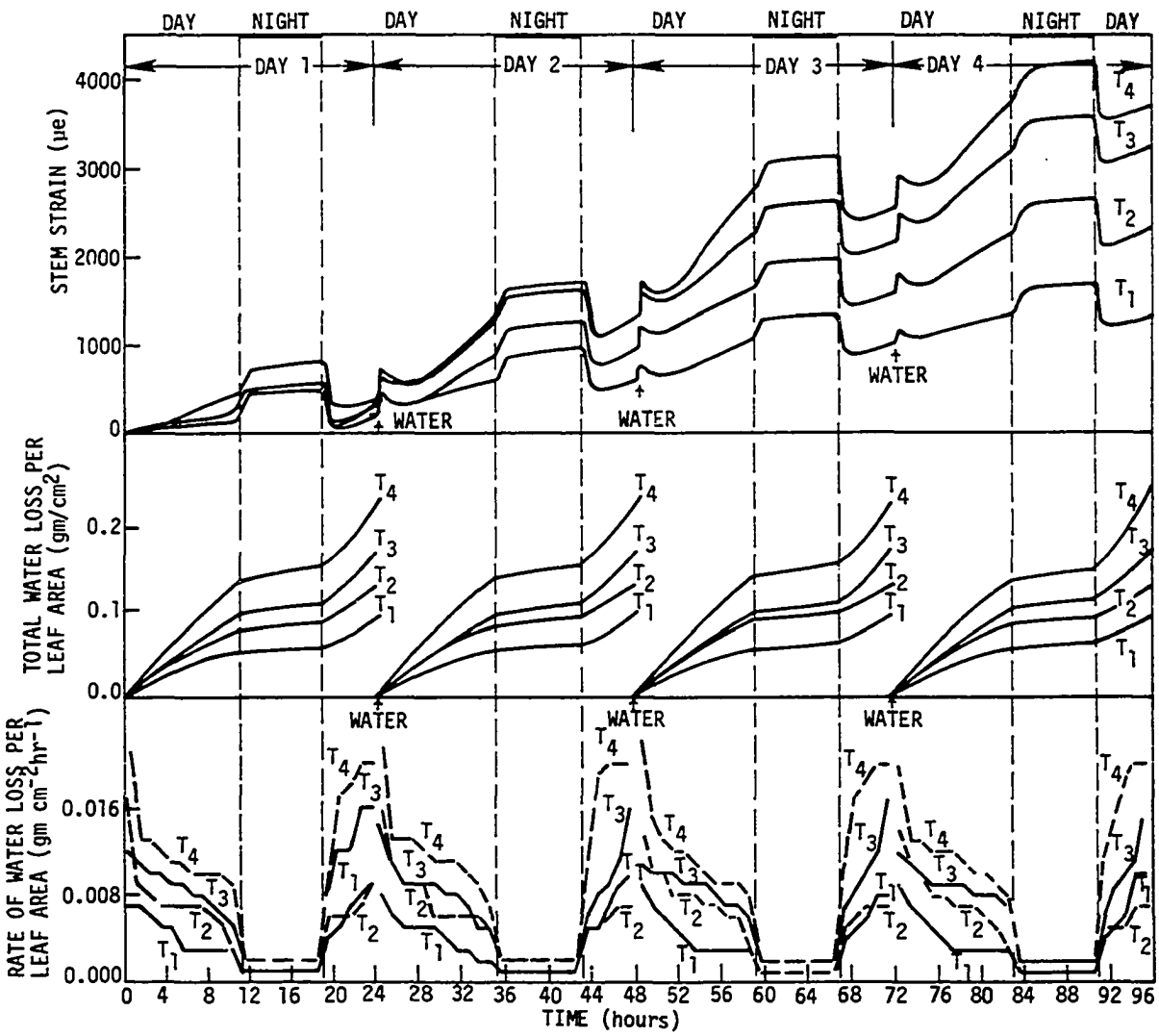

Fig. 26. Variation of stem strain, total water loss per leaf area and rate of water loss per leaf area with time for various temperatures at a light intensity of 26 μ-einsteins $m^{-2}s^{-1}$
T_1 = 55°F; T_2 = 65°F; T_3 = 75°F; T_4 = 85°F.

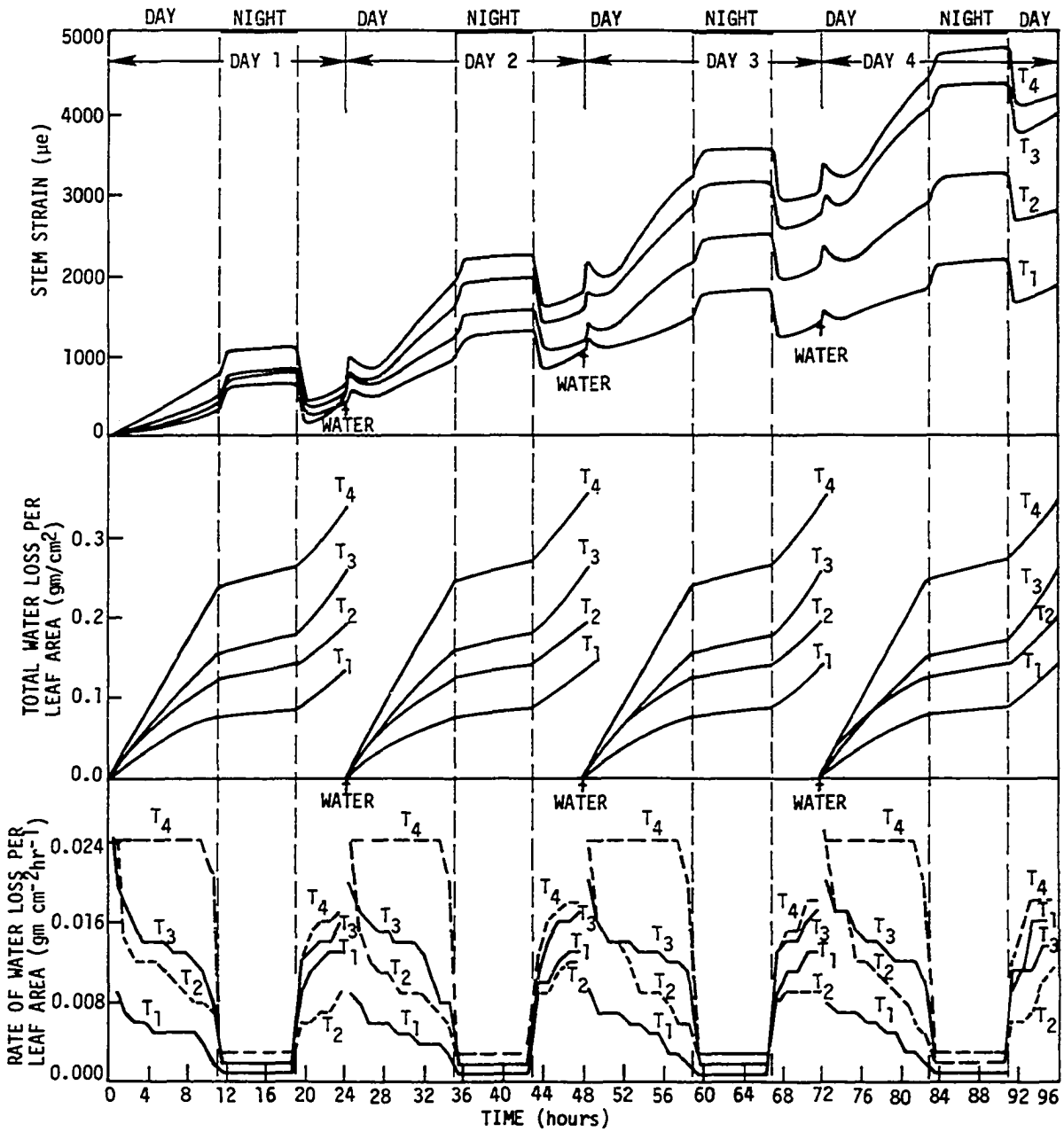

Fig. 27. Variation of stem strain, total water loss per leaf area and rate of water loss per leaf area with time for various temperatures at a light intensity of 100 μ-einsteins $m^{-2}s^{-1}$
T_1 = 55°F; T_2 = 65°F; T_3 = 75°F; T_4 = 85°F.

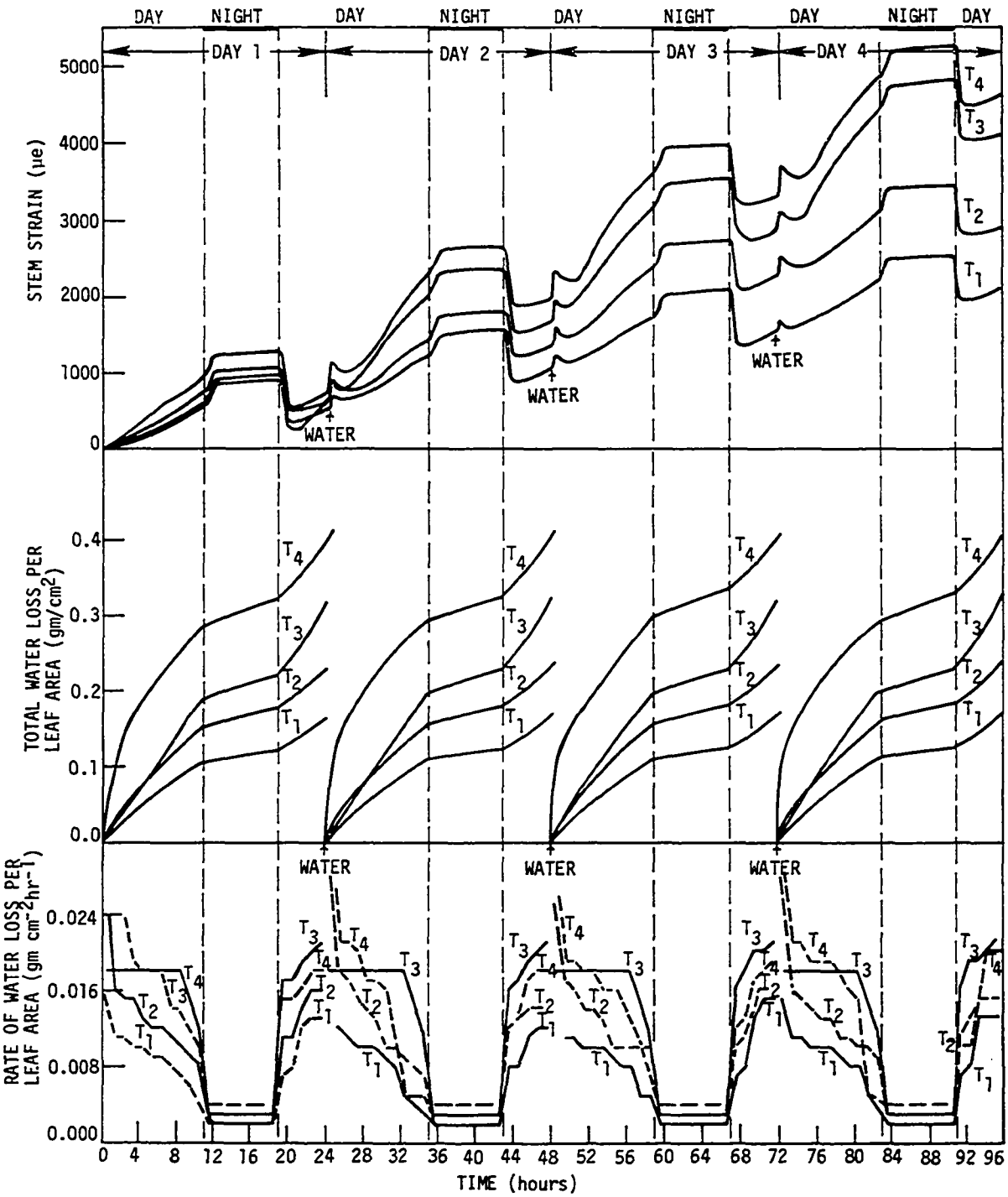

Fig. 28. Variation of stem strain, total water loss per leaf area and rate of water loss per leaf area with time for various temperatures at a light intensity of 180 μ-einsteins $m^{-2}s^{-1}$
T_1 = 55°F; T_2 = 65°F; T_3 = 75°F; T_4 = 85°F.

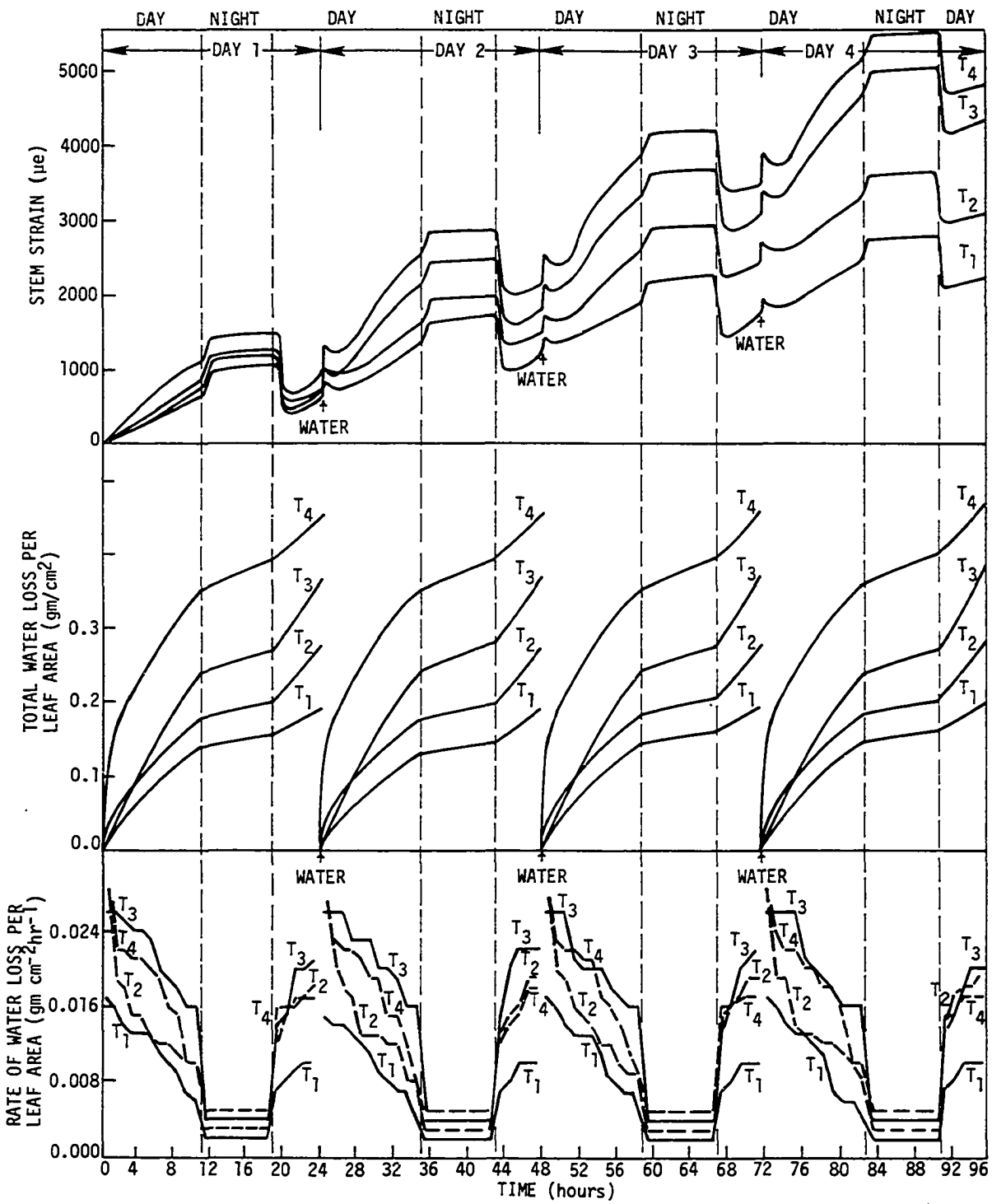

Fig. 29. Variation of stem strain, total water loss per leaf area and rate of water loss per leaf area with time for various temperatures at a light intensity of 330 μ-einsteins $m^{-2}s^{-1}$. T_1 = 55°F; T_2 = 65°F; T_3 = 75°F; 85°F.

watering on the third day for run R_{43}. This difference is 4% of the total strain change for that day or 1.7% of the average value at that time. The total water loss in grams for two such trees, as recorded on the chart, were very different. When reduced to transpiration per unit leaf area basis however, the variation between the two trees was not more than 5 grams for the whole watering cycle. That was 2% of the average value.

In each of Figures 22 to 29 the top graph is a continuous record of the stem strain as it developed over a period of four days in the environmental chamber set to have 8 hours of darkness and 16 hours of light. These redrawn graphs have already been corrected for temperature effects using the result of the temperature tests performed on a freshly chopped piece of stem (Figure 18). The light level did, of course, change instantaneously from one state to the next. The environmental temperature in the chamber, however, did not change instantaneously. New stable conditions took 20 minutes to establish. The actual settling time depended on the extent of the temperature change. The stem strain records clearly show the diurnal behavior of the trees. The total strain change during the day (i.e. lights and temperature on to lights and temperature off) was always larger than the total strain change during the night (lights and temperature

off to lights and temperature on). For R_{41}, Figures 25 and 26, the total strain change during the third day is 1000 με compared to 400 με during the night. Contraction occurred two times in the day. Once when the lights and temperature came on and once after water stress recovery on watering. At any given temperature considered, Figures 22 to 25, the stem strain increased as the light level increased. At any light level considered, the strain increased as the temperature increased except for the first day (see Figures 26 to 29). For light levels L_1 and L_2, the strain for temperature T_3 is the lowest followed by those of T_1, T_2 and T_4 in that order. For light levels L_3 and L_4, the strain for temperature level T_1 is the lowest followed by those of T_3, T_2 and T_4 in that order. It is possible that the trees acclimatize to temperature faster than light for this anomaly in the strain pattern to occur. In other words, the two days acclimatization given to the trees may have been enough for temperature acclimatization but not for light. To check this, the acclimatization time of two days will have to be increased. At any temperature level considered, the strain variations at light levels L_3 and L_4 are closer compared to any of the others, Figures 22 to 25. This can also be noticed by comparing the strains at light levels L_3 and L_4, Figures 28 and 29. The values of L_3 and L_4 however have the largest difference compared to any two consecutive light level values.

This clearly suggests that the strain increase at any temperature is nonlinear with light intensity (see discussion on page 121).

With reference to the starting point, the general strain pattern was positive throughout the test. Therefore, the trees placed permanent strain on the gages by growing. This was used to assess growth in the tree as discussed later (page 121). The results display a small increase in strain at night. This could be due to the fact that the trees used in the investigation were young and in a relatively fast growing period. Also in general, the populus family of trees is a fast growing one compared to other trees.

The second (middle) graphs in Figures 22 to 29 show the total water loss per unit leaf area in grams/cm^2. The graphs are discontinuous. They start each day after watering to field capacity. The cumulative losses as obtained from the recorder were divided by the respective leaf areas of the trees and the results were plotted from that time on for the remaining 24 hours of each day. The curves display a small water loss during the night. A covered pot of moist soilless mix placed in the growth chamber for 24 hours virtually lost no water even under day conditions. Thus the water loss at night by the trees could not be due to evaporation from the pot. It is possible that the small nightly water loss was just cuticular transpiration or transpiration through the

lenticells on the stem or both. Normally cuticular transpiration on a bright sunny day accounts for about 10% of the total transpiration of some species (54).

The cuticle is a thin waxy covering on top of the leaf just next to the epidermis which is the outermost cell layer of the leaf. The lenticells are pores on the stem and branches. The water loss records in Figures 22-29 do not take into account any increase in biomass. The increase in biomass is expected to be negligible compared to the weight of water evaporated for such a short term investigation.

It is known that when light comes on the stomata of leaves open and trees start transpiring. According to Greulach (54) temperature also influences the opening and closing of the stomata. At temperatures of around 0°C (32°F) or less the stomata of most species remain closed even during the day, whereas at temperatures of around 40°C (104°F) stomata may open at night (54). Between 0°C and 28°C (32°F and 82.4°F) the degree of stomatal opening in some species has been found to be proportional to the temperature (54). For example, Devlin (55) quotes Wilson as having reported that for cotton under constant light intensity the stomatal aperture is proportional to temperature from 5°C to 25°C (41°F to 77°F). This seems also to be the case for the young populus clone. As night temperatures increased, the water loss during the night increased. For example at light intensity level L_1,

Figure 26, the total water loss during the night at temperatures T_1, T_2, T_3 and T_4 are 0.05, 0.08, 0.12 and 0.15 gm cm^{-2} respectively. This conclusion is true for the day also - that is, at any light intensity level considered, Figures 26 to 29, the transpiration increased as the day temperature increased which is not contrary to expectation. The only exception to this conclusion occurs during the first few hours after watering for temperature levels T_2 and T_3 when the total transpiration at temperature level T_2 was higher than that of level T_3, Figures 26 to 29. This anomaly occurred at all light levels considered. The period of time during which the total transpiration at temperature level T_2 was higher than that of level T_3 varied with the day and there is no general pattern.

At any temperature level considered the total transpiration at any time increased as the light level increased. This is not contrary to expectation because the opening of the stomata increases as the light intensity increases. The relationship is not linear though. This is shown in Figure 33 for the case of total transpiration for a day.

The highest total water loss per unit leaf area was obtained in R_{44}, followed by R_{43}, R_{34} and R_{42}, Figures 24 and 25. The lowest was recorded for run R_{11} followed by R_{12} and R_{21} which lost about the same amount of water, Figures 22 and 23.

The third (lowest) graphs in Figures 22 to 29 show the average rate of water loss per unit leaf area (gm cm^{-2} hr^{-1}) over periods of one hour as read from the second graph. The average value was computed by reading the water loss on each hour computing the average over that hour and plotting it as a central difference on the half hour. For example:

The total water loss at hour 6 for R_{41} = 0.076 gm cm^{-2}

The total water loss at hour 7 for R_{41} = 0.065 gm cm^{-2}

The average rate of water loss = 0.076 - 0.065

= 0.011 gm cm^{-2} hr^{-1}

This value is plotted at time 6 1/2 hours. Straight lines connect these data points. From these rate of transpiration graphs the following conclusions can be made:

1. In all cases the rate of water loss was constant at night. This is due to the fact that the water loss at night was linear with respect to time (see second graph in Figures 22 to 29).
2. In all cases the rate of transpiration was high immediately after watering and it reduced with time. This should be expected because by the time the tree was watered it had used almost all the water supplied to it during the previous watering.
3. When light and temperature triggered on the rate increased rapidly. This is not surprising because the stomata of the leaves open at the onset of light.

4. At temperature levels T_1, T_2 and T_3 the rate of transpiration increased with increasing light intensity. At temperature level T_4 however, the rate of transpiration increased in the order L_1, L_3, L_4 and L_2. That is rate of transpiration was highest at light level L_2 when the temperature level was T_4 (Figures 22 to 25). The variation of a number of biological processes have the tendency of increasing from a low value to a maximum value and then leveling off or decreasing as the dependent variable increases. This seems to be what is happening at the temperature T_4. Thus if the rate of transpiration at T_4 at any time is plotted against light intensity the curve will increase with increasing light intensity to a maximum value around light level L_2 and decrease again, or level off as the light intensity increases (see Figure 30a).
5. The lowest night rate was 0.001 gm cm^{-2} hr^{-1} and this occurred for R_{11}, R_{12} and R_{21}, Figures 22 and 23 or Figures 26 and 27. The highest night rate was 0.005 gm cm^{-2} hr^{-1} and it occurred during R_{44}, Figures 25 and 26.

7. At light levels L_1 and L_2 the rate of transpiration during the day before darkness was highest for temperature level T_4 followed by T_3, T_2 and T_1 in descending order, Figures 26 and 27. Thus the rate increased as the temperature increased as expected. At light levels L_3 and L_4 however the order is T_3, T_4, T_2 and T_1 in descending order, Figures 28 and 29. The phenomenon mentioned above is likely to be occurring here too. That is at light levels L_3 and L_4, a plot of rate of transpiration against temperature at any time will peak around T_3 (see Figure 30b). This is not an unusual biological phenomenon.
8. After day break, the rates were quite clustered together with a pattern which cannot easily be explained. The low transpiration rate at T_4 for L_4 after day break may however be explained by the fact that at temperatures above 86°F the stomata of some species close or reduce in aperture. The temperature effect of the light added to the high temperature of 85°F may be high enough to contract the stomata of the tree thereby giving low rates of transpiration. Also the trees were given the same amount of water (a liter or a little more gave field capacity conditions). For R_{44} the total

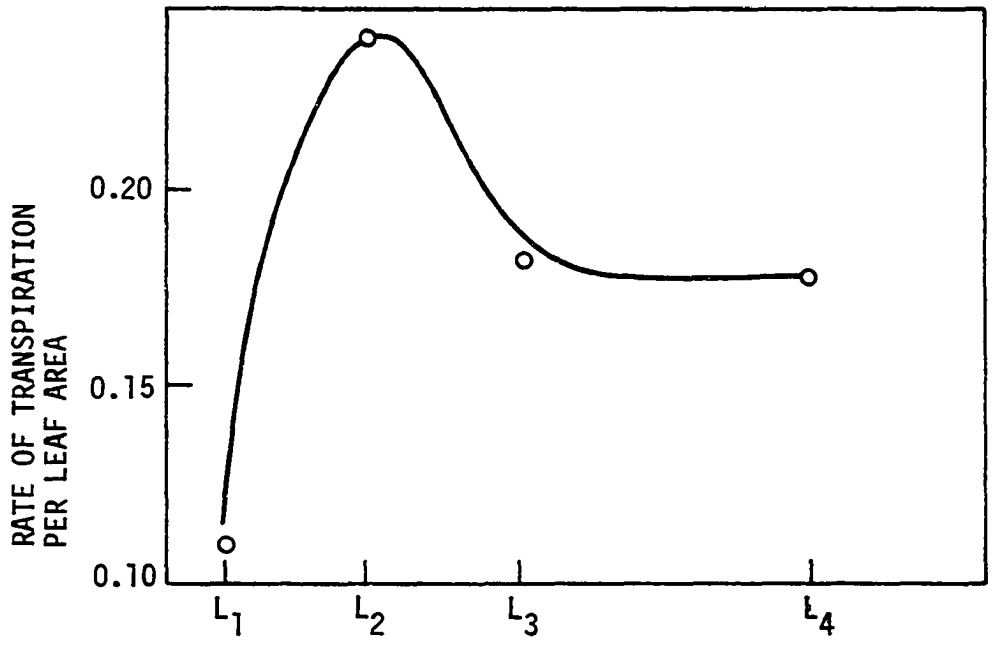

Fig. 30a. Rate of transpiration on 6th hour of first day vs light at 85 °F

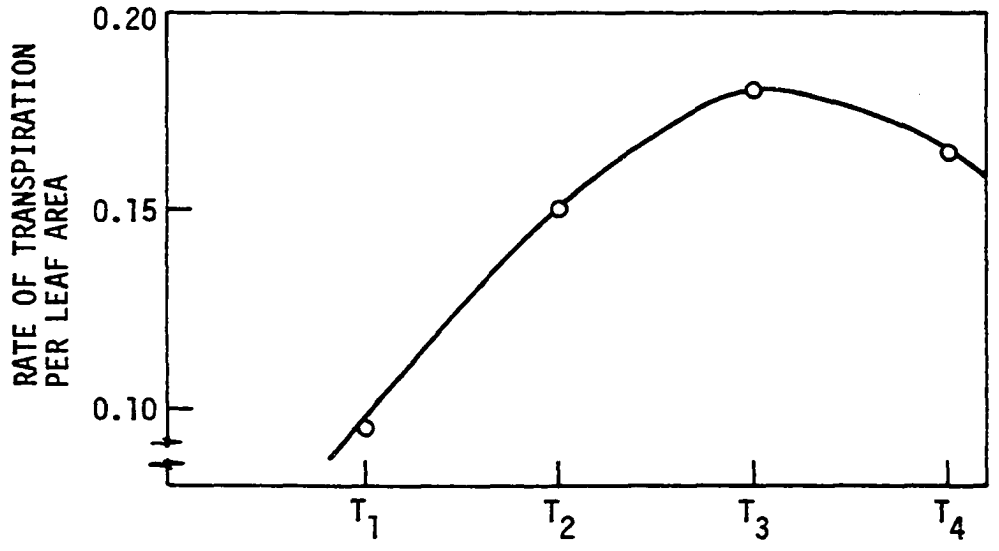

Fig. 30b. Rate of transpiration on 6th hour of second day vs temperature at 180 μ-Einsteins m^{-2} s^{-1}

transpiration for a day was a liter in one case. It is possible that after day break, the soil moisture became limiting for this run thereby giving low rates of transpiration.

The maximum strain recovery on watering for each run was read for the times the trees were watered from Figures 22 to 29. The readings so obtained were averaged for each test run. For example the maximum strain recovery for R_{41}, Figure 25 or Figure 26 are 350 με, 380 με and 350 με giving an average of 360 με. The average times taken to recover these maximum strains were calculated in a similar way for the various runs. From the strain graphs (see top graphs in Figures 22 to 29), it is obvious that when the light and the temperature went off the strain in the gage increased and when the light and the temperature came on the strain in the stem decreased. The respective stem strain increases and decreases as the light and the temperature went off and on did not vary much from day to day for the various runs. For example for R_{41}, Figure 25 or Figure 26, the stem strain increases when the light and temperature went off were 270 με, 300 με, 320 με and 300 με giving an average of 298 με. These strain values were read from the point at which the light and the temperature went off up to the point of maximum strain during the night. All the runs took almost the whole night to reach this maximum value. The maximum stem strain

decrease when the light and the temperature came on for R_{41}, Figure 25 or Figure 26, were 520 με, 580 με, 670 με and 620 με giving an average of 598 με. These stem strains were read from the point at which the light and the temperature triggered on up to the minimum point reached before the stem started increasing in strain again. The times taken to achieve these strain reductions were also read, and averaged. These maximum average stem strain values and the average times taken to reach these values are given in Table 1. It is amazing to note how close these strains and times are for the various runs.

From Table 1 it is seen that the numerical value of the decrease in stem strain when the light and the temperature came on varied for the different runs but it was always much higher than the numerical value of the increase in stem strain when the light and the temperature went off.

The average strain recovery on watering is plotted against light intensity in Figure 31a. The average recovery times for these strains are plotted against light intensity in Figure 31b. The average strain recovery on watering at any light intensity considered increased as the temperature increased. The average recovery time is seen to be independent of light intensity. The curves obtained for the other columns in Table 1 are as shown in Figures 32a to 32d. Very little can be said about these graphs in the form of explanation.

Table 1. Average strain changes and average times for the changes

Test run	Average amount of strain recovery on watering (με)	Average strain recovery time on watering (minutes)	Average stem strain change when light and temperature come on (με)	Average stem strain change when light and temperature go off (με)	Average time for maximum stem contraction when light and temperature come on (minutes)
R_{11}	150	25	445	250	72
R_{12}	155	25	558	300	76
R_{13}	170	25	648	250	80
R_{14}	200	25	715	300	98
R_{21}	220	15	515	300	82
R_{22}	220	15	540	300	85
R_{23}	233	15	615	300	91
R_{24}	273	15	670	250	104
R_{31}	260	15	512	300	87
R_{32}	240	15	563	300	90
R_{33}	243	15	790	300	93
R_{34}	317	15	814	300	110
R_{41}	360	10	598	298	89
R_{42}	362	10	666	300	90
R_{43}	373	10	630	250	96
R_{44}	393	10	820	300	110

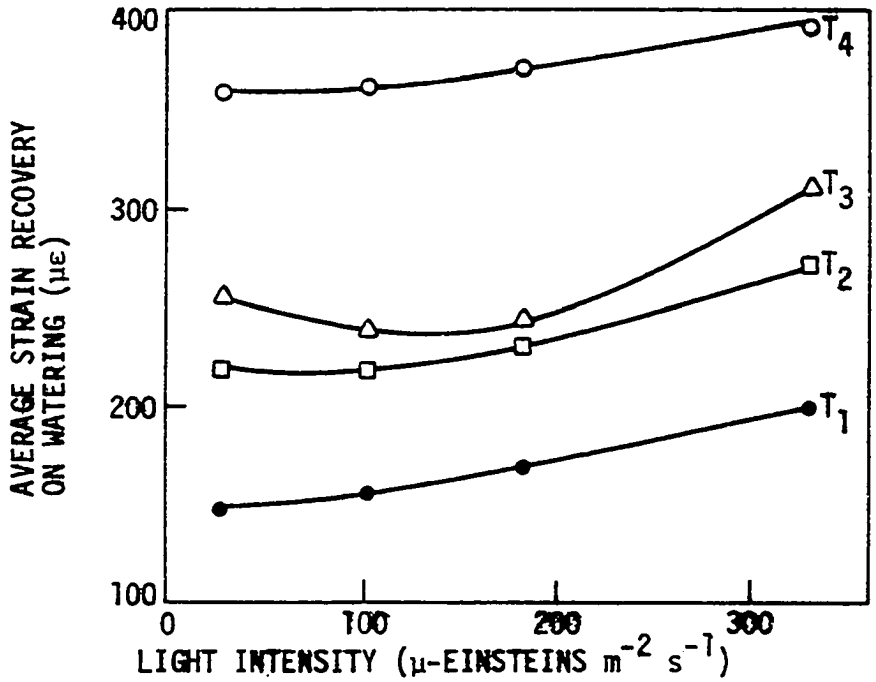

Fig. 31a. Average strain recovery on watering vs light intensity T_1 = 55 °F; T_2 = 65 °F; T_3 = 75 °F; T_4 = 85 °F

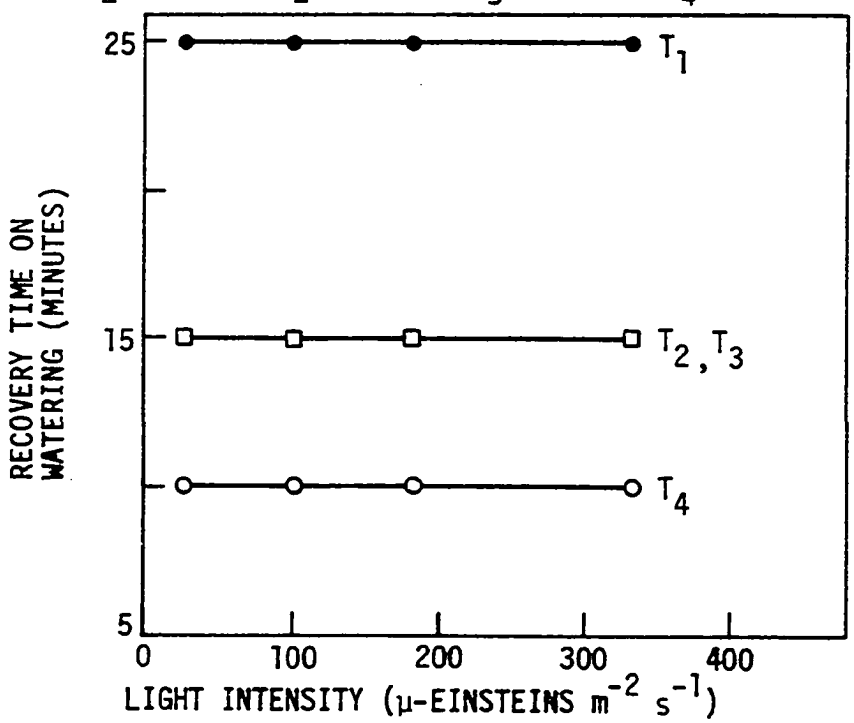

Fig. 31b. Average strain recovery time on watering vs light intensity T_1 = 55 °F; T_2 = 65 °F; T_3 = 75 °F; T_4 = 85 °F.

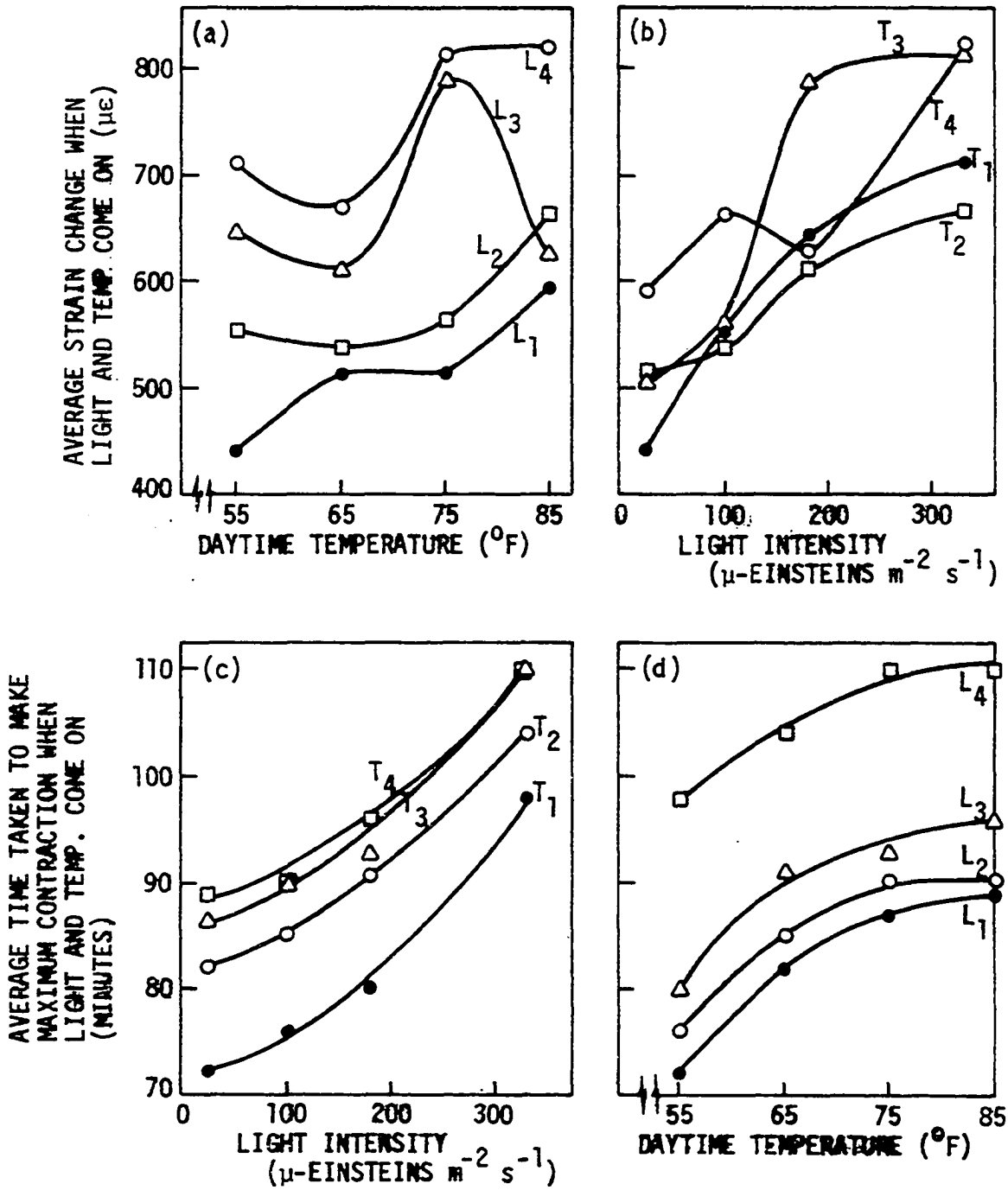

Fig. 32. Variations of stem strain change and average time for the change with temperature and light intensity.

It is worth noting, however, tnat the average time taken to achieve maximum contraction when light and temperature came on increased as the light intensity increased for a given temperature within the temperature domain and light intensity domain considered (Figure 32c). From Figure 32d it is seen that the average time taken to achieve maximum contraction when light and temperature came on increased with temperature. The rate is high at temperatures between 55°F and 70°F after which the slopes become gentle.

The total water loss per watering cycle (one day) per square centimeter of leaf area was calculated for each day for each water loss curve in Figures 22 to 29. The total water loss per watering cycle per unit leaf area did not vary much from day to day as can be seen from these figures. The average total water loss per watering cycle per unit leaf area was worked out over four days for each run. For example for R_{41}, Figure 25 or Figure 26 the total water losses per watering cycle were 0.221, 0.220, 0.225 and 0.230 gm cm^{-2}. This gave an average of 0.224 gm cm^{-2}. Such average water loss per watering cycle per unit leaf area values computed in the manner shown for the various runs were used to plot the graphs in Figure 33. This figure shows that at any temperature level considered, the total water loss per watering cycle per unit leaf area increased as the light

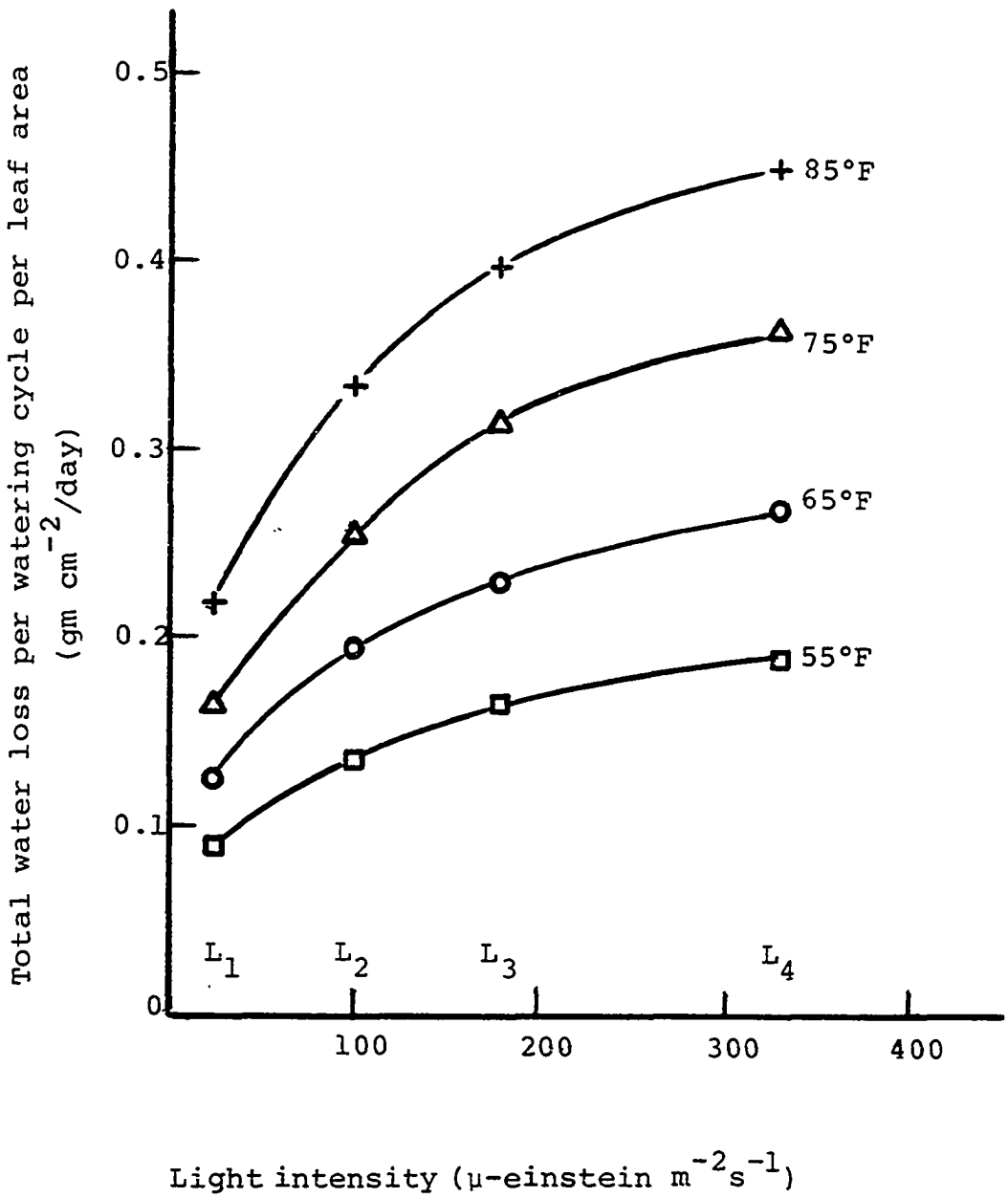

Figure 33. Variation of total water loss per watering cycle per leaf area with light intensity for various daytime temperatures

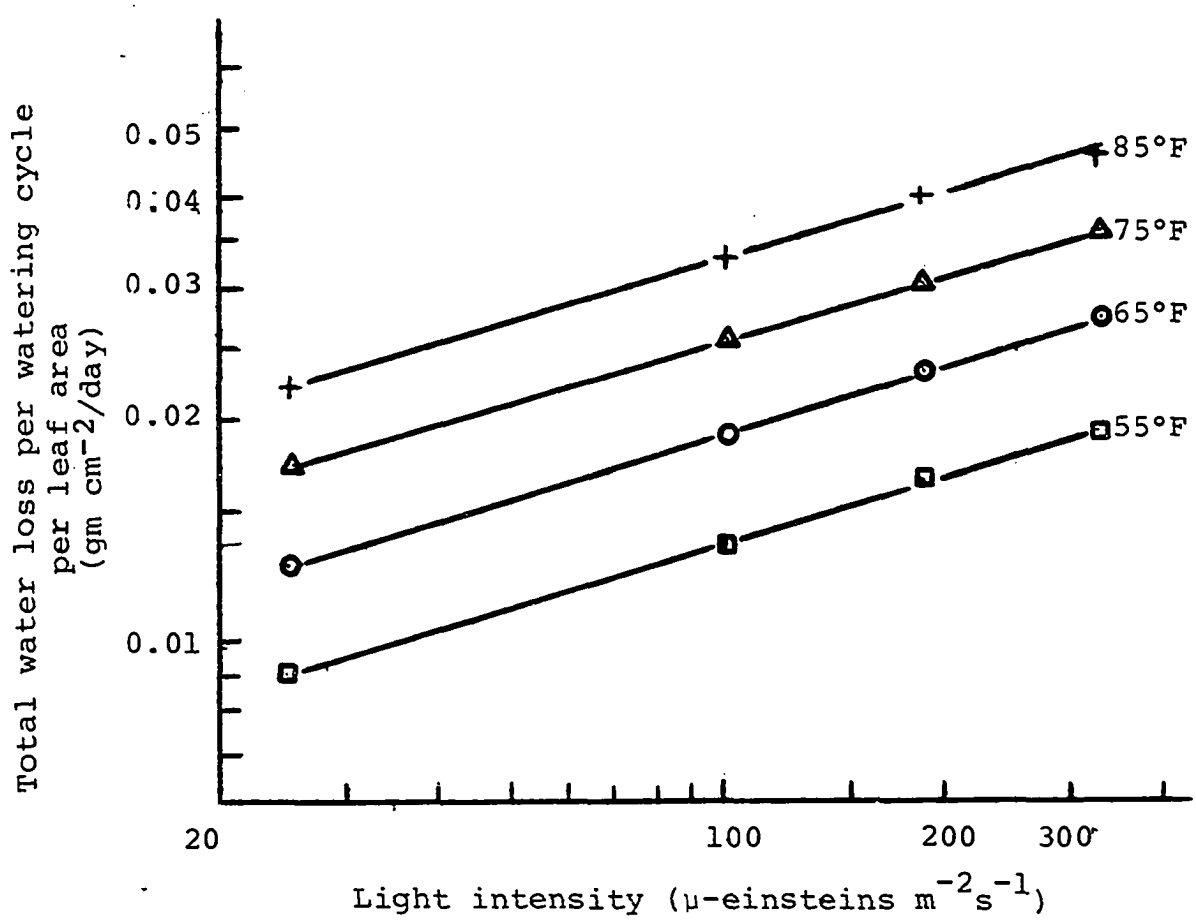

Figure 34. Variation of total water loss per watering cycle per leaf area with light intensity for various daytime temperatures

intensity increased. All the curves have steep gradients at low light levels. As the light level increased the gradients became more gentle. This suggests two things. Either:

1. the curves may level off and saturate at light intensities greater than L_4, i.e. the curves may be asymptotic to some maximum value at light levels higher than L_4, or
2. the curves may hit a maximum value of water loss at some light intensity level and exhibit lower water loss values at light intensities higher than the one which maximizes the water loss. None of these could be tested because higher light intensities were not achievable in the growth chambers used.

The graphs in Figure 33 plotted on a log-log sheet yield straight lines, Figure 34. This means that the total water loss per watering cycle per unit leaf area can be determined from an equation of the form:

$$W_T = cL^{\alpha} \qquad (8)$$

where

W_T = total water loss per watering cycle per leaf area (gm cm^{-2}/day)

c = a constant

L = light level (μ-einsteins $m^{-2}s^{-1}$)

α = a constant

The values of c and α for the various temperature levels are:

	T_1	T_2	T_3	T_4
c	0.034	0.047	0.059	0.088
α	0.2988	0.3051	0.3054	0.2875

Within the limits of experimental errors, α can be taken as 0.3 for the temperature range considered. The total water loss per watering cycle per unit leaf area is thus given by:

$$W_T = cL^{0.3} \text{ gm cm}^{-2}/\text{day} \qquad (9)$$

where c is as given above. It is obvious that c is a function of temperature. When c is plotted against temperature on a semi-log sheet, the graph in Figure 35 is obtained. This means that c and temperature are connected by an equation of the form:

$$c = Ae^{zT} \qquad (10)$$

where

A = a constant

z = a constant

T = temperature (°F)

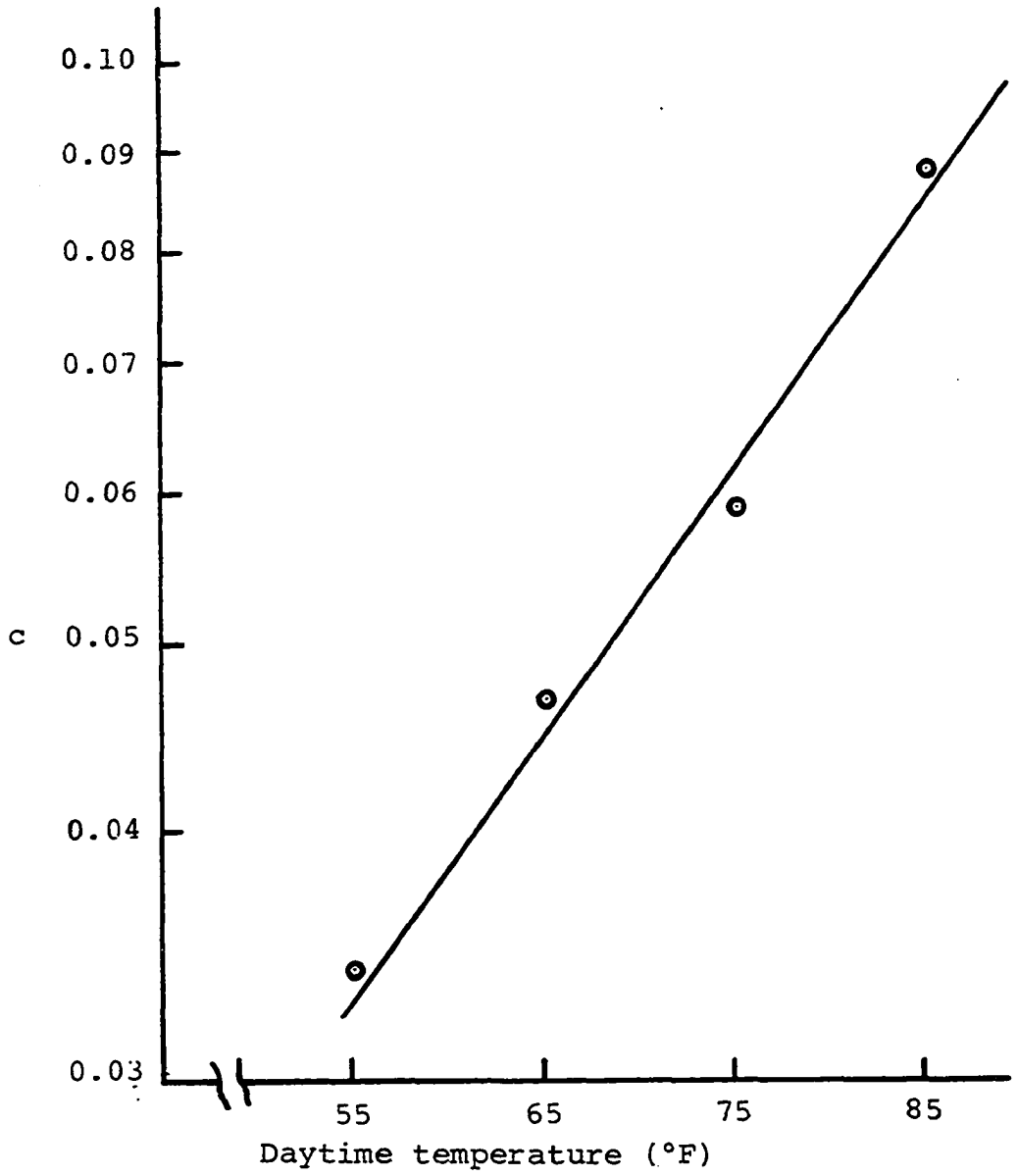

Figure 35. Variation of c with daytime temperature

A works out to be 0.0062, and z = 0.0308. Thus Equation 9 becomes:

$$W_T = 0.0062e^{0.0308T} L^{0.3} \text{ gm cm}^{-2}/\text{day} \quad (11)$$

Therefore within the temperature and light intensity limits considered, the total water loss per leaf area per day can be computed from Equation 11 with a knowledge of T and L. For a day temperature of 60°F and a light level of 180 μ-einsteins $m^{-2}s^{-1}$, Equation 11 gives a W_T of 0.187 gm cm^{-2}/day.

The total water loss per day per unit leaf area for the various runs were plotted against temperature for the various light levels considered. The graphs so obtained are displayed in Figure 36. The graphs show that at any light level considered, the total water loss per day per unit leaf area increased linearly with temperature. The lines fan out as the temperature increases. When the lines in Figure 36 are extrapolated, they meet at point P (see dotted lines in Figure 36). It is apparent from the graphs that the trees will not loose any water at 33°F, 34°F, 35°F and 36.5°F for light intensities L_4, L_3, L_2 and L_1 respectively. This is not contrary to expectation since at temperatures around freezing point the stomata of most species close even during the day. Due to the linearity of the graphs in Figure

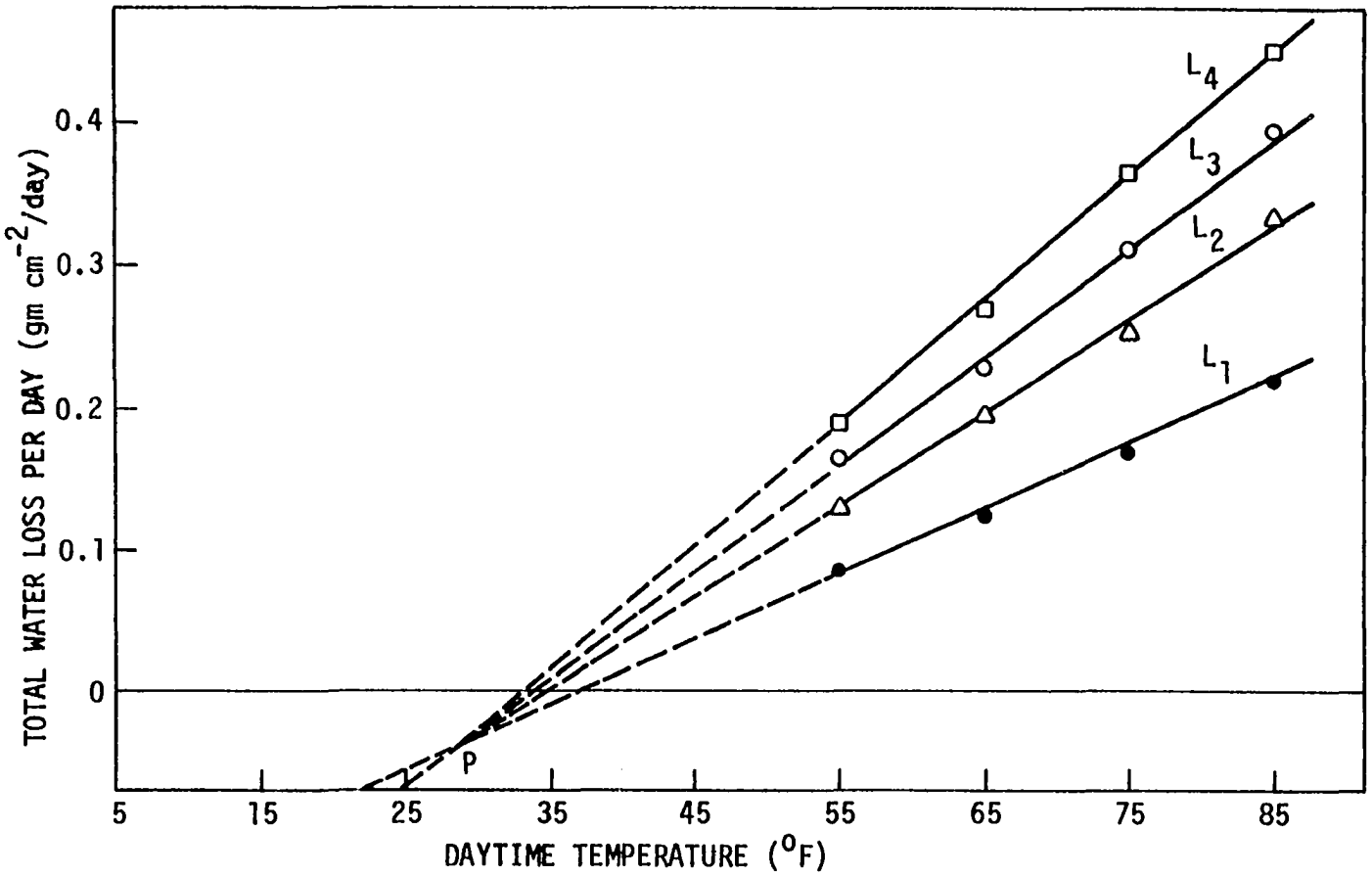

Fig. 36. Variation of total water loss per leaf area per day with day temperature for different light intensities

36, the total water loss per day per unit leaf area can be determined from an equation of the form

$$W_T = \beta + mT \tag{12}$$

where

W_T = total water loss per day per unit leaf area (gm cm^{-2}/day)

β = a constant (gm cm^{-2}/day)

m = a constant (gm cm^{-2}/°F)

T = day temperature (°F)

The values of β and m for the various light intensities are:

	L_1	L_2	L_3	L_4
β	-0.151	-0.232	-0.266	-0.294
m	0.0043	0.0066	0.0078	0.0088

Both β and m appear to be functions of light intensity, L. The positive values of β plot as a straight line against L on a log-log graph (see Figure 37). Therefore, β is of the form

$$\beta = -\phi L^n \tag{13}$$

where ϕ and n are constants. From the plot ϕ = 0.0647 and n = 0.268. Thus β is given by

$$\beta = -0.0647\ L^{(0.268)} \tag{14}$$

Light intensity, L and m (Equation 12) plot as a straight line

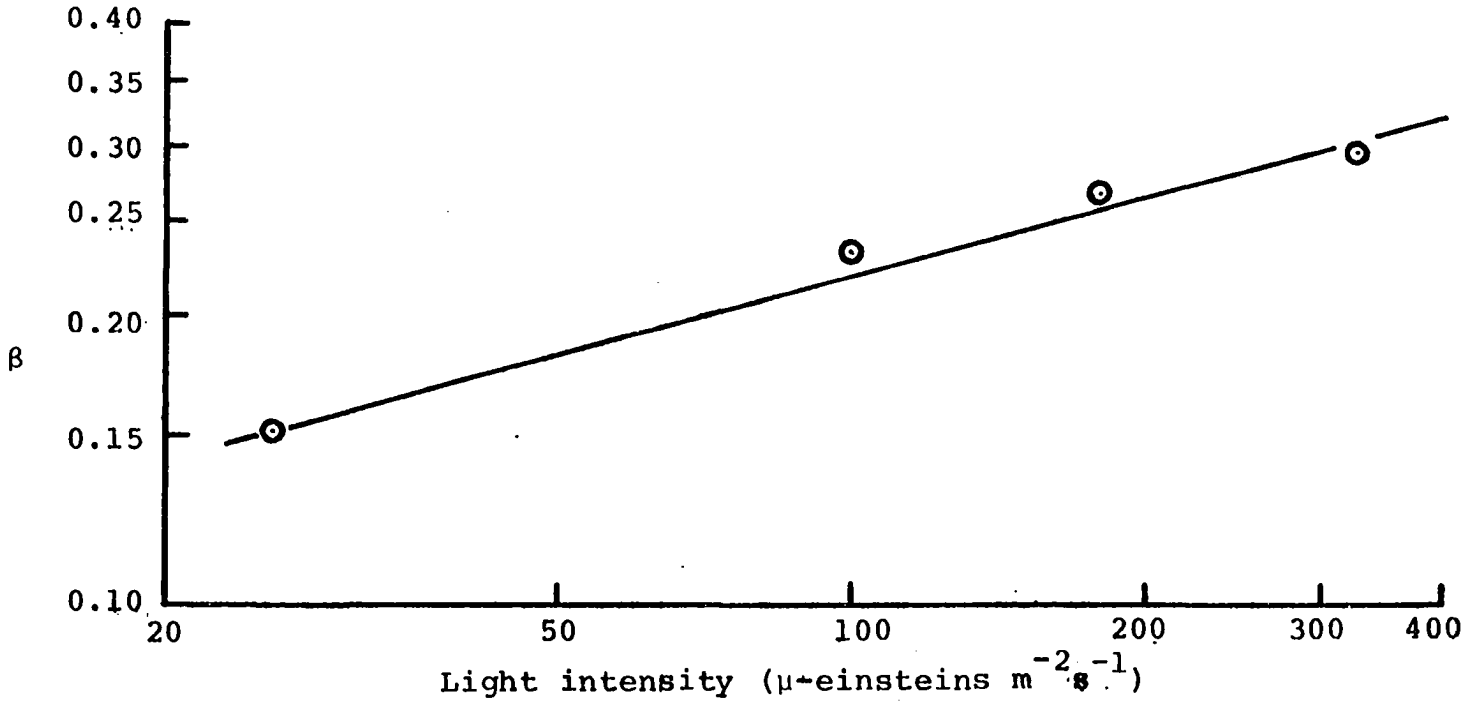

Figure 37. Variation of β with light intensity

on semi-log graph (Figure 38). Thus L and m are related in this form:

$$L = \gamma e^{\psi m} \quad \text{or} \quad m = \ln(L/\gamma)/\psi \tag{15}$$

where

γ is a constant, ψ is a constant,

γ works out to be 2.37,

ψ works out to be 560.

Thus

$$m = \ln(L/2.37)/560$$

$$m = (\ln L - \ln 2.37)/560$$

$$m = (\ln L - 0.863)/560 \tag{16}$$

Equation 12 then becomes:

$$W_T = -0.0647\ L^{(0.268)} + \frac{(\ln L - 0.863)T}{560} \tag{17}$$

Therefore with a knowledge of the day temperature and the light intensity, the total water loss per day per unit leaf area can be computed from either Equation 11 or Equation 17. For a day temperature of 60°F and a light intensity of 180 μ-einsteins $m^{-2}s^{-1}$ Equation 17 gives a W_T of 0.204 gm cm^{-2}/day which compares well with the 0.187 gam cm^{-2}/day given by Equation 11 for the same temperature and light conditions. For the same light and temperature conditions, Figure 36 gives a W_T value of 0.200 gm cm^{-2}/day.

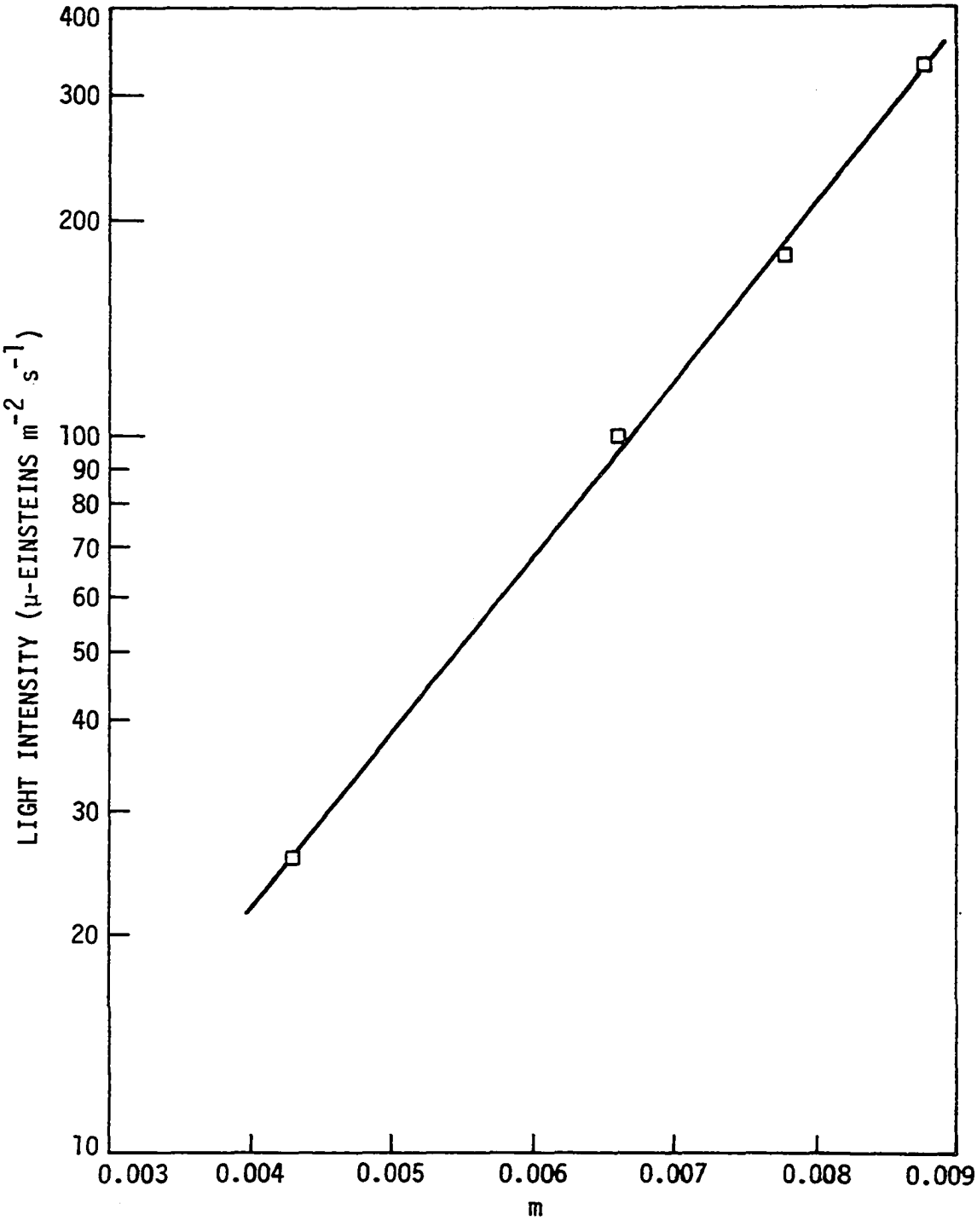

Fig. 38. Variation of light intensity with m.

Using the middle of the period of darkness as reference points, the total increase in strain between the first night and the fourth night were calculated for each of the test runs from Figures 22-29. The values so obtained were the permanent strain increases imparted to the gages by the stem in three days. These permanent strain values are plotted against light intensity in Figure 39 and against temperature in Figure 40. In all cases considered, the permanent increase in strain over the three days increased as the light intensity increased, Figure 39. The curves peak at about 180 μ-einsteins $m^{-2}s^{-1}$ light intensity for day temperatures of 65°F and 75°F. At 55°F and 85°F day temperatures, however, the curves will peak at a higher light intensity. This peak does not quite show in Figure 39 due to light intensity limitations in the growth chamber. These curves show that at 75°F and 85°F, the permanent strain imparted to the trees do not differ much. This can also be seen from Figure 40.

The permanent strain values used for plotting the graphs in Figures 39 and 40 were converted to permanent growth values by multiplying the strain values by the diameters of the trees at the points where the gages were mounted. These growth values are tabulated (Table 2b, p. 137) for the trees used for the various runs. The averages of these growth values have been used in plotting the graphs of

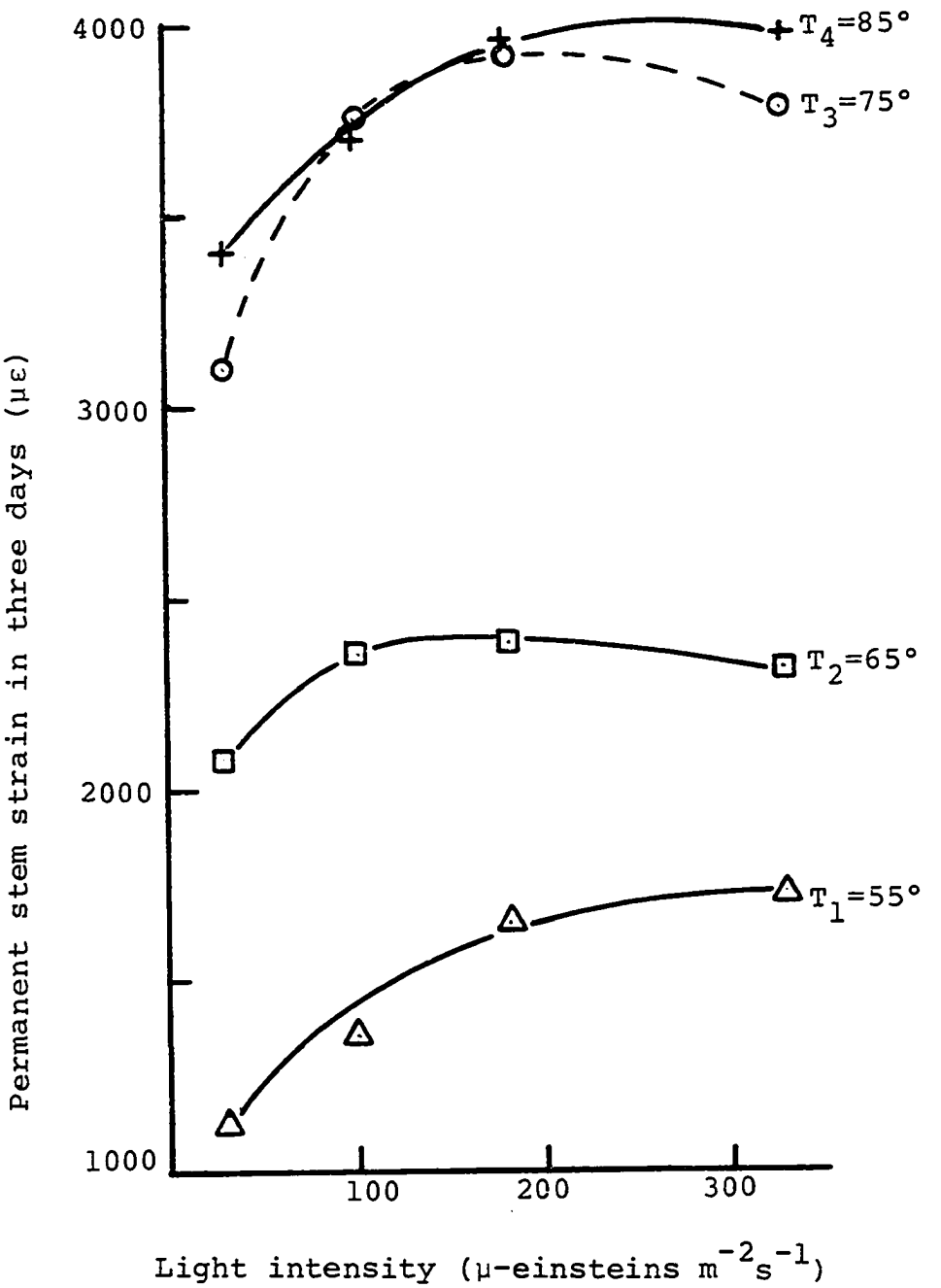

Figure 39. Permanent stem strain variation with light intensity for various temperatures

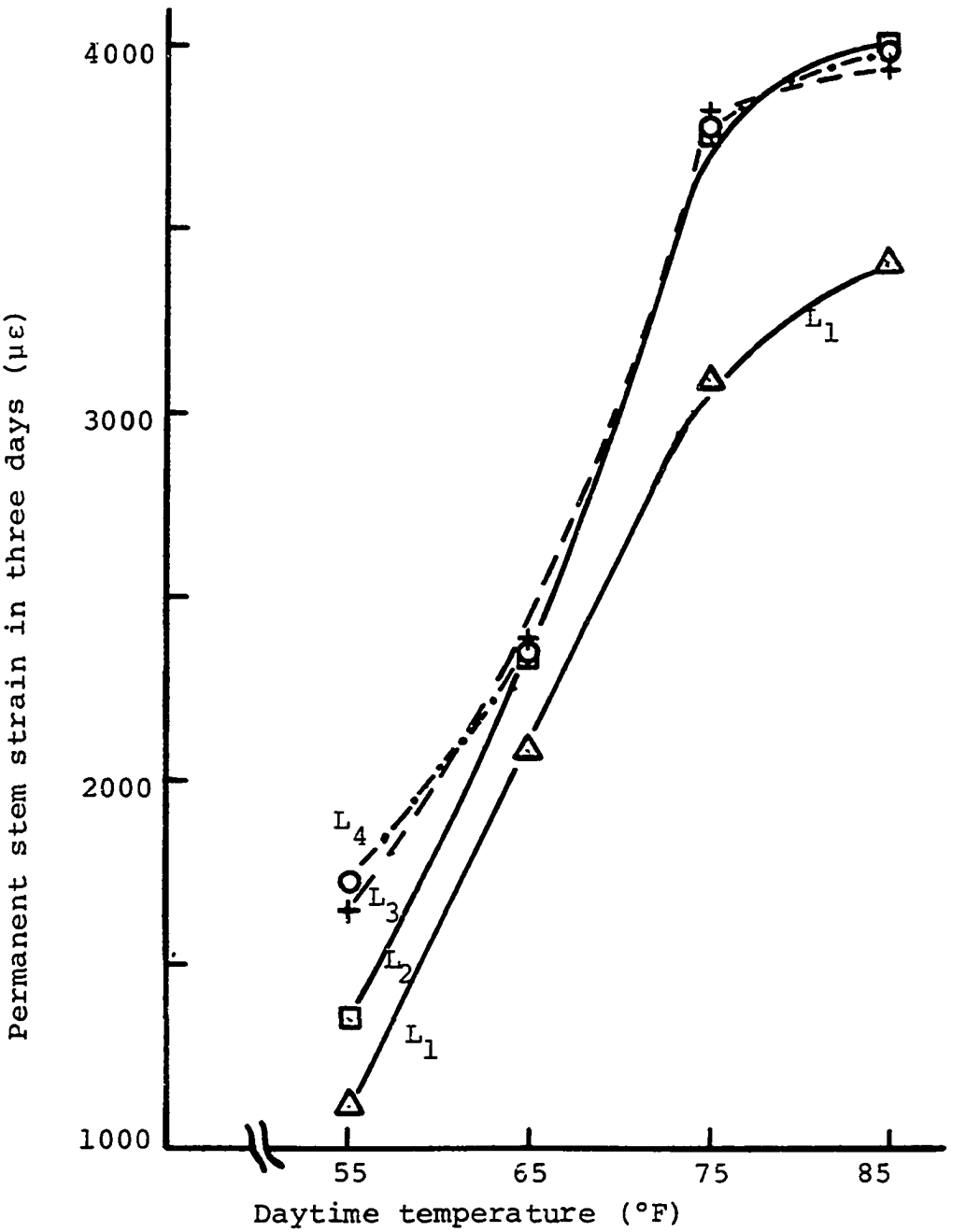

Figure 40. Permanent stem strain variation with daytime temperature for various light intensities

growth over three days against light intensity in Figure 41, and against temperature in Figure 42. The conclusions that can be made from these figures are:

1. As light intensity increased, growth increased for a given temperature. Fasehun and Gordon (56) also found this conclusion to be true for vertical growth for populus clones 5323, 5326 and 5328 under green house conditions. Williamson and Splinter (57) also working in a growth chamber found that diametral growth of tobacco increased as the light intensity increased.
2. As temperature increased, growth increased for a given light intensity. Williamson and Splinter (57) also found this conclusion to be true for tobacco under growth chamber conditions.
3. Growth did not increase much from a day temperature of 75°F to 85°F.

The conclusions 1 and 2 above have been known for a long time. A major contribution here, however, is the ability to get detailed measurements of diametrical growth over short time intervals.

Figure 41 plots as straight lines on semi-log graph, Figure 43. Therefore, the variation of growth with light intensity within the range considered is of the form

$$L = De^{rG} \quad \text{or} \quad G = \frac{\ln L - \ln D}{r} \tag{18}$$

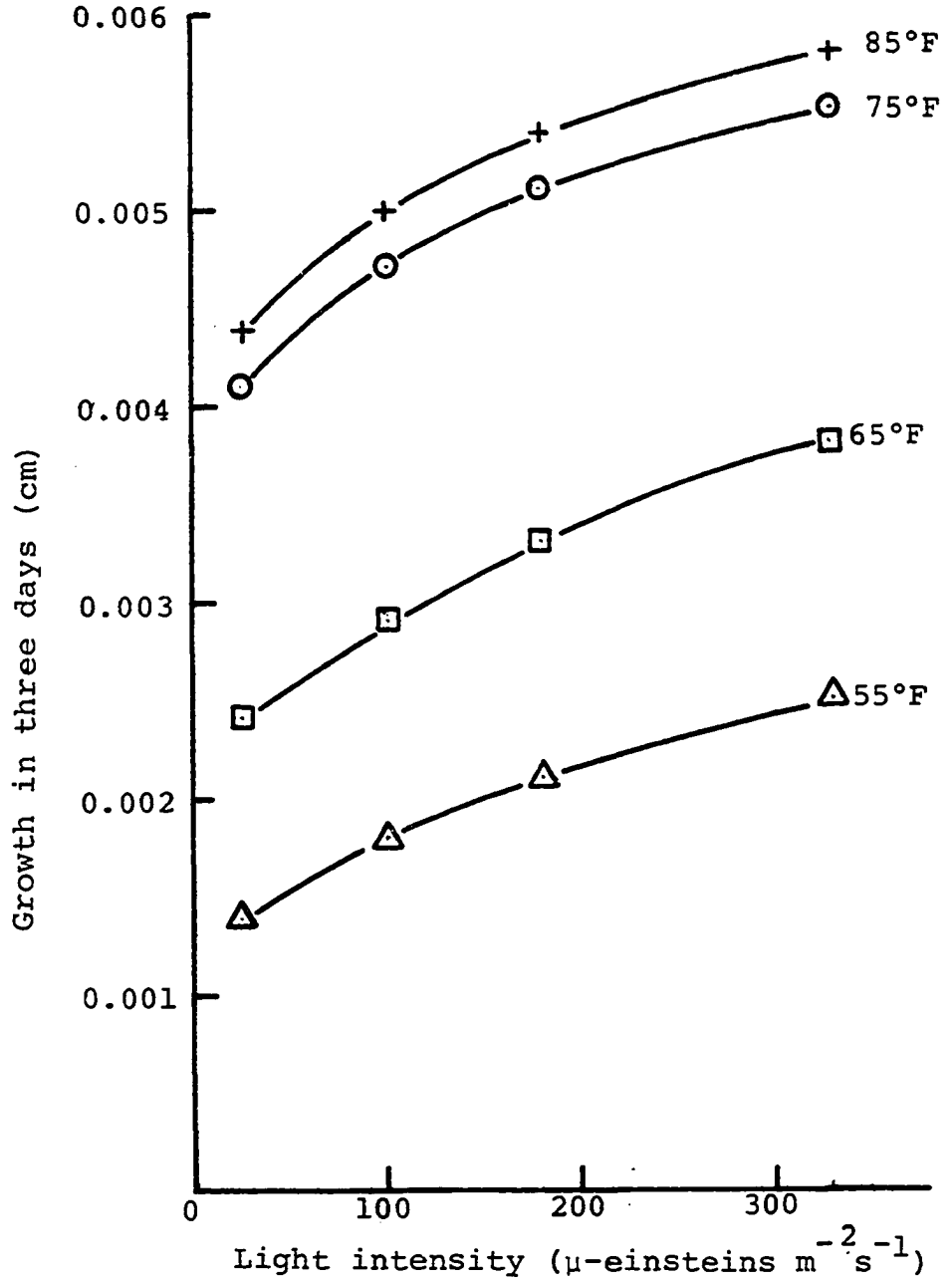

Figure 41. Variation of growth with light intensity for various day temperatures

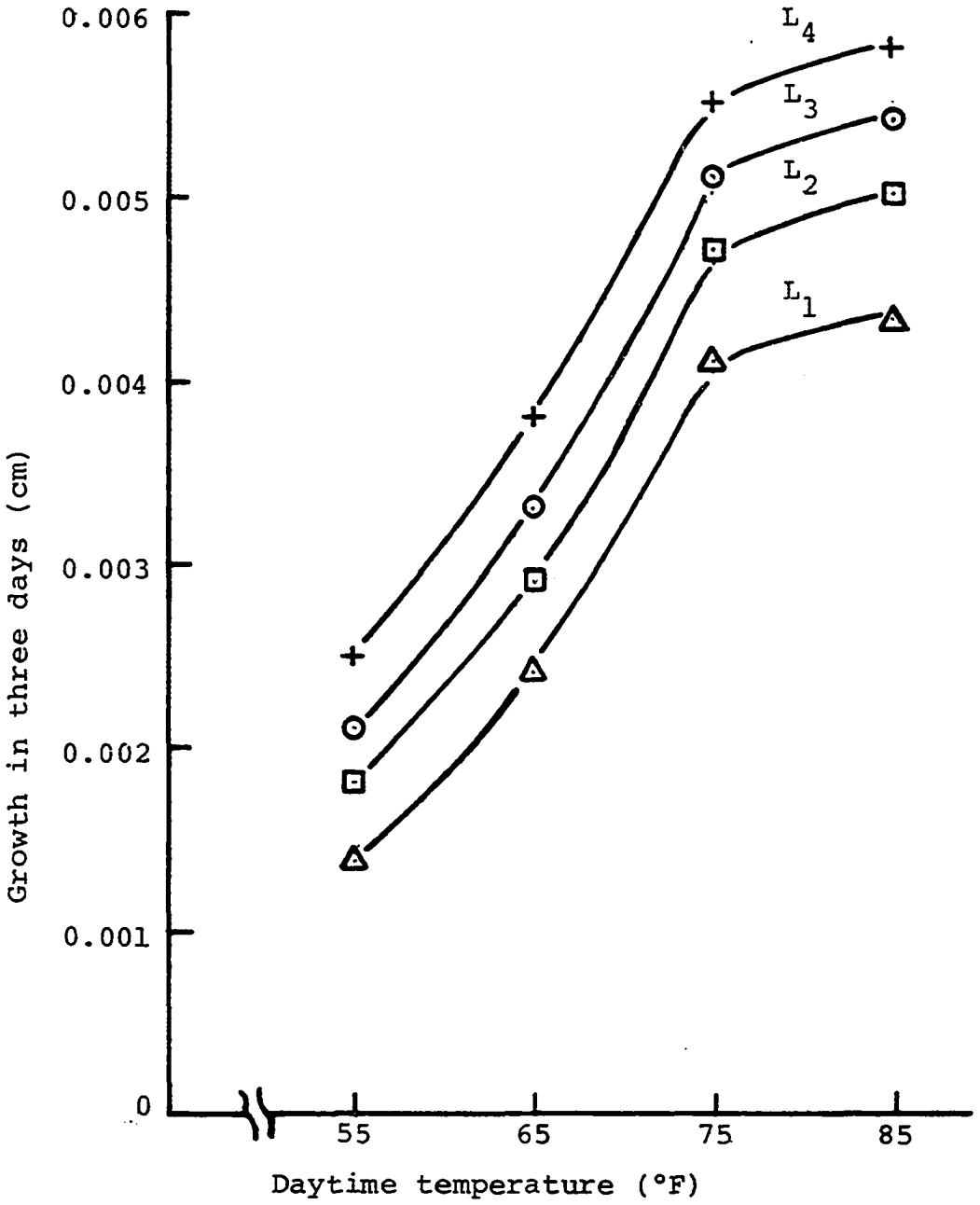

Figure 42. Variation of growth with daytime temperature for various light intensities

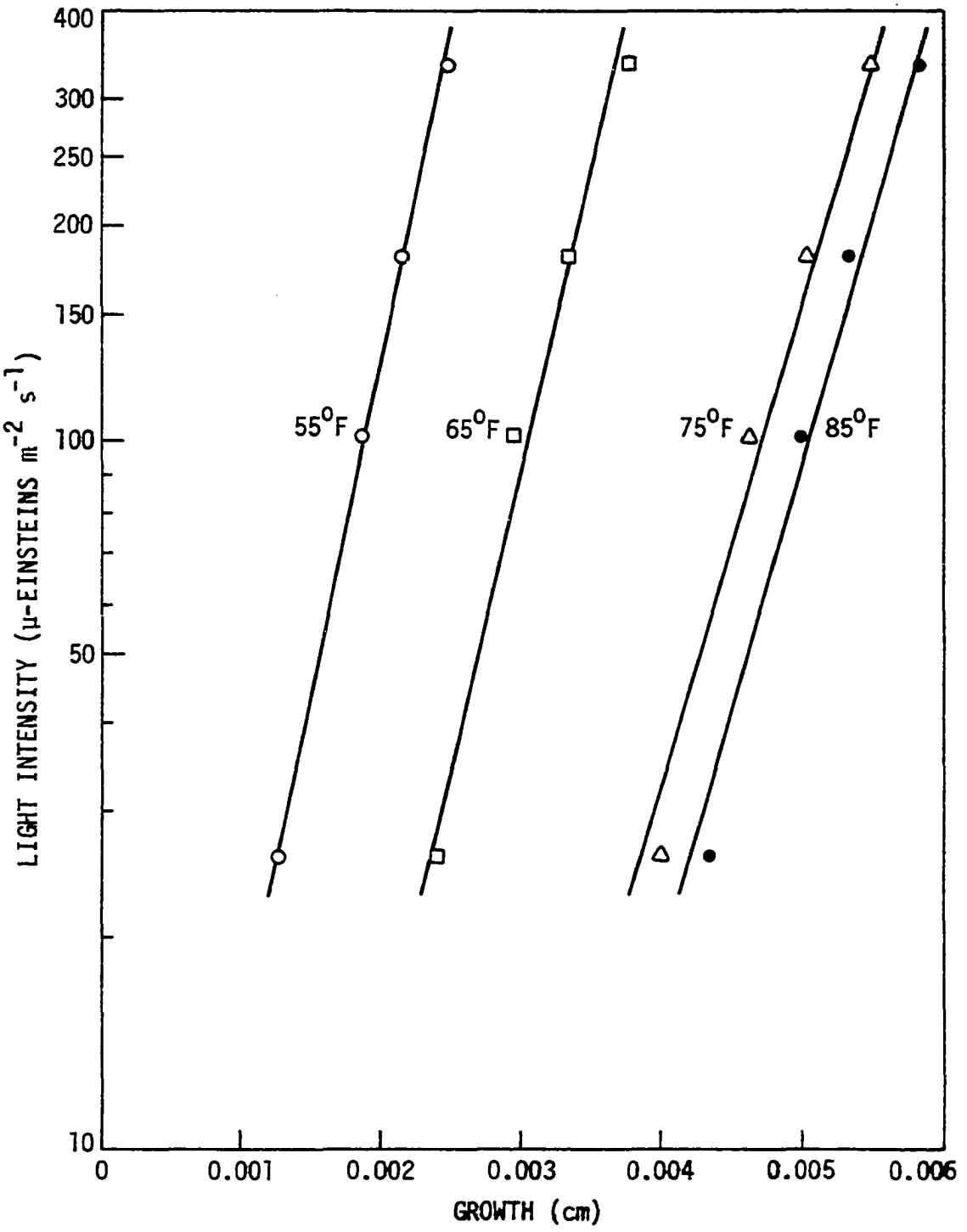

Fig. 43. Graph of light intensity against growth for various day temperatures.

where

G = growth (cm)

L = light intensity (μ-einsteins $m^{-2}s^{-1}$)

D = a constant

r = a constant

The values of D and r for the various temperatures are:

	T_1	T_2	T_3	T_4
D	1.428	0.3927	0.0390	0.0172
r	2234.6	1814.8	1666.4	1721.2

Both D and r are functions of T (see Figures 44 and 45). The variation of D with T is logarithmic (D and T plot as a straight line on a log-log graph), Figure 44 while the variation of r with T is a second order curve, Figure 45. D can therefore be written as

$$D = kT^n \tag{19}$$

where k and n are constants. k works out to be 7.8×10^{18} and n is -10.74

$$\therefore D = 7.8 \times 10^{18} T^{-10.74} \tag{20}$$

The second order equation relating r and T is:

$$r = 1.355 T^2 - 205 T + 9420 \tag{21}$$

Equation 18 then becomes

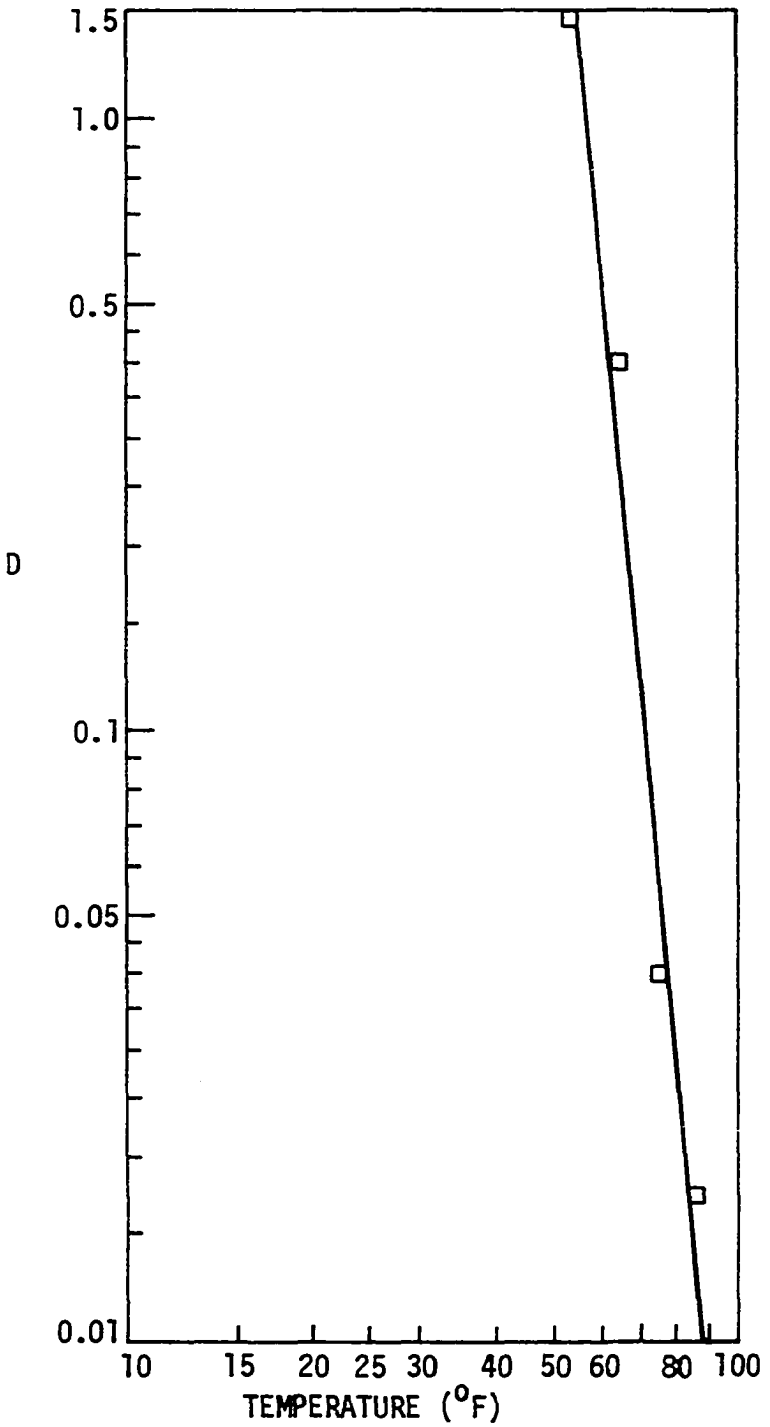

Fig. 44. Graph of D against temperature

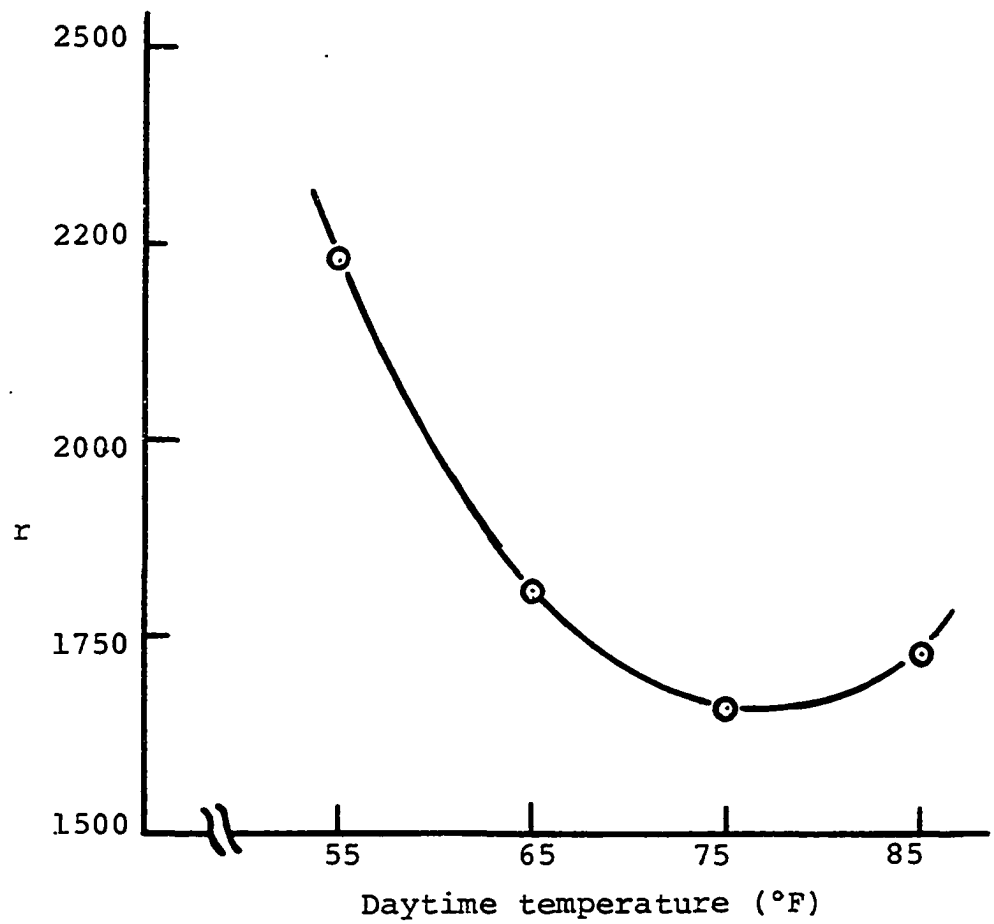

Figure 45. Variation of r with daytime temperature

$$G = \frac{\ln L - \ln(7.8 \times 10^{18}T^{-10.74})\,cm}{1.355T^2 - 205T + 9420} \qquad (22)$$

Growth within the temperature and light intensity range considered can thus be assessed using Equation 22. For example the equation gives growth at 60°F and 180 μ-einstein $m^{-2}s^{-1}$ light intensity as 0.00284 cm.

Between the temperature range T_1 and T_3, the growth curves in Figure 42 plot as straight lines on semi-log graph (see Figure 46). This means that within this temperature range, growth can be modelled by the equation

$$G = He^{QT}\ cm \qquad (23)$$

where H and Q are constants. H and Q values for the various light intensities are

	L_1	L_2	L_3	L_4
H	6.6×10^{-5}	13.2×10^{-5}	19.4×10^{-5}	29×10^{-5}
Q	0.055	0.0474	0.0434	0.039

H plots linearly with L on a log-log sheet, Figure 47. Therefore H and L are connected by the relation:

$$H = NL^k \qquad (24)$$

where N and k are constants. N and k work out to be 9.72×10^{-6} and 0.579 respectively.

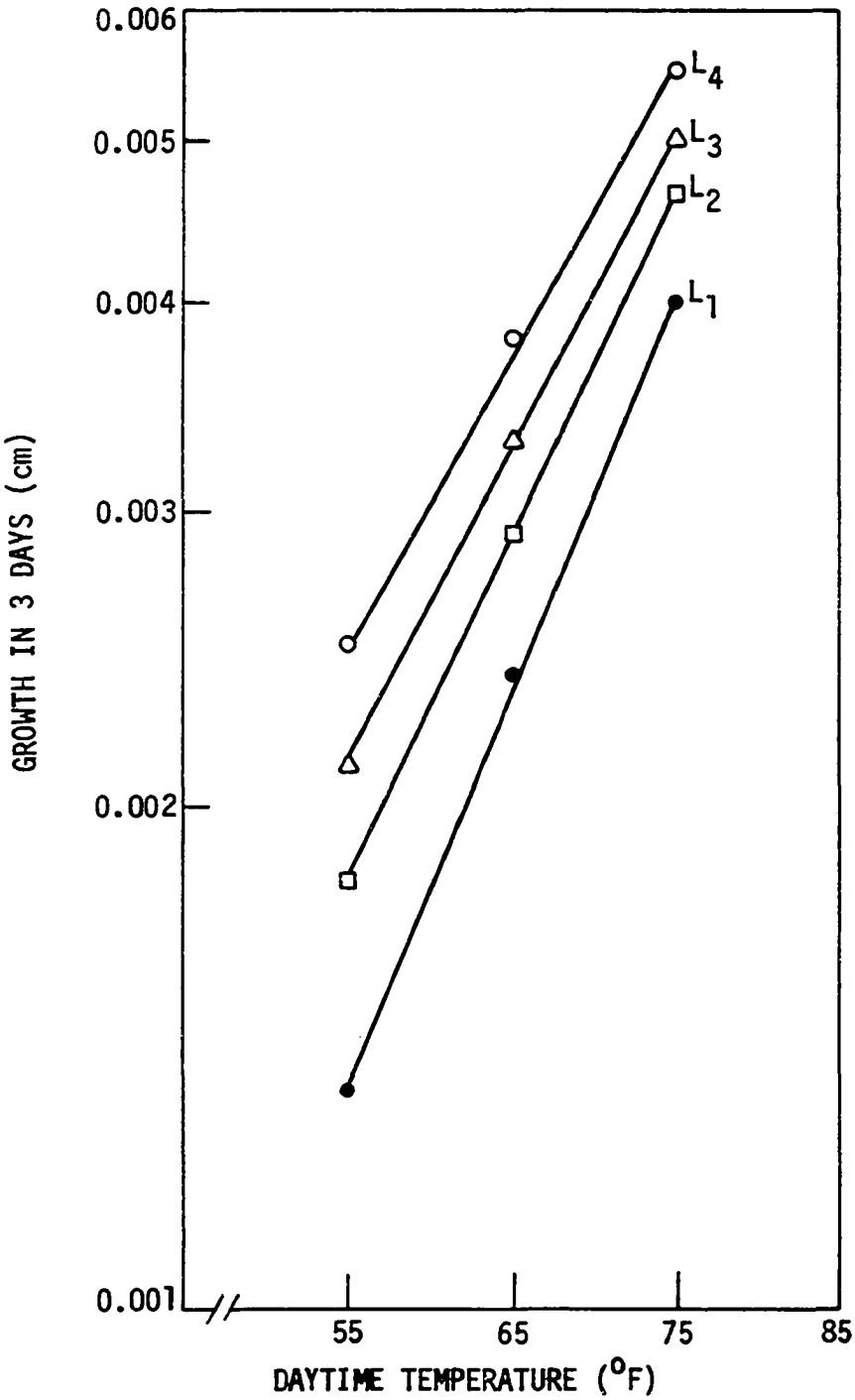

Fig. 46. Variation of growth with day temperature

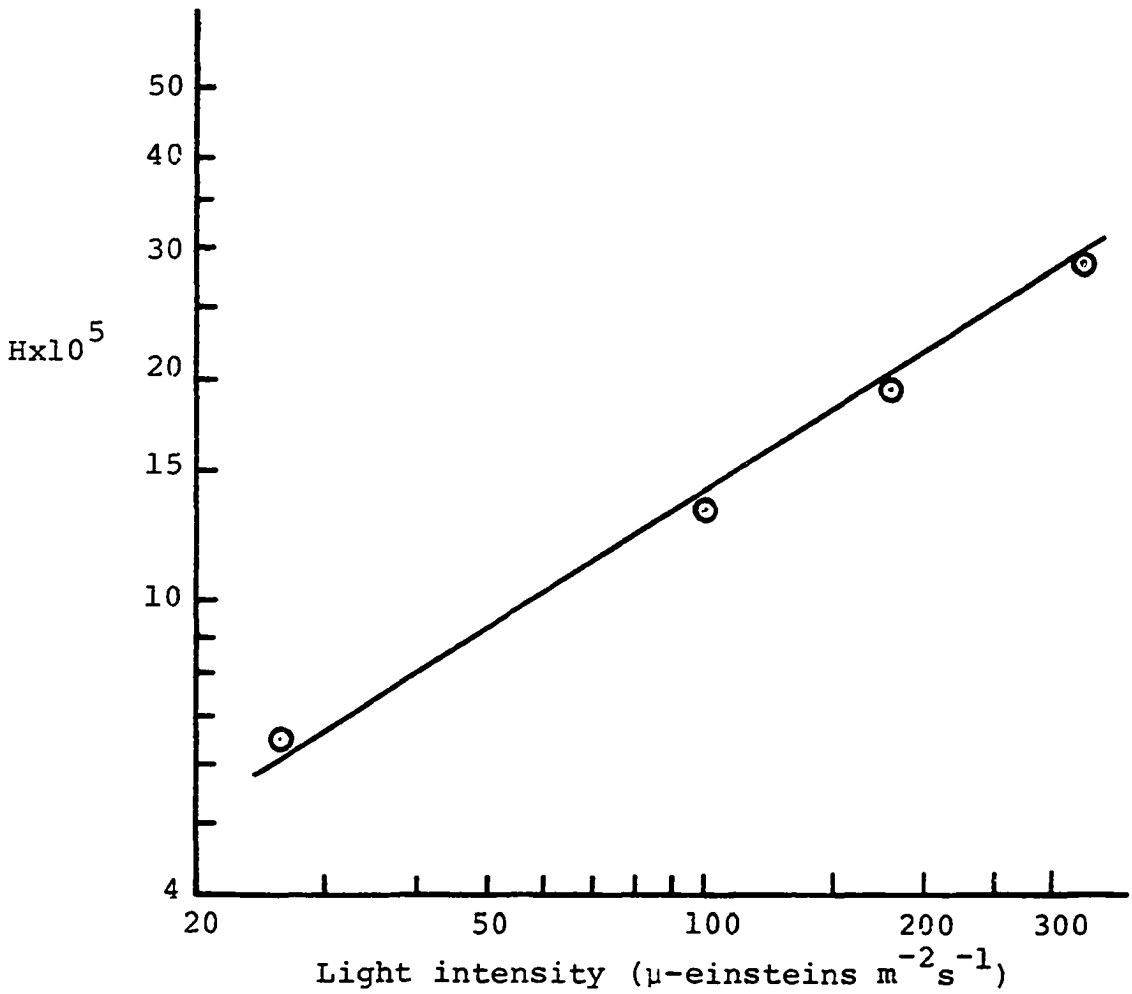

Figure 47. Variation of H with light intensity

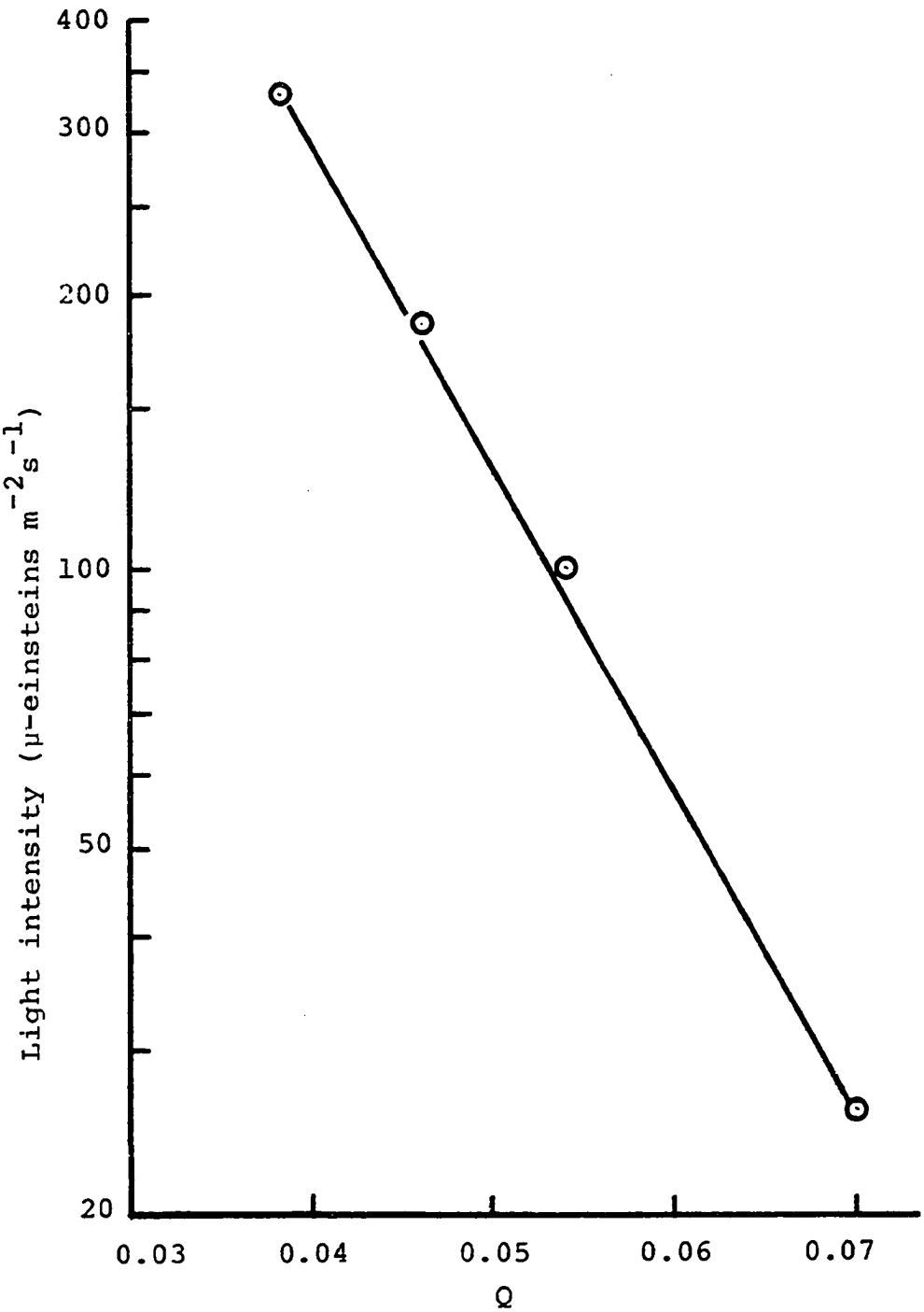

Figure 48. Variation of light intensity with Q

$$\therefore H = 9.72 \times 10^{-6} L^{0.579} \quad (25)$$

L and Q plot linearly on semi-log sheet, Figure 48. Thus Q and L are related by the equation:

$$L = Me^{PQ} \quad (26)$$

where M and P are constants.

$$\therefore Q = \frac{\ln L - \ln M}{P} \quad (27)$$

M and P are equal to 17.655×10^4 and -159.47 respectively.

$$\therefore Q = \frac{\ln L - 12.08}{-159.47}$$

$$\therefore G = 9.72 \times 10^{-6} L^{0.579} e^{\left(\frac{\ln L - 12.08}{-159.47}\right) T} \text{ cm} \quad (28)$$

for

$$55 \leq T \leq 75.$$

This equation gives a growth value of 0.00262 cm for $T = 60°F$ and $L = 180$ μ-einsteins $m^{-2}s^{-1}$ which compares well with the value of 0.00284 cm given by Equation 22 for the same light and temperature levels. For these light and temperature levels, the graph in Figure 42 gives a growth of 0.00262 cm.

The trees used for the test runs were selected in a statistically random manner as mentioned previously. The

transpiration and growth at the four light levels and four temperature levels could thus be analyzed as a 4x4 completely randomized factorial experiment. An analysis of variance was made on the results of the total transpiration per unit leaf area per day and the growth. In the analysis the results are fitted with a straight line or curve (58). The results used for the analysis of variance are as shown in Tables 2a and 2b.

Table 2a. Total transpiration per unit leaf area per day x 10^3 gm cm^{-2}/day

	L_1	L_2	L_3	L_4
T_1	88	136	165	220
	92	134	165	180
T_2	130	191	222	285
	120	199	238	255
T_3	176	260	309	363
	176	240	331	367
T_4	224	342	415	460
	236	358	405	441

Sometimes the form of the fit is suggested by subject-matter knowledge. A model commonly used is a polynomial. For example models for transpiration and growth for a 4x4 factorial experiment will be of the form:

Table 2b. Growth in three days x 10^6 cm

	L_1	L_2	L_3	L_4
T_1	1358	1650	2211	2227
	1328	1740	2015	2167
T_2	2351	2800	3330	3362
	2449	2816	3374	3452
T_3	4122	4550	5150	5213
	4000	4450	5005	5317
T_4	4350	4831	5280	5440
	4374	4891	5452	5560

$$W_T = \alpha_0 + \alpha_1 L + \alpha_2 T + \alpha_3 LT + \alpha_4 L^2 + \alpha_5 T^2 + \alpha_6 L^2 T + \alpha_7 LT^2 + \alpha_8 L^3 + \alpha_9 T^3 + \varepsilon_1 \quad (29)$$

and

$$G = \beta_0 + \beta_1 L + \beta_2 T + \beta_3 LT + \beta_4 L^2 + \beta_5 T^2 + \beta_6 L^2 T + \beta_7 LT^2 + \beta_8 L^3 + \beta_9 T^3 + \varepsilon_2 \quad (30)$$

where

W_T = total transpiration per unit leaf area per day (gm cm^{-2}/day)

G = growth (cm)

L = light intensity (μ-einsteins $m^{-2}s^{-1}$)

T = temperature (°F)

$\varepsilon_1, \varepsilon_2$ = error due to uncontrolled variable

$\alpha_1, \alpha_2, \alpha_3, \ldots$ and $\beta_1, \beta_2, \beta_3, \ldots$ are the unknown parameters. The LxT products are the treatment interactions. The method estimates the α and β parameters such that when these estimated values are substituted for the α's and the β's in Equations 29 and 30, the least possible value of the sum of squares of deviations of the predicted values from the actual observations is obtained. Of the variations in the W_T's and G's about their means, some can be ascribed to changes in light and temperature and some cannot be explained by the model. That is:

$$\begin{array}{l}\text{Sum of squares} \\ \text{about the mean}\end{array} = \begin{array}{l}\text{Sum of squares} \\ \text{about regression}\end{array} + \begin{array}{l}\text{Sum of squares} \\ \text{due to regression}\end{array}$$

The variation is due to the two variables L and T and their interactions LT in the case presented here. The analysis of variance breaks up the sum of squares due to L into its linear, quadratic and cubic components. A similar procedure is done to T and the interaction terms. The various degrees of freedom (d.f.), sum of squares (ss), mean squares (ms) and the F values are obtained. The degree of freedom indicates how many independent pieces of information are needed to estimate the parameters α and β. The mean square is obtained by dividing each sum of squares entry by its corresponding degrees of freedom. The F value is obtained by dividing each mean square by the mean square of the

error. These values are compared with values from the F-distribution at a given probability value for significance tests. The analysis of variance output for transpiration is given in Table 3 and that for growth is given in Table 4. This type of analysis of variance is also discussed in references 59 and 60.

The analysis of variance output for transpiration, Table 3, shows that both light and temperature are very significant for transpiration even at the 1% level. This statement is supported by the large F values of 278.31 and 461.19 for light and temperature respectively compared with the value of 4.77 at the 1% level from the F-distribution with 3 and 16 degrees of freedom. Of the effects of light and temperature, the linear components L_L and T_L are the most significant. These have F values of 751.81 and 1375.05 respectively compared to the value of 8.53 at the 1% level from the F-distribution with 1 and 16 degrees of freedom. Similarly, the quadratic component of the light effect is significant but not the quadratic component of the temperature. The cubic components of the effects of both the light and temperature are insignificant. This means that the cubic term of L, the quadratic term of T and the cubic term of T can be deleted from the prediction equation for W_T, Equation 29. The light and temperature interaction has an

Table 3. Analysis of variance for transpiration

Source	df	ss	ms	F
Light (L)	3	122652.8	40884.3	278.31+[a]
L_L	1	110441.0	110441.0	751.81+
L_Q	1	12044.9	12044.9	81.99+
L_C	1	166.9	166.9	1.14
Temp (T)	3	203245.3	67748.4	461.19+
T_L	1	201995.1	201995.2	1375.05+
T_Q	1	1237.5	1237.5	8.42
T_C	1	1126.7	1126.7	7.67
Light*temp	9	9519.0	1057.7	7.20+
L_L*temp	3	6789.5	2263.2	15.41+
L_L*T_L	1	6645.8	6645.8	45.24+
L_L*T_Q	1	28.8	28.8	0.20
L_L*T_C	1	114.9	114.9	0.78
L_Q*temp	3	2358.2	786.3	5.35
L_Q*T_L	1	2245.2	2245.2	15.28+
L_Q*T_Q	1	70.9	70.9	0.48
L_Q*T_C	1	42.7	42.7	0.29
L_C*temp	3	370.7	370.7	2.52
Error	16	2350.5	146.9	

[a] + - means significant.

F value of 7.2. Compared to the 1% level value of 3.78 from the F-distribution at 9 and 16 degrees of freedom, the interaction is significant. This means that the effect of light and the effect of temperature are not independent. The interaction between the linear component of the light effect and temperature is also significant. Out of this type of interaction, however, the only significant one is the $L_L{}^*T_L$ interaction. This is also called a linear by linear interaction. The existence of this interaction means that the slope of the transpiration vs temperature graph varies linearly or almost linearly with light intensity. This however is not quite the case. The variation is a shallow curve which plots linearly on semi-log graph, see Figure 38. The only component of the interaction between the quadratic component of the light effect and temperature which is significant is the $L_Q{}^*T_L$ interaction. Thus the LT and L^2T terms in Equation 29 are significant. The $L_C{}^*$ temp interaction is not significant at the 1% level and so will be all its components. Therefore the L^3T term in Equation 29 can be deleted. Finally the total transpiration per unit leaf area per day can be modelled mathematically as:

$$W_T\Big|_{L_iT_j} = \alpha_0 + \alpha_1 L_i + \alpha_2 T_j + \alpha_3 L_i T_j + \alpha_4 L_i^2 + \alpha_6 L_i^2 T_j + \varepsilon_1 \qquad (31)$$

$i = 1,2,3,4$ and $j = 1,2,3,4$

By similar procedure it is evident from the analysis of variance for growth output, Table 4, that the following terms can be neglected from Equation 30: L^2T, LT^2 and L^3. The growth imparted to the trees in three days can thus be modelled mathematically as:

$$G\Big|_{L_iT_j} = \beta_0 + \beta_1 L_i + \beta_2 T_j + \beta_3 L_i T_j + \beta_4 L_i^2 + \beta_5 T_j^2 + \beta_9 T_j^3 + \varepsilon_2 \qquad (32)$$

$i = 1,2,3,4; \quad j = 1,2,3,4$

The parameters α_0 and β_0 in Equations 31 and 32 respectively are a measure of the means of W_T and G respectively. The values of the α's and β's obtained from the analysis of variance are as tabulated below:

$\alpha_0 = -139.8613$	$\beta_0 = 95491.105$
$\alpha_1 = -14.6634$	$\beta_1 = 67.909$
$\alpha_2 = 3.8014$	$\beta_2 = -4464.949$
$\alpha_3 = 0.3835$	$\beta_3 = 0.330$
$\alpha_4 = 0.3242$	$\beta_4 = -1.549$
$\alpha_6 = -0.0073$	$\beta_5 = 68.453$
	$\beta_9 = -0.336$

Table 4. Analysis of variance for growth

Source	d.f.	ss	ms	F
Light (L)	3	5652723.1	1884241.0	342.98[+a]
L_L	1	4778388.0	4778388.0	869.79[+]
L_Q	1	797331.2	797331.2	145.14[+]
L_C	1	77003.9	77003.9	14.02
Temp (T)	3	54085643.6	18028547.9	3281.68[+]
T_L	1	50984511.0	50984511.0	9280.54[+]
T_Q	1	1473615.3	1473615.3	268.24[+]
T_C	1	1627517.3	1627517.3	296.25[+]
Light*Temp	9	90948.6	10105.4	1.84
L_L*Temp	3	78323.4	26107.8	4.75
L_L*T_L	1	55256.4	55256.4	10.06[+]
L_L*T_Q	1	17154.6	17154.6	3.12
L_L*T_C	1	5912.4	5912.4	1.08
L_Q*Temp	3	8378.6	2792.9	0.51
L_Q*T_L	1	4877.9	4877.9	0.89
L_Q*T_Q	1	665.8	665.8	0.12
L_Q*T_C	1	2834.9	2834.9	0.52
L_C*Temp	3	4246.6	1415.5	0.26
Error	16	87898.5	5493.7	

[a]+ - means significant.

This means that the total water loss per day can be determined from the relation:

$$W_T \times 10^3 = -139.8613 - 14.6634L + 3.8014T + 0.3835LT + 0.3242L^2 - 0.0073L^2T \quad (33)$$

where L is one tenth of the actual L values used in the test runs. This is so because the analysis of variance was run with the L's divided by ten. Also the W_T's were multiplied by a factor of 10^3 in the analysis of variance. Hence the factor of 10^3 on the left hand side of Equation 33. For a light intensity level of 180 μ-einsteins $m^{-2}s^{-1}$ and a day temperature of 60°F, Equation 33 gives a W_T value of 0.201 gm cm^{-2}/day. This compares well with the value of 0.204 gm cm^{-2}/day given by Equation 17 and 0.187 gm cm^{-2}/day given by Equation 11 for the same light intensity and temperature levels. It can also be recalled that for the same light intensity and temperature levels, Figure 36 gives W_T as 0.200 gm cm^{-2}/day.

The growth in three days can also be determined from the relation:

$$Gx10^6 = 95491.105 + 67.909L - 4464.949T + 0.330LT - 1.549L^2 + 68.453T^2 - 0.336T^3 \quad (34)$$

In Equation 34, L is one tenth of the actual L values used in the test runs. The G values were multiplied by a factor

of 10^6 before running the analysis of variance. Hence the factor of 10^6 on the left hand side of Equation 34. For a light intensity of 180 μ-einsteins $m^{-2}s^{-1}$ and a day temperature of 60°F, Equation 34 gives a G value of 0.00253 cm. This again compares well with the values of 0.00262 cm and 0.00284 cm given by Equations 28 and 22 respectively for the same light intensity and temperature levels. It is also recalled that Figure 42 gives a G value of 0.00262 cm for the same light intensity and temperature levels.

SUMMARY

The following are the major conclusions that were drawn from the investigation:

1. The apparent stem strain due to temperature change is only 13 $\mu\varepsilon/°C$.
2. The stem of the trees respond physiologically to small temperature fluctuations.
3. Both temperature and light intensity have remarkable effects on stem strain, growth and transpiration. These increased with increasing temperature and increasing light intensity.
4. The trees lose water at night at a constant rate.
5. The strain recovery time on watering is independent of light intensity. It is a function only of temperature.
6. The total water loss per unit leaf area per day can be assessed from any of the formulae below:

$$W_T = 0.006e^{0.03T} L^{0.3} \text{ gm cm}^{-2} \qquad \text{(i)}$$

$$W_T = -0.0547L^{(0.268)} + \frac{(\ln L - 0.863)T}{560} \text{ gm cm}^{-2} \qquad \text{(ii)}$$

$$W_T \times 10^3 = -139.8613 - 14.6634L + 3.8014T + 0.3835LT + 3242L^2 - 0.0073L^2T \qquad \text{(iii)}$$

Equations (i), (ii) and (iii) are good for $26 \leq L \leq 330$ and $55 \leq T \leq 85$.

7. The growth can be estimated from the following formulae:

$$G = \frac{\ln L - \ln(7.8\times10^{18}{}_T{}^{-10.74})}{1.355T^2-205T+9420} \text{ cm} \qquad \text{(iv)}$$

$$G = 9.72\times10^{-6}L^{0.579}\, e^{\left(\frac{\ln L-12.08}{-149.47}\right)T} \text{ cm} \qquad \text{(v)}$$

$$G\times10^6 = 95491.105 + 67.909L - 4464.949T + 0.330LT - 1.595L^2 + 68.453T^2 - 0.336T^3 \qquad \text{(vi)}$$

Equations (iv) and (vi) are good for $26 \leq L \leq 330$ and $55 \leq T \leq 85$. Equation (v), however, is good for $26 \leq L \leq 330$ and $55 \leq T \leq 75$.

BIBLIOGRAPHY

1. Schütte, K. H. and Burger, C. P. "Water Stress Studies on Woody Plants." Proc. of the 1st International Congress of Plant Physiology. Wurzburg, Germany: International Association of Plant Physiology, 1973.

2. Hearn, E. J. Strain Gauges. New York: Pitman Press, 1971.

3. Dove, R. C. and Adams, P. H. Experimental Stress Analysis and Motion Measurements. Ohio: Merrill, 1964.

4. Perry, C. C. and Lissner, H. R. The Strain Gage Primer. New York: McGraw-Hill, 1962.

5. Goldsmith, W. and Taylor, R. L. "Impact on Opthalmic Lenses." Experimental Mechanics, 16 (1976), 81-87.

6. Sherbourne, A. N. and Haydl, H. M. "Postbuckling and Postyielding of Edge-compressed Circular Plates." Experimental Mechanics, 16(1976), 100-104.

7. MacDougal, D. T. "Growth in Trees." Carnegie Institute of Washington Publication, No. 307 (1921).

8. Zaerr, J. B. "Moisture Stress and Stem Diameter in Young Douglas-Fir." Forest Science, 17 (1971), 466-469.

9. Boehmerle, K. "Die Pfistersche Zuwachsuhr." Centralbl. f.d. Gesammte Forstwesen, 9 (1883), 83-93.

10. Friedrich, J. "Zuwachsautograph." Centralbl. f.d. Gesammte Forstwesen, 31 (1905), 456-461.

11. Lassoïe, J. P. "Diurnal Dimensional Fluctuations in a Douglas-Fir Stem in Response to Tree Water Status." Forest Science, 19, No. 4 (1973), 251-255.

12. Mallock, A. "Growth of Trees with Interference Bands Found by Rays at Small Angles." Proc. of Royal Society, Series B90, 186-199. London: Royal Society, 1909.

13. Grossenbacher, K. A. "Diurnal Fluctuation in Root Pressure." Plant Physiology, 13 (1938), 669-676.

14. Grossenbacher, K. A. "Automatic Cycle of Rate of Exudation of Plants." American Journal of Botany, 26 (1939), 107-109.

15. Vaadia, Y. "Automatic Diurnal Fluctuations in Rate of Exudation and Root Pressure of Decapitated Sunflower Plants." Physiologia Plantarum, 13 (1960), 701-716.

16. Merwin, H. E. and Howard, L. "Sap Pressure in the Birch Stem." Botanical Gazette, 48 (1909), 442-458.

17. Schütte, K. H. "The Design of Instruments to Measure Water Stress in Plants." Proceedings of the Convention: Water for the Future. Johannesburg, Republic of South Africa, 1970.

18. MacDougal, D. T. "The Hydrostatic System of Trees." Carnegie Institute of Washington Publication No. 373, (1945).

19. Klepper, Betty. "Diurnal Pattern of Water Potential in Woody Plants." Plant Physiology, 43 (1968), 1931-1934.

20. Huck, M. G., Klepper, Betty and Taylor, H. M. "Diurnal Variations in Root Diameter." Plant Physiology, 45 (1970), 529-530.

21. Whipple, R. L., Ligon, J. B., Burger, C. P. and Coffman, M. S. "Resistance Strain Gages as Physiological Transducers on Trees." Experimental Mechanics, 16 (1976), 329-336.

22. MacDougal, D. T. and Forrest, Shreve. "Growth in Trees and Massive Organs of Plants." Carnegie Institute of Washington Publication, No. 350, (1924).

23. MacDougal, D. T. "Studies in Tree Growth by the Dendrographic Method." Carnegie Institute of Washington Publication, No. 462, (1936).

24. Reineke, L. H. "A Precision Dendrometer." Journal of Forestry, 30 (1932), 692-699.

25. Fowells, H. A. "The Period of Seasonal Growth of Ponderosa Pine and Associated Species." Journal of Forestry, 39 (1941), 601-608.

26. Daubenmire, R. F. "An Improved Type of Precision Dendrometer." Ecology, 26, No. 1 (1945), 97-98.

27. Byram, G. M. and Doolittle, W. T. "A Year of Growth for a Shortleaf Pine." Ecology, 31, No. 1 (1950), 27-35.

28. Fritts, H. C. and Fritts, E. C. "A New Dendrograph for Recording Radial Changes of a Tree." Forest Science, 1, No. 4 (1955), 271-276.

29. Kozlowski, T. T. "Diurnal Variations in Stem Diameters of Small Trees." Botanical Gazette, 128, No. 1 (1967), 60-68.

30. Impens, I. I. and Schalck, J. M. "A Very Sensitive Electric Dendrograph for Recording Radial Changes of a Tree." Ecology, 46, No. 1 (1965), 183-184.

31. Jordan, W. R. and Ritchie, J. T. "Influence of Soil Water Stress on Evaporation, Root Absorption and Internal Water Status of Cotton." Plant Physiology, 48, (1971), 783-788.

32. Klepper, Betty, Browning, V. D. and Taylor, H. M. "Stem Diameter in Relation to Plant Water Status." Plant Physiology, 48 (1971), 683-685.

33. Stansell, J. R., Klepper, Betty, Browning, V. D. and Taylor, H. M. "Plant Water Status in Relation to Clouds." Agronomy Journal, 65 (1973), 677-678.

34. Namken, L. N., Bartholic, J. F. and Runkles, J. R. "Monitoring Cotton Stem Radius as an Indication of Water Stress." Agronomy Journal, 61 (1969), 891-893.

35. Splinter, W. E. "Electronic Micrometer Continuously Monitors Plant Stem Diameter." Agricultural Engineering, 50 (1969), 220-221.

36. Peel, A. J. Transport of Nutrients in Plants. London: Butterworth and Co. Ltd., 1974.

37. Sutcliffe, J. Plants and Water. The Institute of Biology's Studies in Biology, No. 14. New York: St. Martin's Press, 1968.

38. Marais, J. N. and Wiersma, D. "Phosphorus Uptake by Soybeans as Influenced by Moisture Stress in the Fertilized Zone." Agronomy Journal, 67 (1975), 777-781.

39. Sionit, N. and Kramer, P. J. "Effect of Water Stress During Different Stages of Growth of Soybean." Agronomy Journal, 69 (1977), 274-277.

40. Bielorai, H. and Hopmans, P. A. M. "Recovery of Leaf Water Potential, Transpiration and Photosynthesis of Cotton During Irrigation Cycles." Agronomy Journal, 67 (1975), 629-632.

41. Ackerson, R. C., Krieg, D. R., Miller, T. D. and Zartman, R. E. "Water Relations of Field Grown Cotton and Sorghum: Temporal and Diurnal Changes in Leaf Water, Osmotic and Turgor Potentials." Crop Science, 17 (1977), 76-80.

42. Thomas, J. C., Brown, K. W. and Jordan, W. R. "Stomatal Response to Leaf Water Potential as Affected by Preconditioning Water Stress in the Field." Agronomy Journal, 68 (1976), 706-708.

43. Lang, A. R. G., Klepper, Betty and Cumming, M. J. "Leaf Water Balance During Oscillation of Stomatal Aperture." Plant Physiology, 44 (1969), 826-830.

44. Dally, J. W. and Riley, W. F. Experimental Stress Analysis. New York: McGraw-Hill, 1965.

45. Micromeasurements Tech. Note 138-2. Romulus: Micromeasurements Inc., 1975.

46. Micromeasurements Tech. Note 128-2. Romulus: Micromeasurements Inc., 1975.

47. Stein, P. K. Measurement Engineering, Vol. II. Tempe: Stein Engineering Services Inc., 1962.

48. Warnock, F. V. and Benham, P. P. Mechanics of Solids and Strength of Materials. London: Pitman Press, 1965.

49. Faupel, J. H. Engineering Design - A Synthesis of Stress Analysis and Materials Engineering. New York: John Wiley and Sons, Inc., 1964.

50. Freynik, H. S. and Dittbenner, G. R. "Strain Gage Stability Measurements or Years at 75°F in Air." Experimental Mechanics, 15 (1976), 155-160.

51. Troke, R. W. "Improving Strain Measurement Accuracy when Using Shunt Calibrations." Experimental Mechanics, 16 (1976), 397-400.

52. Kuczyski, G. C. "A Note on the Remarkable Stability of the Alloy Used in SR-4 Gages." Testing Topics, 9, No. 3. Philadelphia: Baldwin-Lima-Hamilton Corporation, 1954.

53. Zuuring, H. R. "Indices for the Rapid Early Selection of Populus Clones." Ph.D. dissertation, Iowa State University, Ames, Iowa, 1975.

54. Greulach, V. A. Plant Function and Structure. New York: The Macmillan Company, 1973.

55. Devlin, R. M. Plant Physiology. New York: Reinhold Publishing Corporation, 1966.

56. Fasehun, F. E. and Gordon, J. C. "Difference in Growth Response to Light Intensity by Populus x euramericana Clones." Iowa State Journal of Research, 51, No. 3 (1977), 265-270.

57. Williamson, R. E. and Splinter, W. E. "Effects of Light Intensity, Temperature and Root Gaseous Environment on Growth of Nicotiana Tabacum." Agronomy Journal, 61 (1969), 285-288.

58. Barr, A. J., Goodnight, J. H., Sall, J. P. and Helwig, J. T. A User's Guide to SAS. Raleigh, North Carolina: Sparks Press, 1976.

59. Draper, N. R. and Smith, H. Applied Regression Analysis. New York: John Wiley and Sons, Inc., 1966.

60. Snedecor, G. W. and Cochran, W. G. Statistical Methods. Ames, Iowa: The Iowa State University Press, 1967.

ACKNOWLEDGMENTS

The author wishes to express sincere thanks and appreciation to his advisor, Professor C. P. Burger for his valuable suggestions on both the engineering and biological aspects of the study and his graduate committee member Professor R. B. Hall for his useful suggestions on the biological aspects of the study. Many thanks are also due to the author's graduate committee members: Professor C. P. Burger, Professor W. F. Riley, Professor F. M. Graham, all of the Engineering Science and Mechanics Department, Professor S. J. Marley of the Agricultural Engineering Department and Professor R. B. Hall of the Forestry Department for their patience and guidance.

Special thanks are extended to Mr. T. J. Elliot, the technician at the Laboratory of Mechanics, for helping in building some of the equipment, Mr. R. R. Faltonson, The Forestry Research Facilities Supervisor, for providing the trees and many other assistances in the green house and the workers at the E.R.I. electronic shop for their prompt response when any of the research instruments broke down.

Special thanks also go to the author's wife, Esther and daughters Yaa and Afia for their patience, love and moral support.

Lastly, but not the least, the author wishes to thank Pat Gunnells for her excellent typing and suggestions.

APPENDIX A

Table A1. Diameter or circumference measuring devices and their users

Instrument, Designer-User and Year	Quantity Measured	Physical Quantity Correlated to Measurement	Date Type and frequency	Method
Calipas Kaiser, P. (1879)	Diameter change	Diurnal variation in stem	Observer-hourly	The usual use of calipers
Dendrometer Pfister (1883)	Diameter change	Diurnal changes in stem	Observer-when required	Band wrapped around tree trunk. A lever mechanism and a linear scale was used to measure changes in diameter of stem
Dendrometer Friedrich, J. (1905)	Diameter change	Diurnal variation of stem	Observer-when required	Steel band on roller bearings. Change is read directly from scale attached
Dendrometer Mallock, F.R.S. (1917)	Diameter change	Growth	Observer-when required	Light shining through glass prism and glass sheet forms interference bands. Diameter change of tree moves plate in relation to prism. Micrometer screw is used to obtain original angle and is calibrated to give diameter change
Dendrometer MacDougla, D.T. (1918-1934)	Diameter change	Diurnal variation of stem	Chart	Rigid metal frame surrounding tree trunk. Frame had a lever mechanism. Long end of lever carried pen for recording diameter changes
Dendrometer Reineke, L.H. (1932)	Radius change	Growth	Observer-when required	A screw hook is screwed into the sapwood of the tree. A metal tab is affixed to bark. The distance from hook to tab is measured with dial gage micrometer

Table A1 (Continued)

Instrument, Designer-User and Year	Quantity Measured	Physical Quantity Correlated to Measurement	Date Type and Frequency	Method
Dendrometer Powells, H.A. (1941)	Diameter change	Growth	Observer-when required	A hook is screwed into the wood of the tree. A small round headed screw is imbedded in the bark directly beneath the hook. A radial gauge measures the distance between the hook and the screw
Dendrometer Hall, R.C. (1944)	Circumference change	Growth	Observer-when required	A band divided into 0.1 in. scale is fixed around trunk. Overlap contains a vernier. Change is read directly from scale
Dendrometer Daubermire, R.F. (1945)	Radius change	Growth	Observer-when required	A plate is held a fixed distance from the bark of the tree by 3 screws. A pin is screwed into sapwood. The distance from plate to pin is measured with dial gage micrometer
Dendrometer Byran, G.M. Doolittle, W.T. (1950)	Radius change	Growth	Observer-when required	A U-frame is mounted to bark. A grooved lag screw is inserted into sapwood. Distance between groove and U-frame is measured with micrometer calipers

Table A1 (Continued)

Instrument, Designer-User and Year	Quantity Measured	Physical Quantity Correlated to Measurement	Date Type and Frequency	Method
Fritts Dendrograph Fritts, H.C. Fritts, E.C. (1955)	Radius change	Growth	Chart	Mounting plate is attached with 3 bolts to sapwood. Mechanical arm makes contact with bark. Uses lever arm amplification to record on clock driven chart
Dendrometer Schütte, K.H. Preston, R. (1970)	Circumference change	Diurnal variations of stem	Observer-when required	Plastic or rubber tube is fastened securely around the stem. Capillaries are run from this tube (the same can be partially compressed by a band). Height of fluid column gives change
Dendrometer Zaerr, J.B. (1970)	Diameter change	Growth	Observer-when required	Use dial calipers to measure the distance between the heads of two thumb tacks which have been glued to opposite sides of the stem
Dendrometer Lassoie, J.P. (1973)	Circumference change	Diurnal changes in stem	Observer-when required	Band wrapped around stem with pointer. Circumference change is read directly on scale attached

Table A1 (Continued)

Instrument, Designer-User and Year	Quantity Measured	Physical Quantity Correlated to Measurement	Date Type and Frequency	Method
Dendrograph Ninoxata, K. Mitsuru, M. (1956)	Radius change	Growth	Strip chart	Four electrical wires are stretched between a frame and movable arm. The arm is tacked to a tree. As the arm moves with the radius change of the tree, its angle with the frame changes causing two of the wires to elongate and the other two wires to contract. A bridge circuit measures the change in output
Dendrograph Phipps, R.L. Gilbert, G.G. (1960)	Radius change	Growth	Strip chart	Mounting plate is anchored to sapwood. Core of linear voltage displacement transducer is secured to bark
Dendrograph Hawkins, G.W. (1965)	Radius change	Growth	Strip chart	Two stiff arms are attached to an open metal ring. The arms are forced apart while the plant stem is located at the proper position. As the stem changes size, its force changes the curvature of the ring. This change is measured with electrical strain gages

Table A1 (Continued)

Instrument, Designer-User and Year	Quantity Measured	Physical Quantity Correlated to Measurement	Date Type and Frequency	Method
Dendrograph Impens, I.I. Schalck, J.M. (1965)	Radius change	Diurnal variation of stem	Strip chart	Casing of LVDT is anchored to stem using screws. The movable core is attached to a driving pin which is in contact with the bark
Dendrograph Beeman (1966)	Radius change	Growth	Strip chart	Two thin metal bands are fastened together at one end. They are forced apart to form two cantilever beams. The stem is placed between the beams and strain gages are mounted on the beams to measure change in deflection
Dendrograph Namken, L.N. Bartholic, J.F. Runkles, J.R. (1969)	Radius change	Diurnal variation in stem	Strip chart	An LVDT is mounted in a lucite block. The block with sponge inner surface is then bolted to several blocks so as to hold the stem between the inner sponge surfaces
Dendrograph Splinter, W.E. (1969)	Radius change	Diurnal variation of stem	Strip chart	An LVDT is mounted in a movable head which is then attached to base support with rods

Table A1 (Continued)

Instrument, Designer-User and Year	Quantity Measured	Physical Quantity Correlated to Measurement	Date Type and Frequency	Method
Dendrograph Schutte, K.H. Mawmarzh, J. Burger, C.P. (1970)	Circumference change	Diurnal variations of stem	Strip chart	Philips' PR 9814 strain gages are mounted either directly to the bark of the tree or on a thin metal band which fastened around the stem. A temperature compensating circuit is used. A Baldwin SR4 bridge is used to measure gage output. Results were contrary to all classical botanical information
Dendrograph Klepper, Betty Browning, Douglas Taylor, Howard (1971)	Radius change	Diurnal variations in stem	Strip chart	An LVDT with holder is clamped to an anchored rod. The core is held to the stem with spring pressure
Dendrograph LaPoint, Grant Van Cleve, Keith (1971)	Diameter change	Diurnal variations of stem	Strip chart	A frictional pressure band holds the apparatus to the tree. An LVDT is used. The core is moved by stiff wires connected to the opposite side of the holder
Dendrograph Kinerson, Russell S, Jr. (1973)	Diameter change	Diurnal variations of stem	Strip chart	A linear motion potentiometer is fastened to a template. The template is clamped around the tree

Table A1 (Continued)

Instrument, Designer-User and Year	Quantity Measured	Physical Quantity Correlated to Measurement	Date Type and Frequency	Method
Dendrograph Whipple, R.L. Ligon, J.B. Coffman, M.S. Burger, C.P. (1976)	Circumference change	Diurnal variations in stem	Strip chart	Micro-measurements MW 84 94-4. Foil strain gages are bonded to the tree stem. The four gages are connected in standard bridge configuration to a Northern Technical Services digital strain indicator. Output is recorded on a potentiometric strip chart recorder

APPENDIX B

Table B1. Physical properties of trees used for each light and temperature combination

Run (Rab)	Tree no.	Tree height (cm)	Stem diameter at point where gage was mounted (cm)	Number of leaves	Leaf area cm^2
R_{11}	1	90	1.235	28	3476
	2	80	1.207	42	4347
R_{12}	1	102	1.222	35	3443
	2	96	1.289	55	3704
R_{13}	1	92	1.340	20	3636
	2	105	1.221	25	3226
R_{14}	1	98	1.291	26	2744
	2	89	1.256	25	2895
R_{21}	1	95	1.133	33	4039
	2	95	1.180	72	4400
R_{22}	1	106	1.192	25	1735
	2	103	1.198	34	2576
R_{23}	1	105	1.402	35	3500
	2	100	1.421	52	3982
R_{24}	1	90	1.446	36	3233
	2	99	1.484	24	3156
R_{31}	1	97	1.330	48	3241
	2	104	1.290	101	5026
R_{32}	1	87	1.213	50	4525
	2	82	1.187	28	2347
R_{33}	1	98	1.346	105	5025
	2	95	1.309	57	3285
R_{34}	1	89	1.381	23	3071
	2	89	1.409	34	3398
R_{41}	1	93	1.279	69	3538
	2	102	1.287	72	4200

Table B1 (Continued)

Run (Rab)	Tree no.	Tree height (cm)	Stem diameter at point where gage was mounted (cm)	Number of leaves	Leaf area cm^2
R_{42}	1	95	1.306	40	3122
	2	97	1.322	85	4875
R_{43}	1	90	1.337	56	2510
	2	101	1.380	63	3443
R_{44}	1	94	1.369	34	2500
	2	86	1.399	32	3674